NASA/CR-2009-215933

# Trajectory-Oriented Approach to Managing Traffic Complexity

*Trajectory Flexibility Metrics and Algorithms and Preliminary Complexity Impact Assessment*

*Husni Idris, Robert Vivona, and Tarek Al-Wakil*
*L3 Communications, Billerica, Massachusetts*

September 2009

# NASA STI Program . . . in Profile

Since its founding, NASA has been dedicated to the advancement of aeronautics and space science. The NASA scientific and technical information (STI) program plays a key part in helping NASA maintain this important role.

The NASA STI program operates under the auspices of the Agency Chief Information Officer. It collects, organizes, provides for archiving, and disseminates NASA's STI. The NASA STI program provides access to the NASA Aeronautics and Space Database and its public interface, the NASA Technical Report Server, thus providing one of the largest collections of aeronautical and space science STI in the world. Results are published in both non-NASA channels and by NASA in the NASA STI Report Series, which includes the following report types:

- TECHNICAL PUBLICATION. Reports of completed research or a major significant phase of research that present the results of NASA programs and include extensive data or theoretical analysis. Includes compilations of significant scientific and technical data and information deemed to be of continuing reference value. NASA counterpart of peer-reviewed formal professional papers, but having less stringent limitations on manuscript length and extent of graphic presentations.

- TECHNICAL MEMORANDUM. Scientific and technical findings that are preliminary or of specialized interest, e.g., quick release reports, working papers, and bibliographies that contain minimal annotation. Does not contain extensive analysis.

- CONTRACTOR REPORT. Scientific and technical findings by NASA-sponsored contractors and grantees.

- CONFERENCE PUBLICATION. Collected papers from scientific and technical conferences, symposia, seminars, or other meetings sponsored or co-sponsored by NASA.

- SPECIAL PUBLICATION. Scientific, technical, or historical information from NASA programs, projects, and missions, often concerned with subjects having substantial public interest.

- TECHNICAL TRANSLATION. English-language translations of foreign scientific and technical material pertinent to NASA's mission.

Specialized services also include creating custom thesauri, building customized databases, and organizing and publishing research results.

For more information about the NASA STI program, see the following:

- Access the NASA STI program home page at *http://www.sti.nasa.gov*

- E-mail your question via the Internet to help@sti.nasa.gov

- Fax your question to the NASA STI Help Desk at 443-757-5803

- Phone the NASA STI Help Desk at 443-757-5802

- Write to:
  NASA STI Help Desk
  NASA Center for AeroSpace Information
  7115 Standard Drive
  Hanover, MD 21076-1320

# Trajectory-Oriented Approach to Managing Traffic Complexity

*Trajectory Flexibility Metrics and Algorithms and Preliminary Complexity Impact Assessment*

*Husni Idris, Robert Vivona, and Tarek Al-Wakil*
*L3 Communications, Billerica, Massachusetts*

# Preface

This document describes exploratory research on a distributed, trajectory-oriented approach for traffic complexity management. The approach is to manage traffic complexity based on preserving trajectory flexibility and minimizing constraints. In particular, the document presents metrics for trajectory flexibility; a method for estimating these metrics based on discrete time and degree of freedom assumptions; a planning algorithm using these metrics to preserve flexibility; and preliminary experiments testing the impact of preserving trajectory flexibility on traffic complexity. While the experiments were performed using distributed scenarios, the fundamental metrics and methods and the insights obtained are relevant to both centralized and distributed control environments. In addition, the metrics and functions may be utilized by the human or the automation, where the human may be the aircraft crew, the airline operations center, or the traffic managers, and the automation may be their decision support tools. Therefore, in this document the term 'aircraft' is used to refer in a general sense to the user or beneficiary of these metrics and functions. The document also describes an early demonstration capability of the trajectory flexibility preservation function in the NASA Autonomous Operations Planner (AOP) platform.

**This page intentionally left blank**

# Table of Contents

## List of Figures

# List of Acronyms

| | |
|---|---|
| 4D | Four Dimensional |
| ADS-B | Automatic Dependent Surveillance – Broadcast |
| AOC | Airline Operations Center |
| AOP | Autonomous Operations Planner |
| ASAS | Airborne Separation Assistance System |
| ATM | Air Traffic Management |
| ATOL | Air Traffic Operations Laboratory |
| ATSP | Air Traffic Service Provider |
| EDA | En-route Descent Advisor |
| ETA | Estimated Time of Arrival |
| FMS | Flight Management System |
| kts | knots |
| NAS | National Airspace System |
| NASA | National Aeronautics and Space Administration |
| NextGen | Next Generation Air Transportation System |
| nmi | Nautical Miles |
| RTA | Required Time of Arrival |
| TFM | Traffic Flow Management |
| UAV | Unmanned Air Vehicle |
| UGV | Unmanned Ground Vehicle |

# List of Symbols

| | |
|---|---|
| ADP | Adaptability |
| RBT | Robustness |
| $(t,s)$ | (time, distance) |
| $(t,x,y)$ | (time, x-location, y-location) |
| $V, V_{min}, V_{max}$ | Ground speed, its minimum, its maximum |

| | |
|---|---|
| Traj | Trajectory |
| $P_i$ | Probability of trajectory instance $traj_i$ |
| $P_c$ | Probability of constraint situation c |
| $P_f$ | Probability of feasibility |
| $P_{f,c}$ | Probability of feasibility in constraint situation c |
| $f(t,s)$ or $f(t,x,y)$ | Number of feasible trajectories from (…) to destination |
| $f_c(t,s)$ or $f_c(t,x,y)$ | Number of feasible trajectories from (…) to destination in constraint situation c |
| $i(t,s)$ or $i(t,x,y)$ | Number of infeasible trajectories from (…) to destination |
| $i_c(t,s)$ or $i_c(t,x,y)$ | Number of infeasible trajectories from (…) to destination in constraint situation c |
| $N(t,s)$ or $N(t,x,y)$ | Number of all trajectories from (…) to destination |
| $b(t,s)$ or $b(t,x,y)$ | Number of feasible trajectories from current state to (…) |
| $g(t,s)$ or $g_k(s)$ or $g(t,x,y)$ or $g_k(x,y)$ | Number of trajectories from k=(…) to next time step |
| $\varepsilon$ | Duration between time increments |
| $h_i$, $h_{min}$, $h_{max}$ | Heading with its maximum and minimum values |
| $Q(t, x, y)$ | Cost function |

# 1 Introduction

The Next Generation Air Transportation System (NextGen) is expected to receive up to three times the current traffic demand by the year 2025 [1]. In order to handle the expected increase in air traffic NextGen will introduce major transformations in Air Traffic Management (ATM); three examples of which are net-enabled information access, performance-based services, and aircraft trajectory-based operations [1]. Net-enabled information access will substantially increase information availability promoting greater shared awareness of system operations among users and service providers. Net-enabled information access is exemplified by emerging technologies such as the Automatic Dependent Surveillance Broadcast (ADS-B) which enables sharing of aircraft-based position and intent information among airborne and ground-based agents. Performance-based services will make access to National Airspace System (NAS) resources, such as runways and airspace volumes, dependent on the equipage and capability of the aircraft. This performance dependence promotes users to equip their aircraft and service providers to provide access to scarce NAS resources according to performance levels of aircraft. Trajectory-based operations will manage NAS resources by requiring aircraft to precisely follow custom-made four dimensional (4D) trajectories consisting of a specified path and along-path time conformance requirements. Trajectory-based operations promote prescribing and accurately following trajectories that ensure separation and optimize traffic flow management over different time horizons.

These NextGen capabilities enable a more optimal allocation of functions among the agents of the air traffic system [2]. One such allocation scheme proposes moving the ATM system towards a distributed control architecture [3], [4]. This distributed architecture delegates to the pilot more authority in determining and modifying the aircraft trajectory; currently this authority resides mainly with the ground-based controller. The premise is that distributed control mitigates the controller workload as a constraint against increasing airspace capacity, because introducing more traffic introduces additional responsible decision makers (pilots) enabled by advanced sensor, communication, and decision support technologies.

While the architecture of the ATM system becomes less centralized and more distributed, its goal remains to achieve objectives such as maintaining safety and efficiency at acceptable levels. A key research question asks whether a distributed control architecture will be capable of satisfying these ATM objectives. A positive answer has important implications on the new role of centralized control, taking on higher level supervisory control functions such as dynamic scheduling, as opposed to lower level active control, thus enabling capacity gains and cost savings. Therefore, in the distributed control architecture each individual aircraft is responsible for generating and maintaining a trajectory that achieves the ATM objectives for that flight in addition to any self-interest objectives. To this end it is critical to design the distributed architecture with appropriate elements that ensure individual aircraft actions achieve the overall ATM objectives.

## 1.1 Research Questions

As shown in Figure 1-1, the ATM system ensures high level objectives such as safety, stability, cost effectiveness, among other objectives. To ensure these objectives, constraints are imposed on aircraft trajectories. For example to ensure safety separation requirements are imposed between aircraft and to ensure stability, required times of arrival are scheduled to maintain demand below capacity. This research deals with two newly proposed functions for the distributed ATM system: a trajectory flexibility preservation function and a trajectory constraint minimization function. The trajectory flexibility preservation function enables an aircraft to plan its trajectory such that it preserves a requisite level of maneuvering flexibility in accommodating unforeseen disturbances, stemming for example from other traffic and from weather activity. The trajectory constraint minimization function enables ground-based agents, in collaboration with air-based agents, to impose just enough constraints on trajectories to achieve ATM objectives, such as separation assurance and flow management.
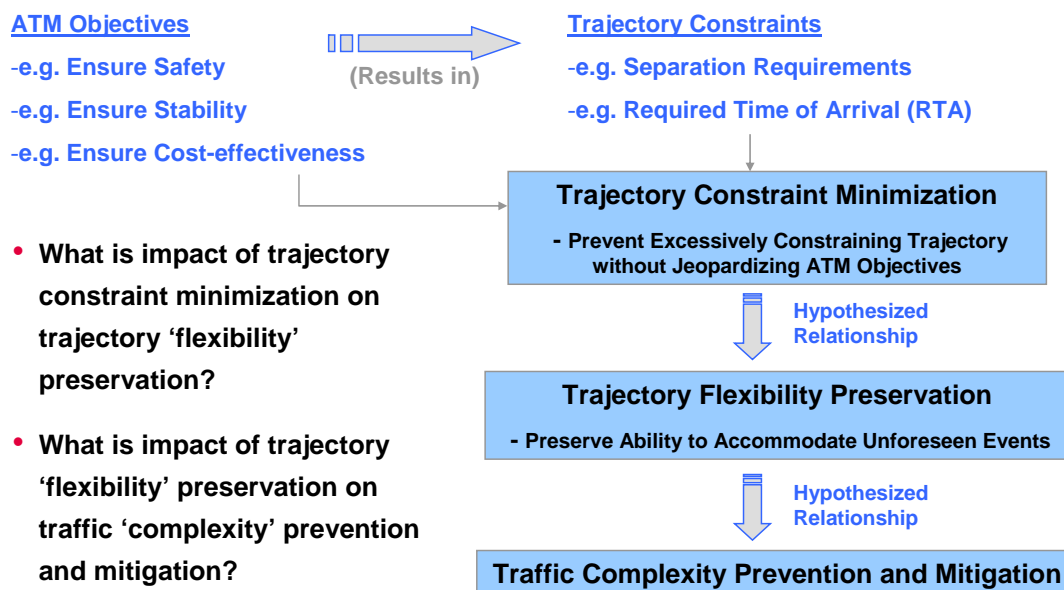


**Figure 1-1 Main functions and their hypothesized relationships**

The objective of this research is to investigate the relationships between these functions and their impact on the aggregate ATM system performance. Namely, this research will test two underlying hypotheses displayed in Figure 1-1:

a. by each individual aircraft preserving its own trajectory flexibility, aggregate system objectives, such as maintaining acceptable traffic complexity (complexity defined as proneness to compromising safety), are naturally achieved, and

b. by minimizing the constraints imposed on a trajectory, without jeopardizing the intended ATM objectives, the trajectory flexibility is increased, and hence traffic complexity is further mitigated.

## 1.2 Literature Review

Literature on three main topics related to this research is summarized: distributed separation assurance, motion planning, and traffic complexity.

### 1.2.1 Distributed Airborne Based Conflict Resolution

Research on distributed ATM has focused on the investigation of sharing the primary function of separation assurance between pilots and controllers. Currently this authority resides mainly with the ground-based controller, except in emergency situations and some visual situations. To maintain workload at an acceptable level, controllers are assisted by automation such as the Center TRACON Automation System [5], [6]. In a distributed control architecture, each aircraft (i.e., pilot/automation system) is responsible for maintaining separation from surrounding traffic. Pilots are assisted by cockpit automation, known generally as Airborne Separation Assistance Systems (ASAS).

Prior research on distributed ATM concentrated on the investigation of sharing the primary function of separation assurance between pilots and controllers. ASAS research has produced a number of prototypes, algorithms, and experiments. The research presented in this paper is in support of the Autonomous Operation Planner (AOP) – a NASA-developed research model of an airborne automation system built for the study of advanced distributed air-ground operational concepts [7], [2]. It provides an integrated suite of capabilities for separation management and trajectory planning from the flight deck perspective, including conflict detection and resolution, and trajectory constraint conformance. AOP has been used in both batch and human-in-the-loop simulation studies for assessment of the feasibility of self separation. For example, in a recent batch simulation study [8] AOP was used to analyze the safety performance of a self-separation conflict resolution function that utilizes a genetic algorithm approach [9]; earlier versions of which are reported in [10] and [11]. It was performed in the distributed simulation platform of NASA's Air Traffic Operations Laboratory (ATOL), which includes a grid of interconnected, medium fidelity aircraft simulators, each flown by a computer-based pilot model. The study simulated a range of traffic densities up to five times the current level, with random traffic patterns, running more than 10000 flights over 168 simulation hours. While a large number of conflicts were observed due to the high and randomized traffic, the study demonstrated the effectiveness of the conflict resolution algorithm, while testing only strategic lateral maneuvering with multiple sources of uncertainty. AOP was also used in early human-in-the-loop experiments of mixed distributed and centralized separation assurance, which showed promising effects on workload and efficiency [12]. Other ASAS efforts include the Mediterranean Free Flight Program where early experiments also showed positive results of self separation operations [13], [14].

A number of other research efforts investigated and reported algorithms suitable for conflict resolution in a distributed control environment: Hill, et al. suggested a satisficing game theoretic approach for distributed air traffic control [15]. Wollkind, et al. reported a cooperative negotiation algorithm for conflict resolution, by trading shared utility information using a monotonic concession protocol [16]. Versteegt and Visser used

traffic complexity as a criterion to resolve conflicts in a free flight sector while reducing the traffic load [17].

Using hybrid control, Tomlin et al [18], [19] analyzed the safety of trajectory patterns with continuous dynamics between discrete states. They used relative geometry of kinematics for modeling the continuous state evolution between discrete states, which were turns between straight segments. They analyzed a worst case scenario based on a game theoretic assumption that each aircraft assumes the worst action by the other.

### 1.2.2  Motion Planning in Robotics and Other Moving Agent Systems

Significant research has been conducted in the area of robotics for planning coordinated motion and trajectories of robots and autonomous vehicles of different types. This work which concentrated in the late eighties and the nineties has been reinvigorated recently in the context of multiple rovers and multiple unmanned air and ground vehicles (UAV and UGV) for applications such as space exploration and hazard area operations. In such applications autonomous aerial or ground vehicles are expected to coordinate their motions to avoid each other and other obstacles while achieving certain goals.

In general this problem involves deriving a world model based on partial information of the objects surrounding each vehicle including current and intended states of obstacles and other moving vehicles. This information is available through sensing and communication, such as through vision sensors and data links. Then motion plans for each vehicle are generated in a centralized or distributed fashion to reach its destination while avoiding the obstacles and other objects.

One of the earlier approaches to motion planning is based on geometrically defining the environment, using methods such as Voronoi diagrams [20], and planning trajectories through geometric entities or cells. These approaches are mainly used to plan trajectories off-line.

One popular approach is based on artificial potential fields proposed by Khatib [21]. In this approach obstacles are modeled as repellers and goals as attractors. The approach is attractive because it allows adaptive on-line motion planning, in a reactive manner while vehicles move. The most serious shortcoming of this approach is the risk of deadlock due to local minima and of oscillations near obstacles and in narrow passages [22]. However the use of potential fields is still a popular approach and has been suggested for navigation of unmanned vehicles using actual magnetic field sensors [23], [24]. Shimoda [25] applied an artificial potential field approach in the trajectory space (the space of the actuation degrees of freedom of a vehicle) to account for kinematic constraints, uneven terrain as well as avoiding moving obstacles. Two advantages were described for using the degrees of freedom space as opposed to the conventional Cartesian space: directly computing actuation command inputs that obey the vehicle constraints and easily expressing the terrain constraints in terms of actuation variables.

Randomized motion planning approaches avoid the deadlock problem inherent in potential field approaches. One such approach uses probabilistic road maps by randomly selecting milestones from the robot's configuration space and connecting them to produce collision free paths [26]. This approach was described in Hsu 1997 and

extended to account for any kinodynamic constraints by building the roadmap in the space-time domain [27], [28], [29].

Lamiraux [30] used randomized exploration trees (introduced previously by Barraquand [31] and extended in LaValle [32]) from the initial state and from the goal state, and then potential field methods to modify the two resulting partial trajectories such that they connect. Combining randomized exploration trees and trajectory deformation using potential fields reduced the size of the trees and the exploration time. The paper has a mathematical formulation for a generic perturbation of a trajectory using artificial potential field approach, which is based on earlier work of Lamiraux [33]. When a local minimum results in the potential field modification, further tree exploration is used to avoid the deadlock.

Clark et al. [34] reported an approach to robot planning motion based on dynamic networks. They proposed centralized control within networked vehicles and decentralized when not networked. Centralized control used priority rules within networked vehicles.

### 1.2.3 Traffic Complexity

Traffic complexity is essential to this research because of the need to test and demonstrate the impact of trajectory flexibility preservation and constraint minimization on traffic complexity.

The vast majority of the air traffic control literature dealing with complexity has tackled the complexity issue focusing on factors that make the air traffic situation more complex and result in an increase of controller workload, ultimately limiting the airspace capacity. These studies assumed a centralized environment in which the controller controls traffic within a sector of airspace and the major motivation was to approximate controller workload, and hence sector capacity, by a more realistic measure than a simple traffic count, as it is the practice today. The approaches used in these efforts include:

Kopardekar and Magyarits [35] listed a large number of factors (from a number of studies) that affect traffic complexity (and hypothetically controller workload) along with associated metrics. The metrics were mostly derived from the airspace geometry based on the notion of dynamic density, and included, for example, aircraft count and density, sector geometry, traffic mix and distribution, traffic flow structure, mix of aircraft types and performance characteristics, and weather. Then using the linear regression technique, they found the factors/metrics that best fit controller workload data. The workload data was obtained from subjective controller ratings of the difficulty to control traffic scenarios of different complexities.

Histon et al. [36] and Davison et al. [37] emphasized cognitive elements of complexity, in particular the use of structure by controllers to simplify the control cognitive processes. Examples of structure that they determined include standard flows, grouping of traffic, and critical points such as merge points. Athenes et al. [38] developed and analyzed a metric that measures the effect of uncertainty and time pressure on controller workload. They used objective measures such as heart rate to demonstrate the validity of their metrics.

Delahaye and Puechmorel [39] introduced several complexity metrics based on traffic geometry (proximity, convergence, sensitivity to control maneuver) and traffic flow pattern organization or disorder (topological entropy). They extended the entropy metric effort building linear and nonlinear dynamical system models to fit actual aircraft trajectories [40]. Building on this effort, Ishutkina et al. [41] estimated traffic complexity by the ability of a mathematical linear program to interpolate a vector flow field between aircraft positions and velocities, given a set of constraints on speed and turn rate. These efforts tend to be computationally expensive and were demonstrated for simple 2 dimensional situations.

Aigoin [42] used clustering techniques to measure complexity. Granger and Durant [43] analyzed the impact of the cluster size of aircraft in conflict. Clustering techniques were also used by Billimoria and Lee [44] to determine airspace congestion independent of sectors.

Relevant to a distributed control environment, Riley et al. [45] analyzed the pilot perception of airspace complexity. This study built on the controller perception studies by Koperdekar and Magyarits [35]. It reduced the list of factors to the ones relevant to a pilot resolving conflicts and used pilot ratings and regression to analyze the factors that represent pilot perception the best. Then a neural network model was used to create a complexity prediction utility.

Some efforts were made to use complexity prediction for traffic flow management decision aid. These efforts include Sridar et al. [46] and Masalonis et al [47].

Little literature has been found and reviewed dealing with the minimization of constraints and its effects. For example, Ishutkina et al. [41] suggest a lineal program formulation that determines the minimum number of constraints that should be relaxed in their vector field formulation.

## 1.3  Report Outline

In this report, Section 2 describes conceptually how the two functions of trajectory flexibility preservation and constraint minimization operate in a distributed control architecture that includes self separation. The concept and its underlying hypotheses are illustrated through hypothetical scenarios involving conflict resolution and flow management. Then, a functional analysis is described where each of the three functions is decomposed into monitoring and action components, and the interaction and information flow between them is demonstrated schematically. Section 2 is based on material published in [48]. Section 3 defines the notion of trajectory flexibility in an analytical framework of an aircraft trajectory solution space. In this framework flexibility is defined in terms of robustness and adaptability to disturbances. For simplicity the framework assumed a single degree of freedom, namely speed. Also in this section metrics for robustness and adaptability are presented. Section 4 presents a method for estimating the robustness and adaptability metrics under simplifying assumptions of discrete time and speed. Furthermore, the impact of constraints is illustrated through analysis of a trajectory solution space with speed variation along the aircraft path, and in simple constraint situations involving meeting multiple times of arrival and resolving a conflict. Sections 3 and 4 are based on material published in [49] and [50]. Section 5

generalizes the metrics definition and estimation methodology to the heading degree of freedom. It also presents an example analyzing a simple scenario with traffic and time constraints. The material in Section 5 is based on material published in [51] and [52]. Section 6 presents an analysis of the impact of trajectory flexibility preservation on traffic complexity based on material published in [52]. In this analysis, the impact of using the robustness and adaptability metrics on traffic complexity is analyzed. Two scenarios are analyzed in two-dimensional en route airspace, where each aircraft must meet a required time of arrival (RTA) in a one-hour time horizon using speed and heading degrees of freedom. Simultaneously, each aircraft preserves its trajectory flexibility, using the defined metrics, to mitigate the risk of loss of separation with the other aircraft. The effects were quantified using traffic complexity metrics based on Lyapunov exponents [40], flow pattern consistency, and proximity. The experiments showed promising results in terms of mitigating complexity as measured by these metrics. Section 7 presents initial thoughts on the constraint minimization function. The research described in this report focused mainly on the trajectory flexibility preservation function. This was intended because this function is more central to testing the hypothesis of the impact of trajectory flexibility preservation on traffic complexity. The constraint minimization function is expected to further increase trajectory flexibility and hence mitigate traffic complexity. This function will be studied more thoroughly in future extension to this research. Section 8 describes a demonstration of the trajectory flexibility function that was implemented in the AOP platform. The algorithms and experiments supporting the research described in this report were implemented and conducted in a MATLAB environment. However, a limited scope functionality was built in AOP for demonstration purposes. Finally conclusions are presented in Section 1 and future work is summarized in Section 10.

# 2 Concept Definition

Figure 2-1 illustrates the allocation of the three functions: separation assurance, trajectory flexibility preservation, and trajectory constraint minimization in the distributed ATM architecture.
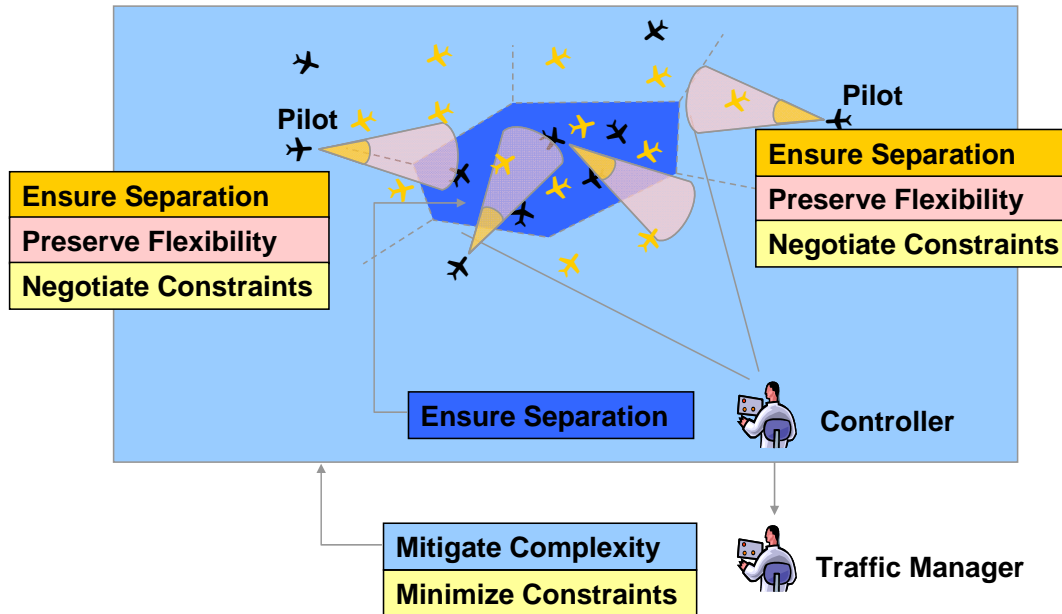


**Figure 2-1 Distributed ATM architecture with separation assurance, trajectory flexibility preservation, and trajectory constraint minimization**

In this mixed-operations, distributed environment, separation assurance is shared between the pilot (for self-separating aircraft) and the air traffic controller (for ground-controlled aircraft) and acts in a time horizon depicted by the shorter cones extending from each aircraft. The flexibility preservation function is a pilot function that complements the pilot's separation assurance function but acts on a larger time horizon as depicted by the extended cone shapes. The constraint minimization function is allocated mainly to the ground based traffic manager to impose just enough restrictions on the aircraft to meet ATM objectives. However, a collaborative role allows the pilot to negotiate constraints with the ground traffic manager. Each of the three key functions, the relationships between them, and their impact on NAS performance indicators such as capacity and complexity, are described next.

## 2.1 Separation Assurance

Separation assurance is the most central function of air traffic control, taking in its time horizon and for safety reasons priority over other functions such as expediting traffic and implementing traffic flow management initiatives. In centralized control, separation assurance is the responsibility of the air traffic controller who monitors and manages aircraft within an airspace volume to maintain the minimum separation requirements. In a distributed control architecture, each aircraft (i.e., pilot/automation system) is

17

responsible for maintaining separation from surrounding traffic. Pilots are assisted in conflict detection and resolution by cockpit automation, such as the AOP system, allowing the pilots to maintain their workload at an acceptable level. As a result of the allocation of separation assurance tasks to pilots, traffic complexity from a centralized perspective (proportional to controller workload and proneness to commit separation violation errors [35] [36] [37] [39]) is reduced because the controller is relieved from the active separation assurance task for self-separating aircraft. In addition, a notion of distributed/automated traffic complexity is introduced that represents the level of proneness to separation violation errors in the new distributed/automated environment. For example, Riley, et al., [45] analyzed a number of factors in terms of how well they represent a pilot's perception of traffic complexity in airborne conflict resolution scenarios. Therefore, traffic complexity may be represented and mitigated differently in a distributed/automated-control environment than in the usual centralized/human-control environment. The premise of the distributed control architecture is that the airspace can accommodate more traffic because the capacity to assure separation is increased through the participation of pilots. Furthermore, as the traffic level increases, the capacity of the NAS in terms of separation assurance increases, because introducing more traffic introduces more pilot decision makers for self separating aircraft, adding scalability of capacity with demand.

Centralized or distributed, resolving predicted separation loss is more critical and required to be more accurate for separation losses that are predicted closer to the current position of aircraft. The further out the predicted loss of separation, the less time-critical their resolution is because prediction is less accurate and the situation is subject to change as time progresses. Separation assurance is, therefore, the most critical function of cockpit automation in the near time horizon taking priority over other functions in this horizon. The strategic separation assurance horizon is typically on the order of tens of minutes. For example, in the current AOP logic, conflict resolution is performed only for conflicts in the next ten minutes from the current aircraft state, and these conflicts are resolved for the next twenty minutes. The separation assurance horizon is depicted as the dark short cone expanding from each aircraft in Figure 2-1.

## 2.2  Trajectory Flexibility Preservation

Trajectory flexibility preservation is envisioned as an airborne function that complements airborne-based separation assurance. The main objective of this function is to plan the aircraft trajectory in a manner that affords the aircraft sufficient flexibility, particularly in preserving its ability to accommodate disturbances. These disturbances may stem for example from other traffic or from weather activity. Flexibility preservation complements separation assurance both within the conflict resolution horizon and outside it within an extended flexibility planning horizon as shown by the extended cone shapes in Figure 2-1.

In the conflict resolution horizon, flexibility is used to select from many conflict resolution solutions one that affords the aircraft more flexibility, for example to adapt to unexpected behavior by the intruder traffic. One example of such behavior is the coincidence conflict situation shown in Figure 2-2. In this situation two separation losses are predicted between two unrelated pairs of aircraft as shown in the left side of the

figure. If the two ownship aircraft maneuvered as shown by dotted lines in the left side of the figure to resolve their respective conflict, without coordination, a new coincidental conflict may arise between them. Although the flexibility preservation function does not explicitly coordinate between the two aircraft, it assists each ownship aircraft in reducing the risk of conflict due to the unpredicted behavior of the surrounding traffic, thus resulting in implicit coordination. Hence with this function, each ownship aircraft may select a more flexible trajectory anticipating the potential behavior of the other aircraft and minimizing the exposure to it. For example, in the right side of Figure 2-2 each of the ownship aircraft decided instead to maneuver away from the other ownship, reducing or eliminating the chance of a coincidence conflict situation.
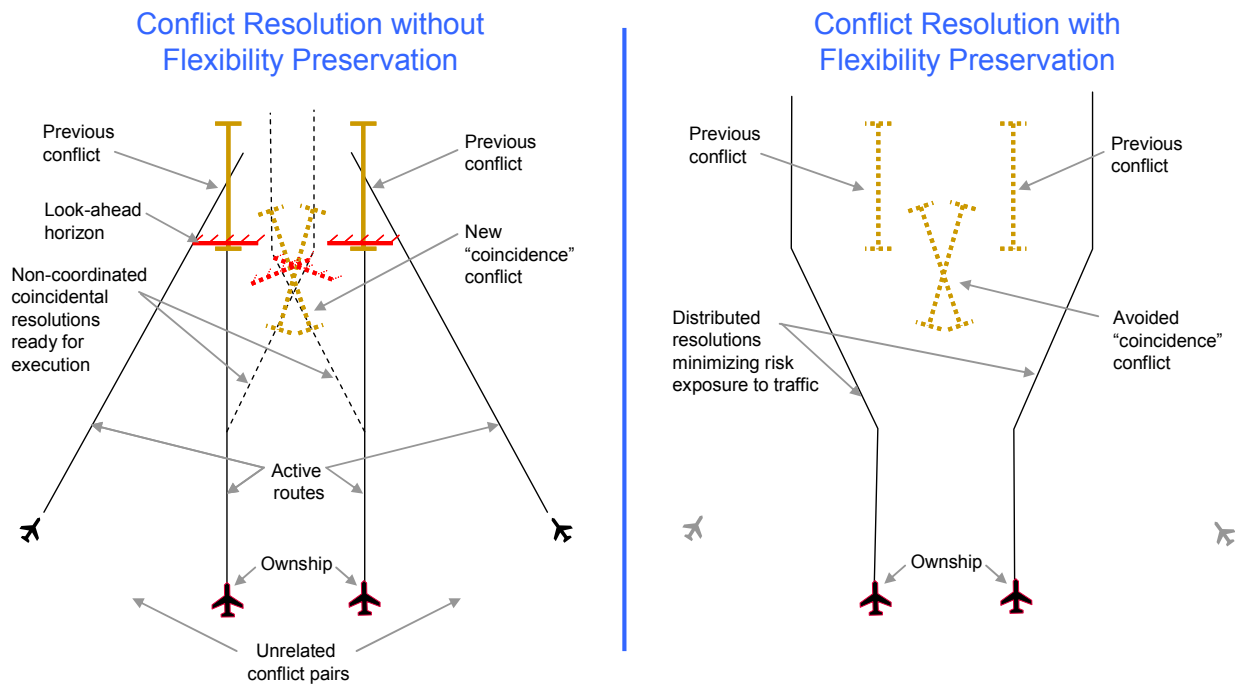


**Figure 2-2 Flexibility preservation avoiding coincidence conflicts**

Outside the conflict resolution horizon and within the flexibility preservation horizon the flexibility preservation function plans the aircraft trajectory to minimize its exposure to disturbances such as weather cells and dense traffic areas. In this long horizon, the possibility of loss of separation is not critical because its prediction is rather inaccurate and does not warrant conflict resolution. While the required separation from the other traffic is not ensured in this horizon, the flexibility preservation function positions the aircraft optimally to reduce the probability of conflict in the future, by minimizing its exposure to weather cells and dense traffic areas. More generally it is hypothesized that the flexibility preservation function results in naturally producing traffic situations that are less complex than without the application of the function.

Figure 2-3 depicts an example involving aircraft maneuvering around convective weather cells. Because of the reduced airspace capacity, aircraft compete for small gaps between the weather cells. On the left side of the figure, each aircraft, while planning its trajectory, assesses its flexibility using a flexibility metric that reflects its exposure to risk and ability to mitigate it. Given the weather and traffic situation, each

aircraft questions whether it should avoid the airspace entirely or modify its trajectory to increase its flexibility. If the aircraft proceeded along their headings as depicted in the left side of the figure, a complex traffic situation arises causing excessive congestion and possibly a high conflict rate in the airspace between the weather cells.

The right side of the figure displays a more structured and streamlined traffic pattern that is hypothesized to result if each aircraft made a decision to increase its flexibility – by limiting its exposure to congestion and proximity to the other traffic and the weather cells. Because the flexibility preservation function results in reducing the traffic complexity in the new distributed environment, the ground controller workload is also reduced, while performing monitoring and supervision roles, as the traffic is more structured and the chance of conflict is reduced.
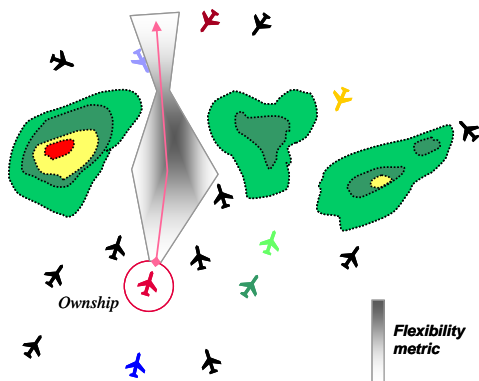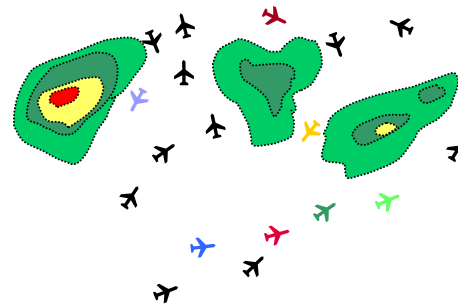


**Figure 2-3 Flexibility preservation avoiding complex traffic situations**

The size of the flexibility planning horizon depends on a number of factors. One important factor is the range of traffic information that is available to an aircraft. If cockpit information about the surrounding traffic is based only on direct ADS-B reception, then the horizon may be limited by the ADS-B reception range. If information is up-linked from the ground then flexibility planning may be available over a greater range, ultimately extending to the destination of the aircraft.

## 2.3 Trajectory Constraint Minimization

Trajectory constraint minimization is envisioned as primarily a ground-based function, with a possible collaboration role for the pilot, as was shown in Figure 2-1. An aircraft trajectory is continually planned to abide by a set of constraints that are imposed on it to achieve ATM objectives. For example, to achieve the objective of safety with respect to collision, an aircraft 4D state should not be within 5 miles and 1000 feet from another aircraft 4D state at any time. In addition, to meet flow management objectives an aircraft is often required to maintain an increased spacing from other aircraft in the same flow or

to absorb a certain amount of delay on the ground or in the air. Constraint minimization is a function by which a traffic manager reduces the amount of constraints imposed on aircraft trajectories to the extent possible without jeopardizing the intended ATM objectives. This is accomplished by imposing just enough constraints to meet the objective; for example, if a single required time of arrival (RTA) at a specified fix will sufficiently meter the traffic flow, multiple RTAs per aircraft are deemed too excessive and hence candidates for relaxation. Such constraint minimization has benefits in terms of more efficient utilization of NAS resources; but it also affords pilots more flexibility as it increases their ability to maneuver freely, with fewer constraints, to accommodate disturbances. Therefore, while constraint minimization is a function performed mainly by the ground-based traffic manager, who has the ability to monitor and achieve ATM objectives that involve a large number of aircraft, the pilot may negotiate constraint reduction from the cockpit perspective. For example, the pilot may determine that certain constraints cannot be met with enough flexibility, and hence may provide useful information to the traffic manager to determine how to adjust the constraints.

Figure 2-4 shows an example demonstrating the hypothesized role and impact of constraint minimization with respect to trajectory flexibility preservation and hence traffic complexity.
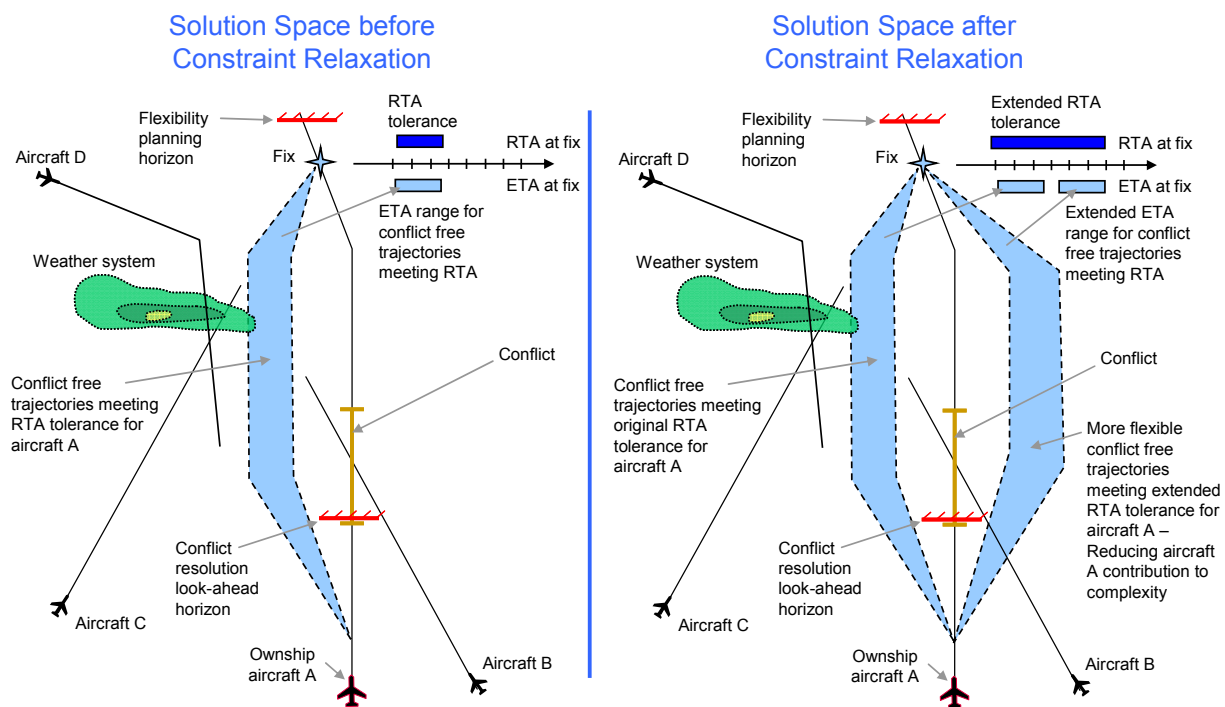


**Figure 2-4 Constraint minimization example – relaxing RTA tolerance**

Aircraft 'A' attempts to plan its trajectory to resolve a predicted loss of separation with aircraft 'B' and at the same time to meet an RTA at a downstream fix. The RTA tolerance initially allows aircraft 'A' to avoid the conflict only by stretching its path to the left, which exposes the aircraft to nearby traffic (Aircraft C and D) and to an inclement weather system (left side of figure). The aircraft has to select from a small set of trajectories (represented by the left-hand shaded region) with expected time of arrival

(ETA) at the fix that lie within the RTA tolerance. These trajectories do not afford the aircraft enough flexibility to accommodate disturbances from the weather and the traffic, and they would increase the contribution of aircraft 'A' to traffic complexity. With this information or independently, the traffic manager relaxes the RTA constraint by increasing the allowable tolerance in meeting it as shown in the right side of the figure. This is done having determined that the ATM objectives intended by the RTA can still be met sufficiently with the increased tolerance. With the extended RTA tolerance, more trajectory solutions become available to aircraft 'A', which is now able to avoid the predicted conflict by maneuvering to the right with no risk exposure to the weather or nearby traffic. As a result, by selecting a more flexible trajectory with less exposure to disturbances from weather and traffic, the contribution of the aircraft to traffic complexity is reduced. In addition, the aircraft is enabled to more reliably meet its RTA constraint and hence achieve the intended ATM objectives.

The constraint minimization function assesses the effectiveness of the constraints imposed on aircraft trajectories in achieving the intended ATM objectives. As shown in Figure 2-5, this is a hierarchical process. ATM objectives are posed at the highest level in abstract terms such as maintaining safety, stability, equity, efficiency, cost-effectiveness, among others. Each high level goal is then mapped into trajectory constraints and objectives that establish the criteria needed to meet the goal. For example, to maintain stability, demand is balanced with capacity; otherwise delays grow unstable. The constraint minimization function assesses if it is possible to relax the demand-capacity balance, for a short duration, without jeopardizing stability. This is done if needed, for example, to accommodate aircraft flexibility needs. Then as shown in Figure 2-5 balancing demand and capacity forms an intermediate goal that results in imposing lower level constraints and objectives on aircraft trajectories. For example, a flow management program may impose on an aircraft meeting an RTA at a fix to achieve the demand-capacity balance. The constraint minimization function then assesses if it is possible to relax the RTA constraint without jeopardizing the balance. One possible method to accomplish this is swapping RTAs between aircraft which does not impact the demand rate but may accommodate aircraft needs. Another example is increasing the tolerance for meeting the RTA (as described in Figure 2-4) or removing redundant RTA constraints at certain locations while keeping them at critical locations.
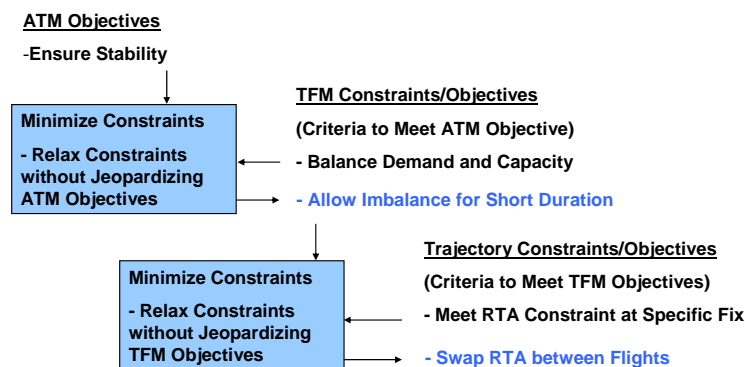


**Figure 2-5 Constraint minimization hierarchy example**

## *2.4 Functional Analysis*

In order to realize the concepts described above, a functional analysis is conducted to identify key functions and the information flow between them. Figure 2-6 depicts a diagram of the key functional blocks and information flows for the three main functions: separation assurance (A), flexibility preservation (B) and constraint minimization (C). The functional relationships depicted are abstractly independent of the allocation/sharing of functions between the air or ground agents. However, for this discussion the allocation proposed above is assumed.

At the heart of the functional diagram in Figure 2-6 is a trajectory generation engine. It generates a trajectory for an aircraft given as input the set of all constraints imposed on it, some by cockpit concerns and some from controllers, traffic managers and company operators. Both the airborne and the ground systems may contain a trajectory generation engine to support their functionalities. The diagram separates inputs to trajectory generation coming from the separation assurance function, the flexibility preservation function, and the constraint minimization function.
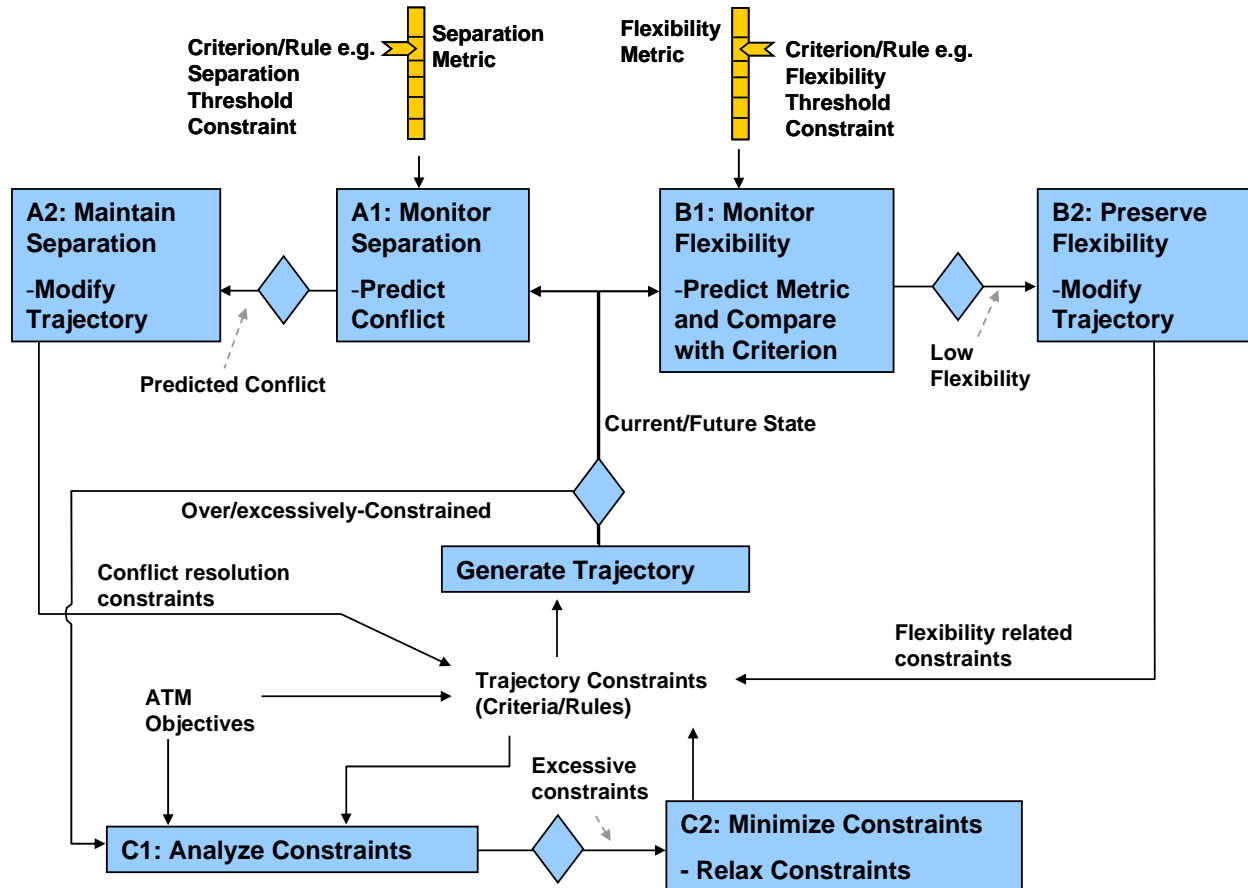


**Figure 2-6 Functional framework**

To simplify the analysis, each function is divided into only two components, a monitoring/assessment component to identify the need for action and a solution/action component to select a solution and implement it. The separation assurance function monitors the current and predicted future states of all aircraft within its horizon and

predicts loss of separation based on the separation requirement criteria (A1 in Figure 2-6). The metric is the estimated separation between aircraft and the criteria are the separation requirements which are well established for ground-based control for each type of airspace and aircraft. (For example, the separation requirements are: 5 miles horizontally or 1000 feet vertically for the en-route airspace.) If a loss of separation is predicted, the separation assurance function selects a conflict resolution solution (A2) and sets the corresponding constraints (conflict resolution advisories) to the trajectory generation engine. This is performed on board by a cockpit system like AOP and/or on the ground by a controller decision support tool like the En-route Descent Advisor (EDA) [6].

Similarly the onboard flexibility preservation function monitors the current and future states of the aircraft and of all aircraft within its horizon and predicts a flexibility metric that measures the risk exposure of the aircraft to disturbances such as from weather and traffic (B1). It compares this measure to criteria that dictate an acceptable level of flexibility. Based on this assessment, if the predicted flexibility is low, the flexibility preservation function selects more flexible solutions (B2) and advises the trajectory generation engine by setting the corresponding constraints and objectives. Unlike the classical separation assurance function, the flexibility metrics and criteria are not well established and are the main subject of this report and ongoing research. Preliminary investigations will be discussed in the next sections and more mature results will be presented in follow-on reports and papers.

Finally, the ground-based constraint minimization function monitors the constraints imposed on aircraft trajectories for the aircraft within its horizon, and analyzes their effectiveness in achieving the intended ATM objectives (C1). If opportunities to reduce constraints without jeopardizing the intended objectives are identified, these constraints are relaxed (C2) and conveyed to the trajectory generation engine. In this mode the constraint minimization function is continuously performed by the ground-based manager/automation identifying opportunities to reduce constraints and afford aircraft more flexibility as long as the ATM objectives are sufficiently met. Action to minimize constraints may also be invoked from the aircraft. An aircraft may determine that its flexibility is insufficient and can only be increased by relaxing certain constraints imposed on it. This may occur if an aircraft is either overly constrained or excessively constrained. An overly constrained aircraft is one that cannot find a feasible trajectory that meets all the constraints imposed on it, in which case the trajectory generation fails. An excessively constrained aircraft is one that can find feasible trajectories but ones that are not sufficiently flexible, in which case the flexibility preservation function may indicate a need to relax certain constraints. In such cases the aircraft may invoke the ground-based function to attempt to relax certain constraints with recommendations from the aircraft as shown in Figure 2-6. The multiplicity of the constraints and their types also gives rise to a prioritization among them, which is important when the aircraft is unable to meet all of the constraints. For example, if the aircraft is over-constrained, it may report to the ground-based traffic manager that it is unable to meet an RTA ("Unable RTA") because of a conflict. In this case the traffic manager may relax the RTA constraint ensuring safety at the expense of less important objectives.

# 3  Definition of Trajectory Flexibility and Metrics

In order to define trajectory flexibility and develop metrics and methods for trajectory flexibility preservation and constraint minimization, these notions are posed in the framework of an aircraft trajectory solution space. A trajectory of an aircraft is generated by selecting values for its degrees of freedom over a time horizon. This trajectory is required to abide by a set of constraints that are imposed to achieve certain ATM objectives such as maintaining separation requirements and balancing demand and capacity. Therefore, these constraints define a solution space consisting of the set of feasible trajectories that abide by the constraints. Out of these trajectories the aircraft selects one that optimizes its preferences, which include minimizing fuel burn, delay, and passenger discomfort. Here, the aim is to develop metrics that support selecting a trajectory that preserves flexibility and identifying constraints that may be relaxed without jeopardizing the intended ATM objectives. To provide context, first an example solution space is formulated for an aircraft with only speed as a degree of freedom and with RTA and conflict constraints. Then trajectory flexibility and relevant trajectory characteristics are defined using the example for demonstration.

## 3.1  Trajectory Solution Space with Multiple RTA and Conflict Constraints

A trajectory is represented by a 3-dimensional path (s) and a speed profile (V(s)) that determines the time (t(s)) at each location along the path. Using this representation, Figure 3-1 depicts a simple scenario of a single aircraft required to meet an RTA at a distance d along its path s, as shown in the right side of the figure. The RTA is to be met within a given tolerance in time t. The left side of the figure displays the trajectory solution space of the aircraft in an s-t space, assuming speed is the only available degree of freedom. The set of times that are reachable at any distance s are bound by traveling at maximum speed $V_{max}$ and at minimum speed $V_{min}$. This set is reduced by the RTA tolerance requirement at distance d and the set of feasible trajectories is correspondingly reduced as shown in the figure by eliminating the non-feasible region. The non-feasible region consists of the reachable states that, if reached, the full speed range is not effective in meeting the RTA tolerance. The remaining states are feasible in the sense that, if reached, at least one solution using speed exists to meet the RTA tolerance. Any trajectory that contains non-feasible states (such as trajectory B in Figure 3-1) is infeasible in the sense that it violates the RTA constraint and any trajectory (such as trajectory A in Figure 3-1) that does not contain any non-feasible states is feasible. The set of feasible states is the convex hull bound by straight lines with slopes $V_{min}$ and $V_{max}$ drawn from the current state, a straight line with slope $V_{max}$ drawn through the later RTA tolerance end, and a straight line with slope $V_{min}$ drawn through the earlier RTA tolerance end, as depicted in Figure 3-1.
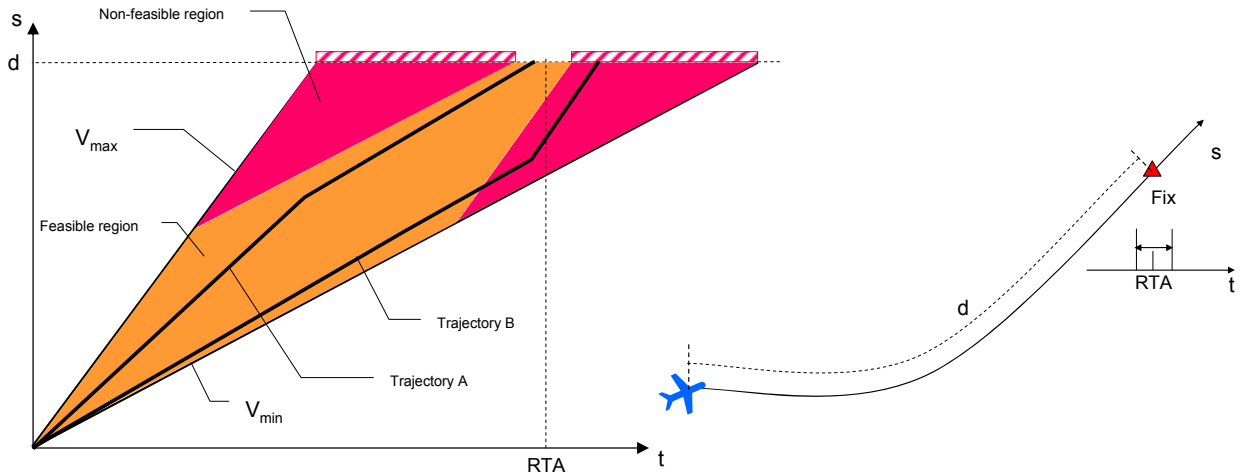
**Figure 3-1 Solution space with single RTA constraint and speed DOF**

Imposing more constraints further limits the trajectory solution space of the aircraft. For example, Figure 3-2 shows the effect of adding a second RTA constraint ($RTA_2$) at distance $d_2$ in addition to a constraint $RTA_1$ at $d_1 > d_2$, along another aircraft path $s_1$. $RTA_2$ may result from a congestion region at distance $d_2$ along $s_1$. On the other hand, path $s_0$, for example, does not go through such congestion and its solution space would be as depicted in Figure 3-1. The feasible region of the solution space along $s_1$ is reduced dramatically (relative to the solution space along $s_0$) to the set of trajectories that meet both RTA tolerances. For example, trajectory B which would be feasible in terms of meeting $RTA_1$ becomes infeasible if $RTA_2$ is imposed because it does not meet $RTA_2$.
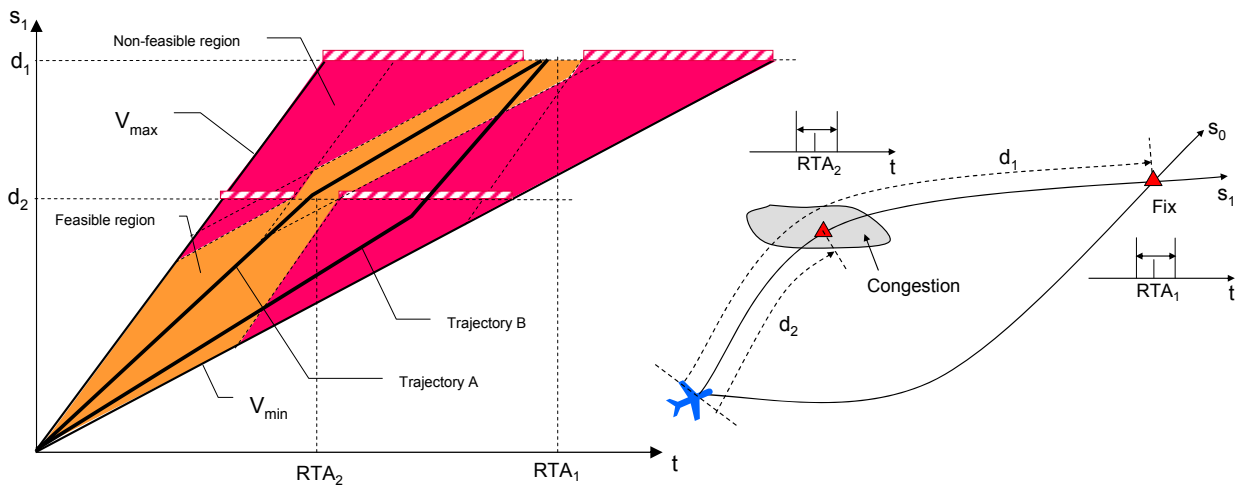


**Figure 3-2 Solution space with multiple RTA constraints and speed DOF**

As depicted in Figure 3-2, the feasible region is the union of the feasible regions between the current state and the first RTA and between each successive pair of RTAs. The feasible region between two successive RTAs is the convex hull between the following lines: Straight lines with slope $V_{max}$ drawn through the earlier tolerance end of the earlier RTA and the later tolerance end of the later RTA, straight lines with slopes $V_{min}$ drawn through the later tolerance end of the earlier RTA and the earlier tolerance

26

end of the later RTA, and horizontal lines drawn at the distances $d_1$ and $d_2$. If the location of RTA$_2$ in Figure 3-2 is shifted to the right or left over time, or its tolerance is reduced, it is possible that no trajectories would be available that meet both RTA$_1$ and RTA$_2$. This occurs when no feasible region connects the aircraft current position to the destination RTA$_1$. In this case the aircraft trajectory is over-constrained as mentioned in Section 2.4 and successful resolution requires relaxation of some constraints. Therefore, as Figure 3-2 demonstrates, relaxing an RTA constraint by, for example, increasing the tolerance or changing the timing has a clear impact on opening up solution space and allowing more feasible trajectories, as was hypothesized by the example in Figure 2-4.

Figure 3-3 adds to the examples above a conflict with an intruder aircraft B (which may also represent a moving weather cell). Along $s_0$ the aircraft is required to meet RTA$_1$ at distance $d_1$ within a tolerance in time, and in addition $s_0$ is impacted by the intruder aircraft B whose separation zone is expected to cross $s_0$ between distances $d_3$ and $d_4$. The geometry and timing of the conflict translates into an elliptical region in the $s_0$-t domain with all points within corresponding to loss of separation. A trajectory that crosses this region loses separation with the intruder and is hence infeasible.[1] As shown in Figure 3-3 the conflict cuts out an additional infeasible region bound by the $V_{max}$ and $V_{min}$ tangents to the elliptical conflict region [53]. Trajectory B is infeasible because of loss of separation with the intruder aircraft while trajectory A is feasible being conflict free and meeting RTA$_1$.

Imposing more constraints further limits the trajectory solution space of the aircraft. For example, along $s_1$ the aircraft is required to meet two RTA constraints within tolerance: RTA$_2$ at distance $d_2$ because of a congestion region, and RTA$_1$ at $d_1 > d_2$, in addition to the impact of the conflict between $d_3$ and $d_4$. For convenience, the geometry in the figure is chosen such that $d_1$, $d_3$, and $d_4$ are equal along $s_0$ and $s_1$. As shown in the diagram at the bottom of Figure 3-3, the solution space is smaller than that along $s_0$; trajectory B is infeasible because of loss of separation with the intruder aircraft or not meeting RTA$_2$ while trajectory A remains feasible by meeting both RTAs and maintaining separation.

---

[1] Idris et al, gives a mathematical formulation of the conflict region for a circular separation zone around an intruder aircraft moving at a constant ground speed across a straight line $s_i$ [53]. The formulas are reproduced in the appendix for reference. In words: The separation zone intersection with the straight line $s_i$ it crosses forms a line segment along $s_i$. The segment starts as a point when the zone first touches $s_i$, grows in size to the diameter length and shrinks to a point when the zone leaves the path $s_i$.
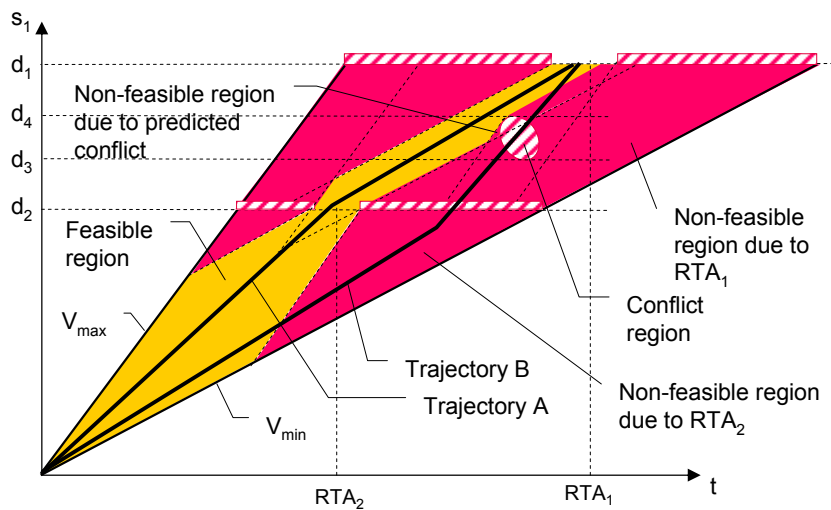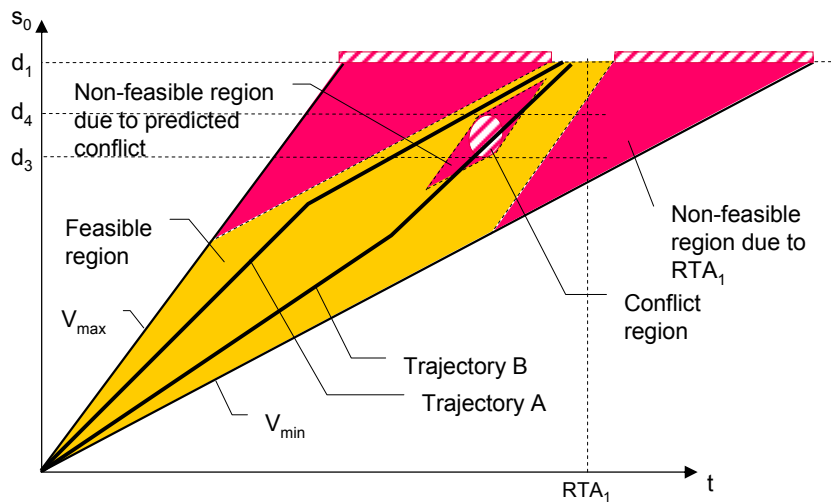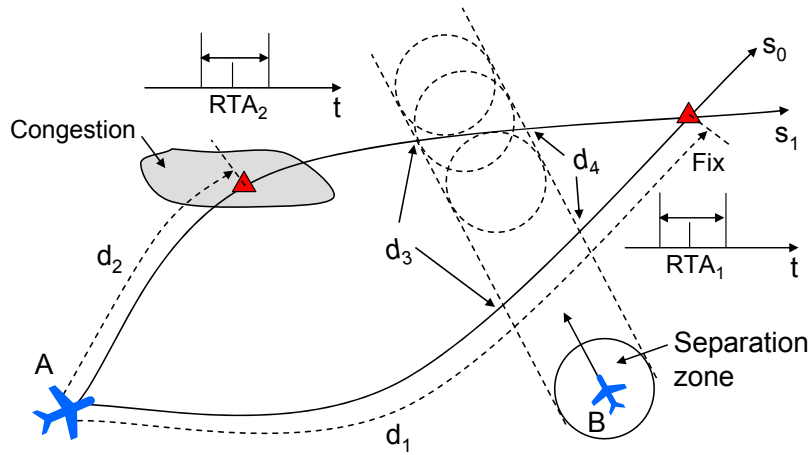
**Figure 3-3 Solution space with RTA and conflict constraints and speed DOF**

The locations and tolerances of RTA$_1$, RTA$_2$ or the conflict region in Figure 3-3, may leave no feasible trajectory that is conflict free and meets both RTAs. In this case the aircraft trajectory is over-constrained and resolution requires relaxation of some

constraints. This example demonstrates how the introduction of additional constraints, such as RTAs and conflicts, reduces the maneuverability of the aircraft by blocking out parts of the solution space. Conversely, relaxing these constraints, when possible without jeopardizing the intended ATM objectives, increases the maneuverability and hence flexibility of the aircraft, as was hypothesized in Sections 2.2 and 2.3. For example, removing $RTA_2$ in Figure 3-3 increases the size of the feasible region and reduces the chance that the prediction of the conflict renders the aircraft over-constrained or excessively constrained. The aircraft may also select path $s_0$, which has less probability of encountering the $RTA_2$ constraint, over path $s_1$ to achieve lower exposure to constraints. The multiplicity of the constraints and their types also gives rise to a prioritization among them, which is important when the aircraft is unable to meet all of the constraints. For example, if the aircraft in Figure 3-3 is over-constrained, it may report to the ground-based traffic manager that it is unable to meet $RTA_2$ ("Unable $RTA_2$") because of the conflict. In this case the traffic manager may relax $RTA_2$ ensuring safety at the expense of less important objectives.

## 3.2  Definition of Flexibility as Accommodation of Disturbances

Given the solution space defined in Figure 3-1 to Figure 3-3, the aircraft selects a trajectory that meets all the imposed constraints, if not over-constrained. If the environment is deterministic, the aircraft proceeds along the trajectory as predicted and the aircraft meets its objectives without violating any constraints. However, disturbances may occur that may alter the images depicted in these figures from what is predicted.

The notion of "trajectory flexibility" is defined here as the ability of the trajectory (and hence the aircraft following the trajectory) to abide by all constraints imposed on it while mitigating its exposure to risks that cause violation of these constraints. Examples of these constraints include the speed limits, RTAs, and separation violations, but in general they include any constraints that intend to achieve ATM and aircraft objectives. They define the trajectory solution space as shown in (Figure 3-1 to Figure 3-3). Risk of constraint violation is represented by disturbances that alter the images depicted in these figures causing the aircraft trajectory to violate or potentially violate constraints. Hence, trajectory flexibility represents the ability of the aircraft to accommodate such disturbances while abiding by the constraints.

Disturbances may be classified into state or constraint disturbances as shown in Figure 3-4. State disturbances result in aircraft state deviations along its trajectory. For example, the aircraft may pass through a turbulence region with uncertain wind speed, which results in the aircraft assuming one of many possible ground speeds in this region, some of which may lead to constraint violation introducing such risk. The disturbance may occur unknowingly; however, if partial information about it is available at the time of prediction, it may be predicted with limited accuracy. For example, if limited information about the variation in the wind speed is available at the time of prediction, such uncertainty in wind speed may be modeled as a localized variation on ground speed as shown in Figure 3-4 and hence a variation in the aircraft trajectory prediction over the prediction horizon. Given discrete representation of speed

uncertainty, the trajectory may be modeled by N trajectory instances (traj$_i$) each with probability P$_i$ where $\sum_{i=1:N} P_i = 1$.
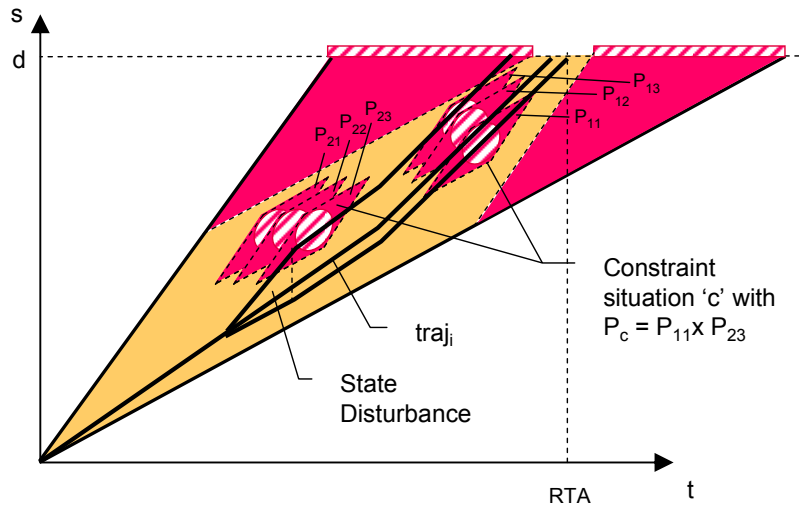


**Figure 3-4 State and constraint disturbances with speed DOF**

Constraint disturbances result in deviations in the constraints that define the aircraft trajectory solution space. They may be new constraints or modifications of currently imposed or known potential constraints. They include many types such as new TFM restrictions or new potential conflicts with traffic or weather cells, of which limited or no information may be available at the prediction time. If some information is available about such disturbances they can be modeled as variations in constraints as shown in Figure 3-4: Assuming discrete representation of the constraint uncertainty, C constraint situations may be predicted each with a probability P$_c$ where $\sum_{c=1:C} P_c = 1$. If each constraint situation c consists of instances of independent constraints, P$_c$ is equal to the multiplication of the individual probabilities of the independent constraint instances. Figure 3-4 shows such an example with discrete probabilistic models of two independent potential conflicts each occurring with three possible instances.

In order to increase its ability to accommodate such disturbances, the aircraft selects out of its solution space a trajectory that affords it sufficient flexibility. Two characteristics have been identified as relevant to measuring flexibility: robustness and adaptability to disturbances. These characteristics are defined and illustrated through an example in analytical terms. The use of the robustness and adaptability characteristics to develop metrics and methods to preserve the flexibility of the aircraft in accommodating different types of disturbances is given in the following sections.

**1. Robustness** is defined as the ability of the aircraft to keep its planned trajectory[2] unchanged in response to the occurrence of a disturbance. A trajectory that can

---

[2] The robustness and adaptability characteristics apply to the full or part of a trajectory plan, such as a path or speed profile.

withstand a disturbance without having to change is more robust than other trajectories that become infeasible when the disturbance occurs. In the context of the RTA/conflict constraint scenario of Figure 3-3 and considering the introduction of the conflict as a disturbance, a trajectory that remains feasible in terms of meeting the tolerances of both $RTA_1$ and $RTA_2$ and avoiding the conflict despite the disturbance, which significantly reduced the solution space, is robust to this disturbance.

**2. Adaptability** is defined as the ability of the aircraft to change its planned trajectory[2] in response to the occurrence of a disturbance that renders the current planned trajectory infeasible. A trajectory that positions the aircraft such that other feasible trajectories remain accessible to it if a disturbance occurred and rendered the current trajectory infeasible is more adaptable than another trajectory for which the disturbance leaves fewer or no feasible trajectories. In the context of the multiple RTA/conflict scenario of Figure 3-3, if trajectory B was selected it becomes infeasible when the conflict is predicted. The conflict reduced the solution space.  However, it left a set of trajectories for the aircraft that are feasible in terms of meeting both $RTA_1$ and $RTA_2$ and resolving the conflict. Therefore, the aircraft is able to adapt to this disturbance over a certain time, for example, by changing its planned trajectory from B to A.

## *3.3  Definition of Trajectory Flexibility Metrics*

Selecting appropriate metrics for measuring flexibility in terms of its two characteristics, robustness and adaptability, ultimately requires generalization to a wide range of situations involving various degrees of freedom and types of disturbances. However, to start, the definition of these metrics are posed in the context of the limited-scope scenario depicted in Figure 3-3, that involves a single aircraft selecting from a set of pre-specified paths to fly between its current position and a destination fix with the ability to vary speed along each path. The aircraft has to meet an RTA at the destination fix regardless of the selected path. Some paths pass through a congestion region which results in a second RTA constraint along these paths at the congestion region. The paths in the scenario may be impacted by one constraint disturbance: a conflict with traffic that crosses the paths.

From an operational perspective, this limited scenario assumes that the aircraft selects a path first and then the speed profile to achieve its objectives. Once the aircraft has selected the path, its only degree of freedom is selecting the speed profile along the path. The decision analyzed here is the selection of the path, where the only objective of the selection is to preserve (or maximize) flexibility (represented by the robustness and adaptability characteristics) in accommodating the conflict disturbance, using the speed degree of freedom. With these assumptions, the decision process is analyzed using initial definitions of metrics that measure robustness and adaptability of each path to the conflict disturbance. It is important to note that this hierarchical decision process may not result in the most flexible trajectory (including path and speed profile). This is because the path is selected first, based on aggregate flexibility metrics, over the set of trajectories that the speed provides along each path. An integrated trajectory selection approach may result in a more optimal trajectory and will be addressed in the generalization to lateral path stretching in Section 5.

In the context of this scenario, the solution space along each path is analyzed in terms of its flexibility to the conflict with the intruder aircraft and meeting the RTA constraint. Figure 3-5 depicts the solution space along a path s that is impacted by an RTA constraint at distance d and a specific instance[3] of the conflict at a location prior to d and a time prior to RTA (as was analyzed in Figure 3-3). The RTA and conflict region divide the solution space into the following regions:
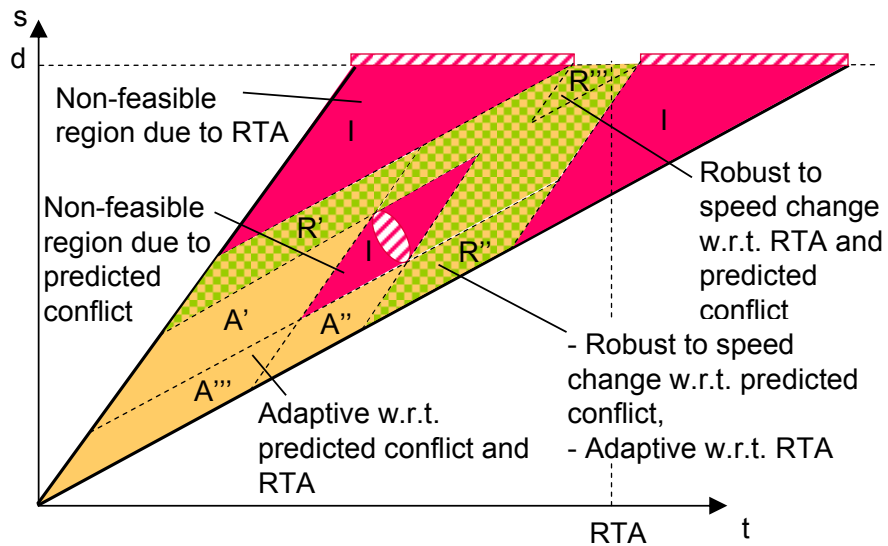


**Figure 3-5 Robust and adaptable states**

1.  Area I consists of the infeasible states which, once reached, violating a constraint (the conflict constraint or the RTA constraint) is unavoidable. These states cannot be part of a feasible trajectory.

2.  Area R consists of robust states which, once reached, constraint violation cannot occur however speed is varied. This region depends on the specific constraint with respect to which robustness is considered. Therefore, R may consist of multiple areas. R' and R" depicted in Figure 3-5 are robust with respect to the conflict but a speed change may still cause violation of the RTA. These states cannot be part of an infeasible trajectory due to the conflict. Area R''' is robust with respect to the RTA and the conflict because any speed change cannot violate either constraint.

3.  Area A consists of adaptable states that may be part of either feasible or infeasible trajectories. Area A is divided into multiple areas in Figure 3-5 indicating which area reaches the R states. States R' can be reached from A' and A''' states, while states in R" can be reached from states in A" and A'''. Therefore, more states can be reached from A''' than from A' or A''.

A <u>robustness</u> metric RBT(traj) is associated with a trajectory (traj) starting from a state (t,s) and ending at another state such as (RTA,d). RBT(traj) is measured with the

---

[3] Other instances correspond, for example, to variability in the intruder aircraft trajectory prediction.

probability of feasibility $P_f$(traj) of the trajectory, which can be estimated with partial information about state and constraint disturbances that represent the risk of constraint violation or infeasibility. Referring to Figure 3-4, with partial information about constraint disturbances and with discrete representation, C constraint situations may be identified each with a probability $P_c$ where $\sum_{c=1:C} P_c = 1$. Similarly, with partial state disturbance information and discrete assumptions of speed and speed change decisions, the trajectory (traj) may be modeled by N instances (traj$_i$) each with probability $P_i$ where $\sum_{i=1:N} P_i = 1$. The probability of feasibility $P_{f,c}$(traj) of the trajectory in a specific constraint situation c is equal to the sum of the probabilities $P_i$ of the set ($F_c$) of trajectory instances traj$_i$ that are feasible in this constraint situation c. Then the robustness metric, RBT(traj), which is equal to $P_f$(traj), is the expected value of $P_{f,c}$(traj) over all constraint situations c of C. This is given in the following two equations, keeping in mind that traj, and hence RBT(traj) can be defined starting from any state (t,s) and ending at any destination state such as (RTA, d):

$$P_{f,c}(\text{traj}) = \sum_{\text{traj}_i \in F_c} P_i$$

$$RBT(\text{traj}) = P_f(\text{traj}) = \sum_{c=1:C} P_c \times P_{f,c}(\text{traj}) \qquad (1)$$

Estimating $P_f$(traj) requires probabilistic models of the state and constraint disturbances. As an example, consider a state disturbance that makes every trajectory from any state (t,s) to the destination e.g., (RTA, d) possible with equal probability. Let N(t,s) be the total number of trajectory instances that start at state (t,s) and end at the destination (in this case (RTA,d)). Note that the number of possible trajectories N varies depending on the state (t,s) at which the trajectory (traj) starts and the state at which it ends (which may be a point such as (RTA,d) or a set of points such as having a tolerance around the RTA). However, the end destination is assumed common among all trajectories that are compared for robustness. Then the probability of each trajectory instance starting at

(t,s) is $P_i(t,s) = \dfrac{1}{N(t,s)}$ and the sum of these probabilities over the set $F_c$ makes

$P_{f,c}(t,s) = \dfrac{f_c(t,s)}{N(t,s)}$ where $f_c$(t,s) is the number of feasible trajectories in the constraint

situation c (i.e., cardinality of the set $F_c$). Finally averaging over the constraint situations C, the following formula can be given for the robustness RBT(t,s) at the state (t,s):

$$RBT(t,s) = P_f(t,s) = \sum_{c=1:C} P_c \times \frac{f_c(t,s)}{f_c(t,s) + i_c(t,s)} \qquad (2)$$

where $i_c$(t,s) = N(t,s) – $f_c$(t,s) is the number of infeasible trajectories in a constraint situation c. Therefore, in this special case, for a common destination, RBT(t,s) may be defined at every state (t,s) representing the start of a trajectory (traj), with all its possible instances from that point to the destination.

An <u>adaptability</u> metric ADP(t,s) is associated with a state (t,s) and is measured by the number of feasible trajectories f(t,s) (with respect to all constraints) that are available for

the aircraft to use at (t,s) to regain feasibility. Figure 3-5 depicts this number at the current state (origin) for a constraint situation (c) consisting of single instances of an RTA and a potential conflict. These constraints divide the total set of trajectories N(t,s) into two mutually exclusive subsets: $f_c(t,s)$ the set of feasible trajectories (with respect to c) which includes all trajectories that lie partially in the regions R (dotted) and $i_c(t,s)$ the set of infeasible trajectories with respect to c which includes all trajectories that lie partially in the regions I (dark). Hence, N(t,s) = $f_c(t,s)$ + $i_c(t,s)$. Then, given the discrete probability $P_c$ of each constraint situation c of C, ADP(t,s) is measured by the expected value of the number of feasible trajectories:

$$\text{ADP}(t,s) = f(t,s) = \sum_{c=1:C} P_c \times f_c(t,s) . \tag{3}$$

Adaptability decreases as the aircraft moves along a trajectory because the number of total trajectories, including feasible trajectories, decreases. This can be seen in Figure 3-5 where the states in area A''' are more adaptable having access to both R' and R'' to adapt to the occurrence of the potential conflict instance, while states in areas A' and A'' are less adaptable having access only to R' or R'' respectively. Once the aircraft is in the shaded regions R' or R'' it is robust to speed changes, with respect to the potential conflict instance shown in Figure 3-5 (since no speed change by state disturbance can result in a conflict and hence the aircraft does not need to adapt to such disturbance). In R' or R'' the aircraft remains adaptive with respect to the RTA (since if a speed change caused its planned trajectory to violate the RTA it can find another speed profile that regains feasibility). Then once the aircraft is in the region R''' it does not need to adapt to speed changes neither with respect to the potential conflict nor with respect to the RTA (since any speed change meets the RTA and is conflict free). Hence, adaptability decreases as the aircraft proceeds transitioning through A''', then from A''' to either A' or A'', then into the shaded regions R' or R'', and finally into the shaded region R'''. Robustness increases as the aircraft proceeds from A to the shaded regions R' or R'' and finally into the shaded region R'''. This can be seen in Equation 2, the special case of robustness to totally random state disturbances: As the number of feasible trajectories (numerator) decreases, the ratio of feasible trajectories to the total number of trajectories increases because the total number (denominator) decreases by infeasible as well as feasible trajectories.

The robustness and adaptability metrics proposed are used in this scenario to compare flexibility among different paths by measuring the set of feasible trajectories that the speed degree of freedom provides along each path. This comparison is used to make a path selection based on properties aggregated over the set of trajectories along the path. The flexibility metric is ultimately used to plan a full trajectory including the heading and the speed profile. This is addressed in the generalization to lateral path stretch in Section 5.

## 3.4  Preliminary Attempts at Analytical Metrics

The calculation of the adaptability and robustness metrics requires estimation of the number of total and feasible trajectories from a state (t,s) to the destination (distance, time, or both). In this subsection, initial attempts at finding a closed-form solution for this

estimate are described. In Section 4, a numerical estimation method is presented making assumptions of discrete time and degrees of freedom. The description uses speed as the only degree of freedom for simplicity.

### 3.4.1 Case with finite time horizon without destination or traffic constraints

The number of feasible trajectories is analyzed for the simplest case with only speed limit constraints. The aircraft flies from a point (t,s) for a time horizon T without any specific destination point at the horizon.

First, the number of feasible trajectories at the point (t,s) is computed assuming that the aircraft makes a finite number of speed changes within the time horizon. For example, the aircraft may be restricted to make speed changes at discrete time instances that are ε apart, between which the speed is maintained constant. In this case the number of changes is (T-t)/ε. Or, the number of speed changes could be set to a finite number N and the timing of changes could be arbitrary.

Each speed change decision is limited to within the minimum and maximum speeds. Therefore, the number of possible speed values at each decision point is equal to the angle $\theta$ between the two lines with slopes $V_{min}$ and $V_{max}$. $\theta = atan(V_{max}) - atan(V_{min})$. It can be seen from Figure 3-6 that the number of trajectories at (t,s) is given by the following equation:

$$f_c(t,s) = \theta^N \quad \text{or} \quad f_c(t,s) = \theta^{(T-t)/\varepsilon}$$

If the assumption of finite number of speed changes is relaxed, the number of feasible trajectories tends to infinity. This can be seen by taking the limit of $f_c(t,s)$ as N tends towards infinity or as ε tends towards zero.

Therefore, the number of trajectories as a metric is ill defined, unless some limitations or assumptions on the operations are imposed. One such limitation is allowing only a finite number of speed changes or a finite duration for each speed decision, as described above. The adaptability metric in this case represents: how many trajectories are available at a point over a time horizon (or to a destination as described next) given a "finite number of maneuverability options" specified by the operational assumption.

This operational assumption may be specified in different manners resulting in different absolute numbers of trajectories at a point. For use in comparative analysis, the operational assumption has to be maintained consistent over the space of solutions that are compared. It amounts to selecting a measurement unit for comparison purposes.
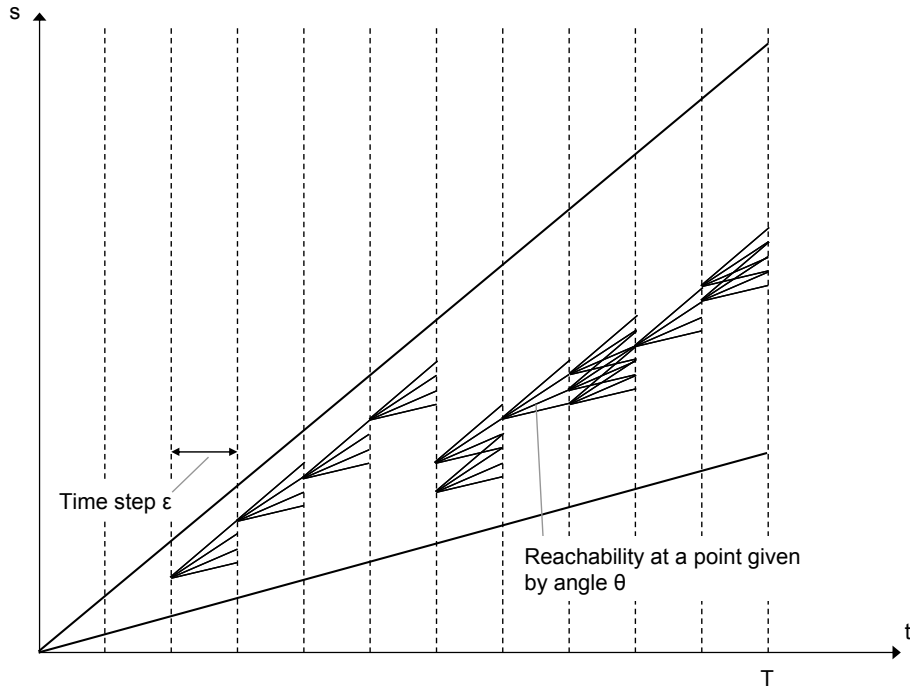
**Figure 3-6 Number of trajectories without destination**

### *3.4.2 Case with point destination constraint*

Adding the constraint of a point destination at the time horizon T, the number of feasible trajectories available at a point (t,s) can be obtained in closed form under restrictive operational assumptions. For example, assume at point (t,s) the aircraft has only one speed change to make before the destination point, while the timing of the change is unlimited. Figure 3-7 shows the geometry of the situation. In this case the number of feasible trajectories available at (t,s) with the aircraft speed at (t,s) being V, is given by the following relationship:

$$f_c(t,s) = | \operatorname{atan}(V_{max}) - \operatorname{atan}((D-s)/(T-t)) | \qquad \text{if } \operatorname{atan}(V) < \operatorname{atan}((D-s)/(T-t))$$

$$f_c(t,s) = | \operatorname{atan}((D-s)/(T-t)) - \operatorname{atan}(V_{min}) | \qquad \text{if } \operatorname{atan}(V) > \operatorname{atan}((D-s)/(T-t))$$

Then this relationship can be used to compute the number of trajectories at a point (t,s) if the aircraft is allowed two speed changes over a time horizon. Figure 3-8 shows the geometry of the situation. An aircraft is able to make two speed changes within a time horizon up to time $T_1 < T$. Then after time $T_1$ up to the horizon T the aircraft has only one speed change.

If the aircraft makes a speed change to a value V at a point (t,s) before $T_1$, then the number of feasible trajectories remaining is given by the above relationship as a function of V, t, and s. Therefore, the number of feasible trajectories available at point (t,s), given a speed change at the point (t,s), is given by integrating the above relationship over the speed range available at (t,s). This integration results in the following formula:

36

**Figure 3-7 Number of trajectories with one speed change and point destination**
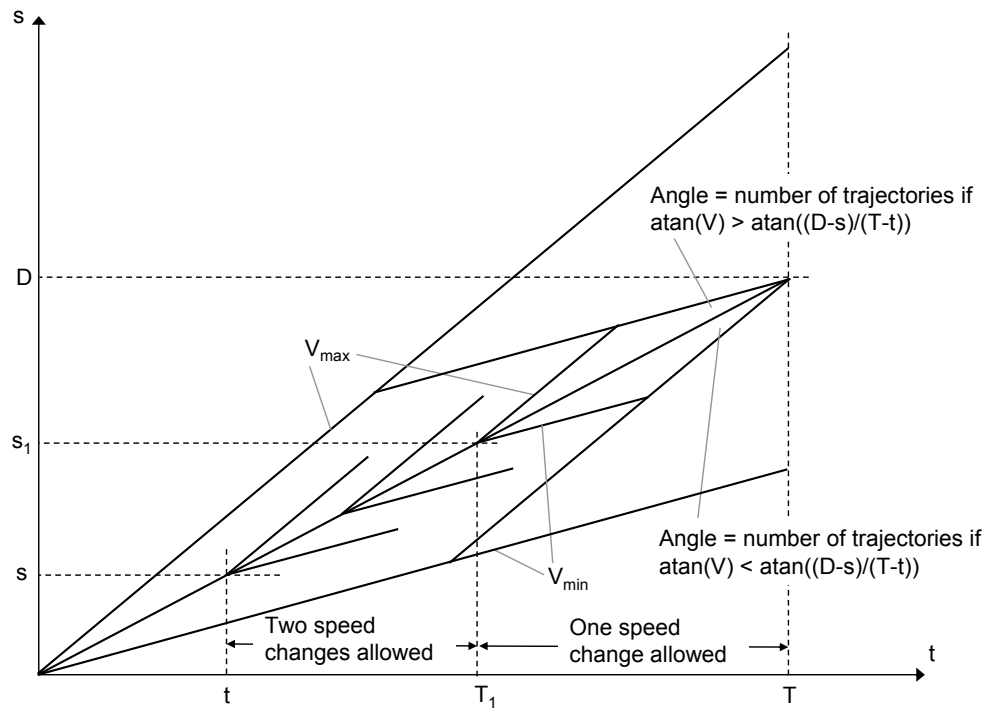


**Figure 3-8 Number of trajectories with two speed changes and point destination**

$$f_c(t,s) = \int_{\mathrm{atan}(V_{min})}^{\mathrm{atan}(\frac{D-s}{T-t})} \{\mathrm{atan}(V_{max}) - \mathrm{atan}(\frac{D-s}{T-t})\} d\theta + \int_{\mathrm{atan}(\frac{D-s}{T-t})}^{\mathrm{atan}(V_{max})} \{\mathrm{atan}(\frac{D-s}{T-t}) - \mathrm{atan}(V_{min})\} d\theta$$

Since s and t are constants in this equation, the result is:
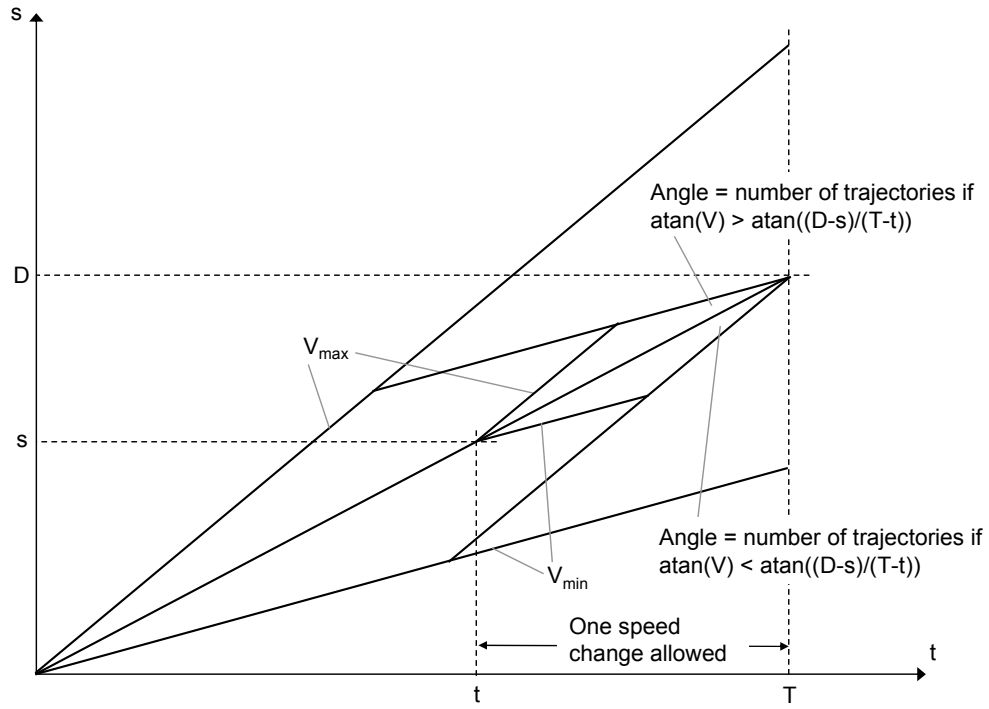
$$f_c(t,s) = \{\mathrm{atan}(V_{max}) - \mathrm{atan}(\frac{D-s}{T-t})\}^2 + \{\mathrm{atan}(\frac{D-s}{T-t}) - \mathrm{atan}(V_{min})\}^2$$

If the speed change is not to occur at (t,s), then the number of trajectories at (t,s) is the integral of this relationship over the line $s_1$-s=V($t_1$ – t), where V is the speed at point (t,s), substituting in the equation above s = $s_1$ = s + V($t_1$-t) and t = $t_1$, and varying $t_1$ starting at t and ending at $T_1$. This integration involves integrating the square of atan, and can be performed using substitution and integration by parts.

Generalizing to N speed changes, this method reduces to a series of integrations over successive horizons, the first allowing N speed changes, the next N-1 speed changes, then N-2 speed changes, and so on up to final horizon allowing only one speed change. While the final few horizons allowing few speed changes may be computed using analytical relationships, the overall integral would require numerical techniques. This approach has not been carried further. Section 4 presents a numerical technique that estimates the number of trajectories using a further restriction on the speed change locations to be at specific time increments.

### 3.4.3 Case with hazard and traffic constraints

When there are traffic or hazard areas, the number of feasible trajectories has to exclude those infeasible trajectories that cross such areas. In the method described above, this is accomplished by performing the integrations over ranges that are feasible. This requires identifying the ranges of angles (speeds) and line segments that intersect such areas. Since these areas are determined geometrically, this can be achieved analytically. However, this analytical approach has not been carried out.

# 4 Estimation of Trajectory Flexibility Metrics using Speed

The calculation of the adaptability and robustness metrics requires estimation of the number of total and feasible trajectories from a state (t,s) to the destination (distance, time, or both). A method is described in the following subsection that estimates this number under assumptions of discrete time and speed. Then an example is given to demonstrate the use of this estimate in trajectory planning.

## 4.1 Estimation Method using Discrete Time and Speed

A method is described in this section that estimates the number of trajectories under the two following simplifying assumptions:

(1) Speed change can only occur at specific discrete instances in time that are $\varepsilon$ apart. Within each time increment the speed is maintained constant.

(2) Speed can take only discrete values $V_i$ between $V_{min}$ and $V_{max}$.

In addition to simplifying the estimation method, these assumptions are reasonable from an operational point of view considering the intended application of the trajectory flexibility metrics. Namely, the metrics are intended for relative comparison of trajectories over a long time horizon suitable for strategic planning (typical of traffic flow management planning horizon) as opposed to tactical maneuvering (where the dynamics of the speed change are relevant).

Under these assumptions, the number of trajectories may be estimated using a convolution and filtering technique. Figure 4-1 demonstrates this method for calculating the number of feasible trajectories $f_c(t,s)$ from any point (t,s) to a time horizon in a constraint situation c that includes an RTA with a tolerance in time and an instance of a potential conflict. The time dimension is discretized into time steps $\varepsilon$-apart. The function $f_c(t,s)$ is estimated for each time step starting from the last time step and proceeding backwards, as follows. Assume the function $f_c(t_j,s)$ at time t = $t_j$ is known. The function $f_c(t_{j-1},s)$ at the previous time step t = $t_{j-1}$ can be obtained by convoluting $f_c(t_j,s)$ and the function $g_k(s)$, which represents the number of trajectories that reach from a point k=($t_{j-1}$,s(k)) at time step $t_{j-1}$ to the next time step $t_j$. The function g is independent of time because of the discretization assumptions. Because of the assumptions of discrete speed values and constant speed between two time steps, there is only one trajectory that reaches from the point k at time step $t_{j-1}$ to each of a set of discrete s-values at time step $t_j$ – each location corresponds to one of the allowable discrete speed values $V_i$ between $V_{min}$ and $V_{max}$. Therefore, the reachability function $g_k(t,s)$ is given by:

$$g_k(t,s)=1 \qquad at \quad (t,s)\in \{(t,s(k)+V_{min}\times\varepsilon,\cdots,(t,s(k)+V_i\times\varepsilon,\cdots,(t,s(k)+V_{max}\times\varepsilon\}$$

$$g_k(t,s)=0 \qquad elsewhere$$

(4)
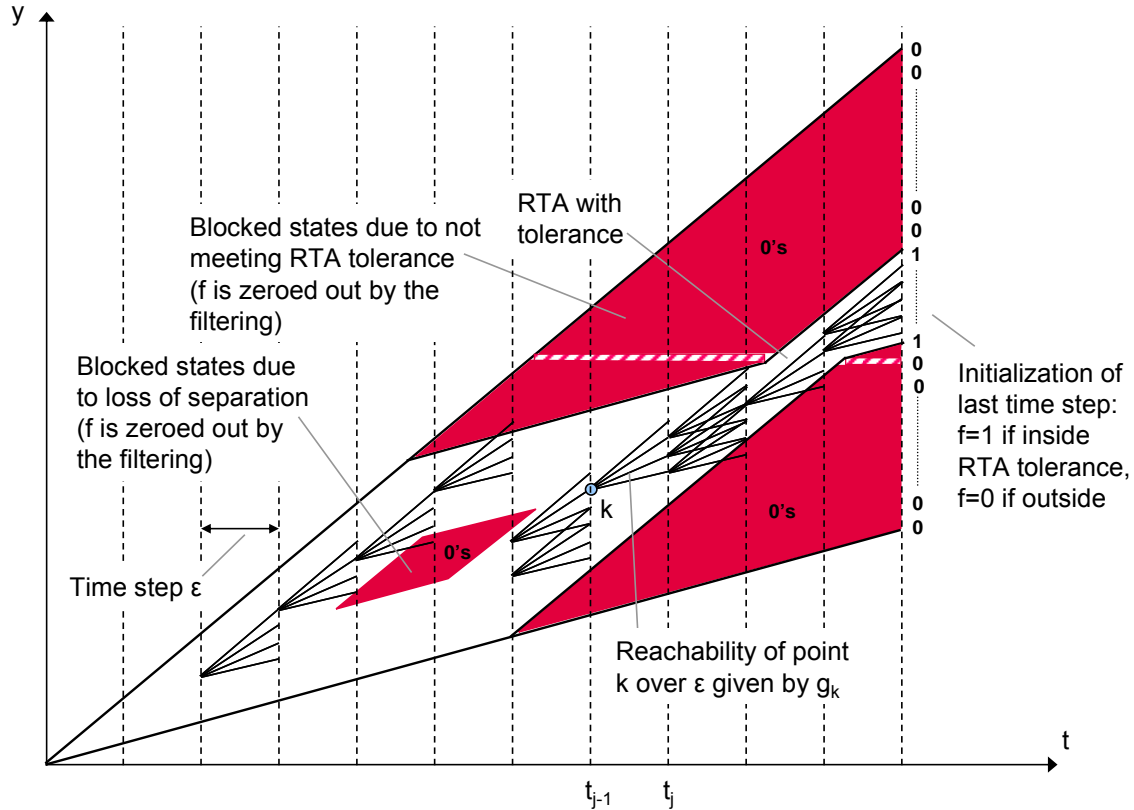
**Figure 4-1 Estimation of number of feasible trajectories with speed DOF**

This convolution operation amounts to calculating $f_c(t_{j-1},s(k))$ at point k by multiplying the values of $f_c(t_j,s)$ by the number of trajectories that reach from point k to $(t_j,s)$ and adding them, and then repeating the operation for each point k along s at time step $t_{j-1}$. Therefore, calculating $f_c(t_{j-1},s(k))$ at every point k along s at time step $t_{j-1}$ amounts to adding the values of the function $f_c(t_j,s)$ that overlap the non-zero part of the function $g_k(s)$. However, if the point k is infeasible (falling in area I of the solution space) then $f_c(t_{j-1},s(k)) = 0$. This requires a filtering step before each convolution operation to zero out the values at infeasible states. Substituting a dummy variable τ to denote sliding the point k along s, the function $f_c(t_{j-1},s)$ is given by the following equation, representing convolution and filtering for infeasibility:

$$f_c(t_{j-1},s) = \sum_\tau f_c(t_j,\tau) \times g(s - \tau) \quad \text{if } (t_{j-1},s) \text{ is feasible}$$

$$f_c(t_{j-1},s) = 0 \quad \text{if } (t_{j-1},s) \text{ is infeasible}$$

(5)

This operation is applied starting from the final time step $(t_f)$ and proceeding backwards to the current state (or origin). The initialization of the final time step is achieved by setting at the final time step $f_c(t_f,s) = 1$ at the feasible states and zero elsewhere as shown in Figure 4-1 (in this case infeasibility is due to not meeting the RTA tolerance). After this initialization/filtering of the final time step, the convolution operation is applied to calculate $f_c(t_f-ε,s)$.

This estimation process is repeated for each constraint situation c. Then, the estimates $f_c(t,s)$ in each constraint situation c are averaged over all constraint situations C to

obtain the adaptability or robustness metrics under probabilistic models of disturbances as described in Equations (1), (2) and (3). To compute the robustness metric RBT (Equation 2), the constraints with respect to which robustness is computed are excluded from the filtering process when computing the total number of trajectories N(t,s) used in the denominator while they are included in the filtering process when computing the numerator.

The convolution operation produces an exponential growth of the number of feasible trajectories $f_c(t,s)$ backwards with time, where the highest number of trajectories is at the current state and it decreases with time towards the destination. This depicts the decrease of adaptability with time. The infeasible regions eliminate trajectories as the function $f_c(t,s)$ is zeroed at infeasible states in each step before proceeding to the previous step. This filtering produces troughs or valleys in the function $f_c(t,s)$ depicting the impact of constraints. The larger the impact of a constraint is, the larger the resulting trajectory elimination. This behavior is demonstrated in the example shown in Figure 4-2 which depicts an implementation of the estimation algorithm in MATLAB. This example consists of an aircraft with two RTA constraints, one without tolerance at (30 min, 150 nmi) and one with 2-min tolerance to reach 50 nmi between 9 and 11 minutes. In addition, the aircraft path is impacted by a potential conflict with an intruder aircraft. The potential conflict may occur at three possible locations due to variation in the speed of the intruder aircraft of (290, 300, 310) kts with probabilities (.20, .35, .45), respectively. Figure 4-2 shows in the t-s plane the trajectory solution space of the aircraft with $V_{min}$ and $V_{max}$ set at 200 and 400 kts, respectively. It also shows, as bars, on a log-scale vertical axis, the average number of feasible trajectories f(t,s), remaining at each point, estimated with time increments of 2 min and speed increments of 10 kn. Figure 4-2 shows the exponential decline of f(t,s) from the origin towards the destination and the filtering out of trajectories in the troughs caused by the potential conflict region and the RTAs.
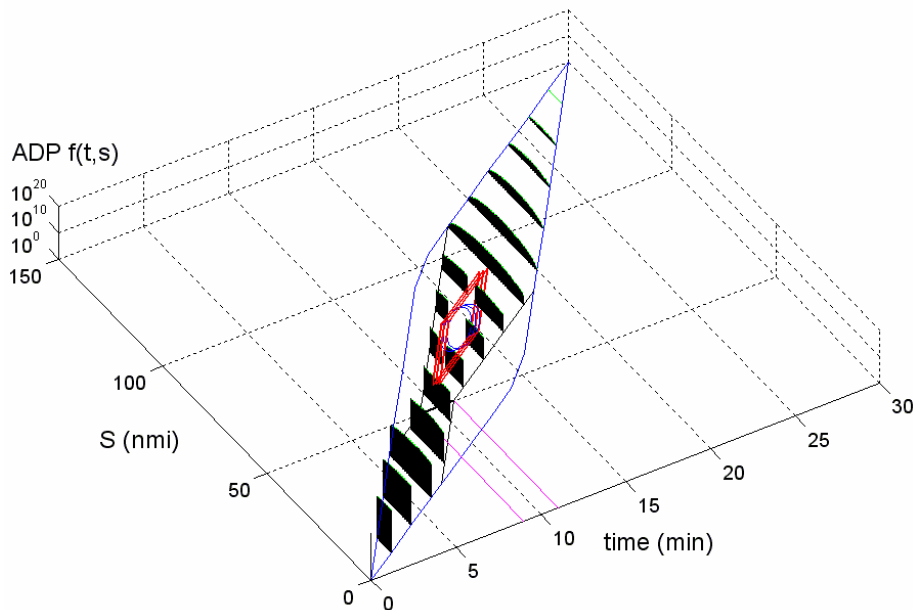


**Figure 4-2 Adaptability estimation example with speed DOF**

Note: An identical convolution/filtering process may be applied in the reverse direction starting from the current state (origin) towards the destination, yielding the number of trajectories (total or feasible) that lead from the origin to each point (t,s). Denoting this number by b(t,s), then for each point to be feasible there should be at least one trajectory to reach it from the current state and at least one trajectory to reach the destination from it. In other words the feasibility condition at a point (t, s) may be written as: $f(t,s) \times b(t,s) > 0$.

## 4.2 Example of Using Metrics for Trajectory Flexibility Preservation

A simple scenario is analyzed to demonstrate how the two metrics used for flexibility, adaptability and robustness described in the previous subsection, can be used in trajectory flexibility planning and constraint relaxation. Preliminary insights are also gained into the hypothesized relationships between such decisions and traffic complexity using a simple indicator of traffic complexity.

### 4.2.1 Analysis Scenario

The scenario analyzed, depicted in Figure 4-3, is a simplified representation of an aircraft (A) planning a trajectory across a stream of traffic to reach a destination fix on the other side of the stream. Only two possible paths are analyzed, $s_1$ and $s_2$, where aircraft A selects one of them and then can vary only speed (between 200 and 400 kts) along the selected path.
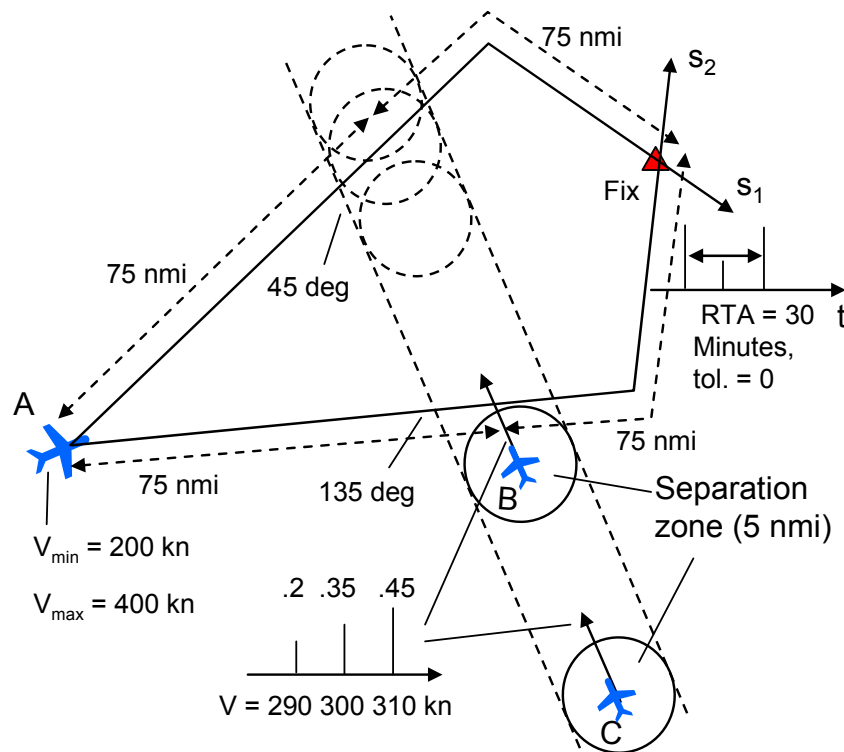


**Figure 4-3 Analysis scenario with speed DOF**

In order to draw the intended insight in this example, everything along the two paths is set to be identical, except for the relative angle (or heading) between aircraft A and the traffic stream crossed: $s_1$ crosses the stream at a relative angle of 45 degrees while $s_2$ crosses it at a relative angle of 135 degrees. Therefore, $s_1$ represents a more aligned direction with the crossed stream while $s_2$ is closer to a head-on situation. Otherwise: Both paths have the same length (150 nmi); both have a single RTA constraint without tolerance at (30 min, 150 nmi); both have a potential conflict centered at (15 min, 75 nmi) $s_1$ with intruder aircraft B and $s_2$ with intruder aircraft C; and both face intruder speed variation of (290, 300, 310) kts with probabilities (.20, .35, .45), respectively. Therefore, the only factor in differentiating between $s_1$ and $s_2$ is the relative heading. This was intended in order to draw insight on the impact of the selection of aircraft A on the orientation of the resulting traffic. The underlying assumption is that if aircraft A selected $s_1$ rather than $s_2$ the resulting traffic situation is more aligned (and less head-on); hence the contribution to traffic complexity is reduced. While traffic complexity involves many other factors, it is assumed here that a more aligned traffic is less complex to manage, everything else being equal.

The selection criterion for the aircraft is to maximize adaptability or robustness, rather than a combination of them, in order to draw insight on the difference between using these two metrics. In a real situation, adaptability and robustness would be traded with each other as well as with other metrics such as fuel efficiency and passenger comfort. Such tradeoffs are a subject for future research. Therefore, the decision criterion for aircraft A is as follows: (1) Aircraft A selects the best speed profile along $s_1$ and $s_2$ based on adaptability (or robustness) and (2) Aircraft A compares these selected speed profiles and selects the path that has the better speed profile based on adaptability (or robustness).

### 4.2.2 Adaptability-Based Trajectory Planning

The adaptability analysis of the scenario is shown in Figure 4-4, using the estimation method of the number of trajectories (Equation 3) with 2-min time increments and 10-kn speed increments. It is clear from Figure 4-4 that the potential conflict along $s_2$ (which is closer to head-on with relative angle of 135 degrees) eliminates many more trajectories than the potential conflict along $s_1$ (which is more aligned with relative angle of 45 degrees). Three-dimensional and two-dimensional views are shown to visually demonstrate the much larger size of the infeasible region due to the 135-degree potential conflict along $s_2$. Also demonstrated in the figure are the three instances of the conflict region due to the three possible speeds of the intruder aircraft with different probabilities. In the 2-dimensional view, the loci of the maximum f(t,s) values are indicated at each time step. An optimum speed profile would attempt to be as close as possible to these maxima while ensuring reachability along the trajectory. There are many algorithmic approaches to find the optimum speed profile, one of which is described in Section 6. For this example, Figure 4-4 shows a feasible speed profile that attempts to stay as close as possible to the f(t,s) maxima starting from the destination point and proceeding backwards to the current state (origin). Most of the optimum points can be connected in the case of $s_1$ while most cannot be connected in the case of $s_2$ further demonstrating the disadvantage of the large conflict region along $s_2$.
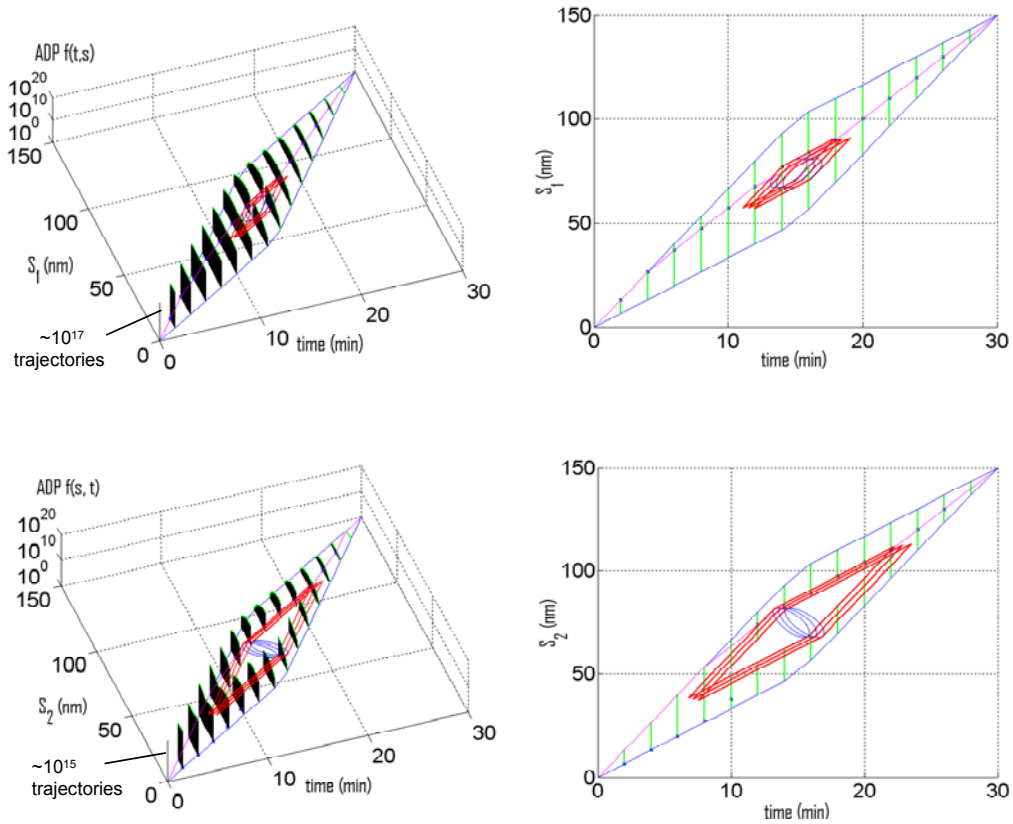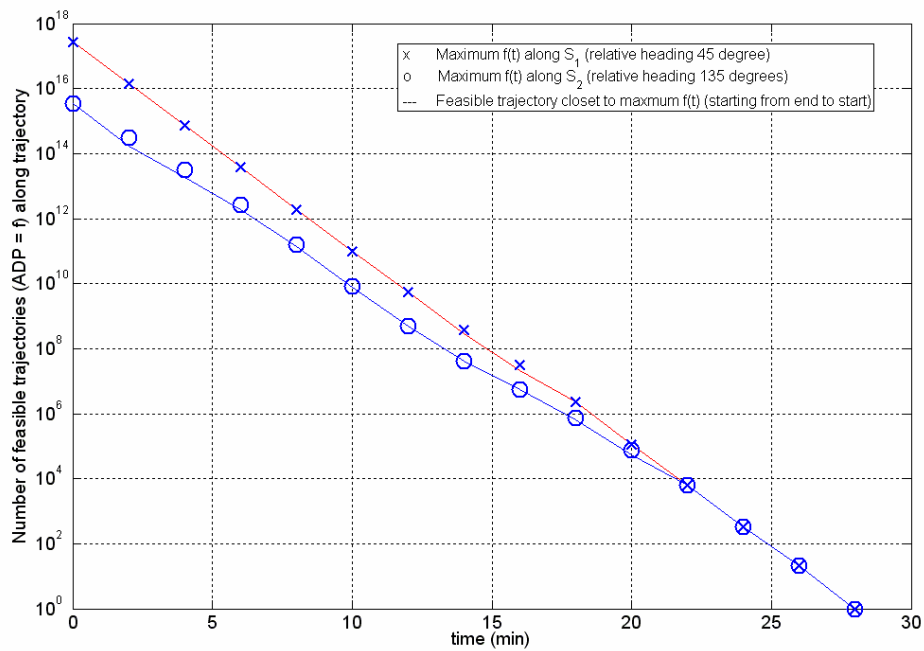
**Figure 4-4 Adaptability analysis with speed DOF**



**Figure 4-5 Route selection based on adaptability with speed DOF**

Figure 4-5 compares the maxima of f(t,s) along $s_1$ and $s_2$ over time. It shows that these maxima along $s_1$, most of which can be connected with a feasible speed profile, dominate their counterparts along $s_2$ at all time steps. This indicates that the most adaptable speed profile along $s_1$ dominates any speed profile along $s_2$, including the one displayed in the figure and the most adaptable. Therefore, aircraft A would select $s_1$ over $s_2$ based on maximizing adaptability. This decision results in a more aligned traffic situation and reduces the contribution to traffic complexity because of increasing traffic alignment.

## 4.2.3 Robustness-Based Trajectory Planning

Figure 4-6 repeats the analysis of Figure 4-4 based on maximizing robustness rather than adaptability, using Equation (2), and assuming totally random state disturbance. For comparability with the analysis of Figure 4-4, in this example, the total number of trajectories N(t,s) allowed by state (speed) variation is limited to the ones that meet the destination (RTA,d). This assumes that meeting the RTA constraint is totally robust to speed changes, and that robustness only with respect to meeting the conflict constraint is considered. The analysis results in a decision similar to the one based on maximizing adaptability, i.e., selecting $s_1$ over $s_2$, because $s_1$ dominates in terms of robustness as well. This is shown further in Figure 4-7 which displays the maximum robustness (ratio) values for both paths and a feasible speed profile that attempts to connect the maxima starting from the destination point backwards. Therefore, the larger conflict region in the case of $s_2$ eliminates a much larger number of total (N(t,s)) and feasible (f(t,s)) trajectories along $s_2$, while keeping their ratio higher for $s_1$ than for $s_2$. Figure 4-6 and Figure 4-7 also demonstrate how robustness (in this special case) increases over time, as opposed to adaptability which decreases over time, reaching a maximum value of 100 percent near the destination. It is also noteworthy that while the adaptively-optimal trajectory tends to stay nearer to the conflict region (maximizing the number of feasible trajectories remaining) the robustly-optimal trajectory tends to stay further away from the conflict region (maximizing the ratio of the feasible trajectories to the total, i.e., minimizing the probability of infeasibility). This highlights the tradeoff between these two metrics. This tradeoff depends on the decision maker's risk attitude. For example, a conservative decision maker may favor robustness to minimize having to accommodate the disturbance. A more risk prone attitude may tolerate a certain chance of having to accommodate the disturbance as long as there is sufficient adaptability.
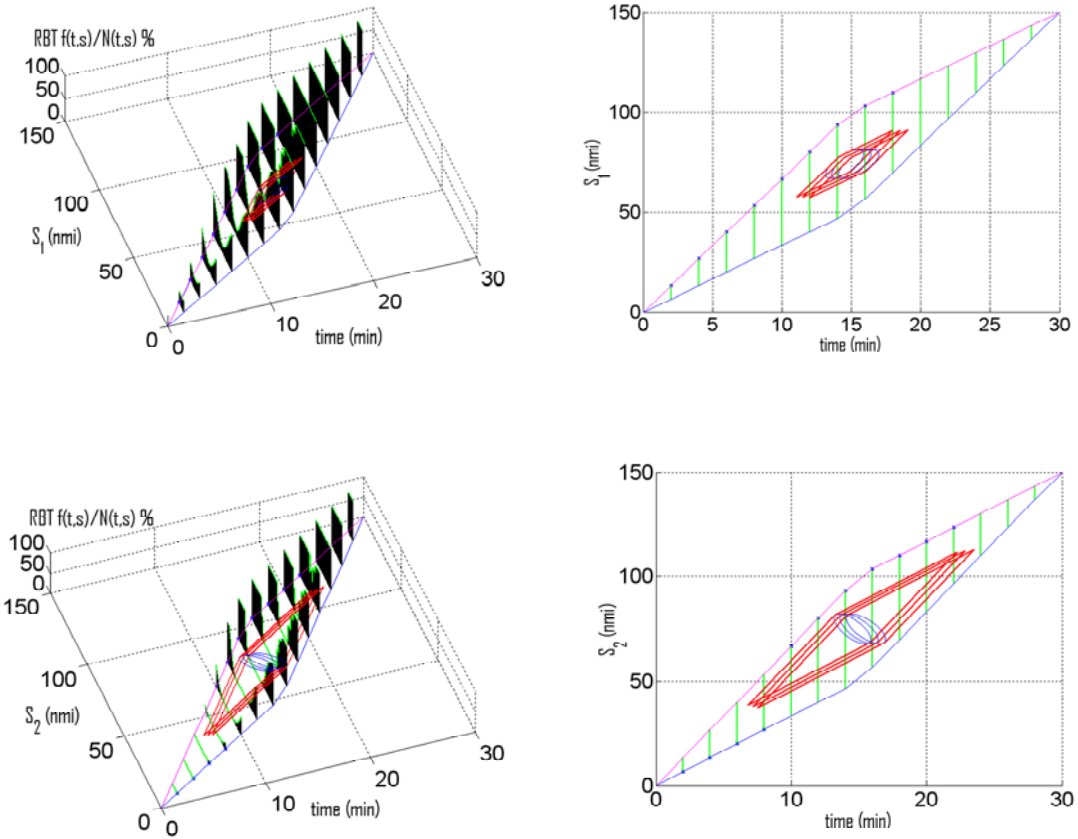
**Figure 4-6 Robustness analysis with speed DOF**
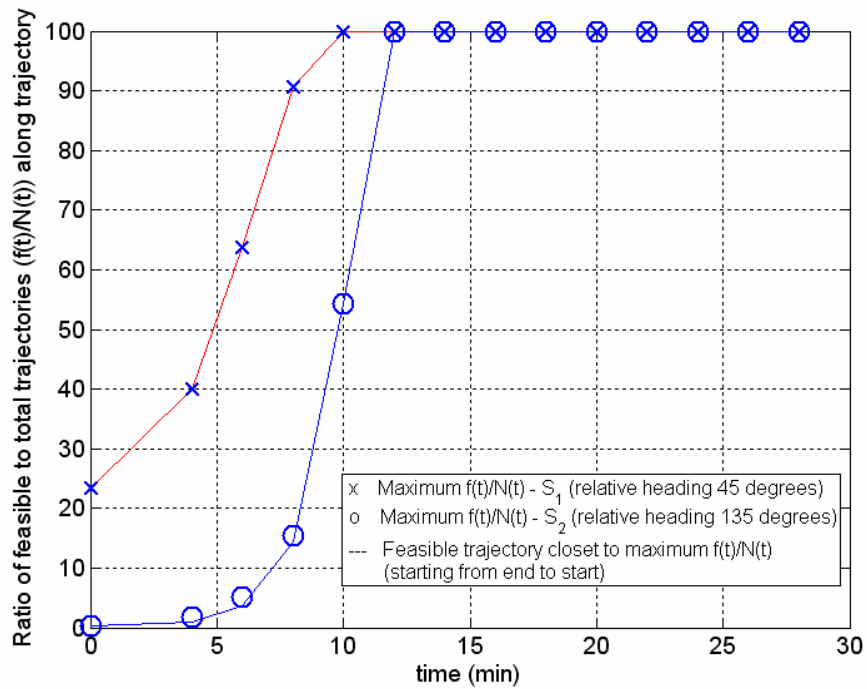


**Figure 4-7 Route selection based on robustness with speed DOF**

### 4.2.4 Note on Constraint Minimization

The adaptability and robustness metrics proposed can be used for assessing the impact of different constraints on the aircraft trajectory in terms of its flexibility. For example, the number of feasible trajectories f(t,s) or its ratio to the total number of trajectories N(t,s) may be compared between situations involving different number and types of imposed constraints. This can be seen by comparing the number of feasible trajectories in Figure 4-2 to the one in Figure 4-4 (for $s_1$ with relative heading of 45 degrees with the intruder aircraft). In Figure 4-2 a second RTA is added to the case in Figure 4-4 resulting in further reduction in the number of feasible trajectories. Removing this second RTA or increasing its tolerance results in increasing this number towards the one of Figure 4-4. Such relative gain from relaxing certain constraints (in terms of adaptability or robustness or a combination of both) can be used to support making decisions about constraint relaxation. Algorithms for using these metrics in making such decisions are a research topic that will be published in future reports.

# 5  Generalization of Trajectory Flexibility to Heading

The previous two sections analyzed the solution space along a path using speed as the only degree of freedom and with RTA and conflict constraints. This section extends that analysis to the solution space for an aircraft with heading and speed as degrees of freedom and with RTA and conflict constraints.

## 5.1  Trajectory Solution Space with RTA and Conflict Constraints

In this section the trajectory solution space is analyzed for an aircraft flying in a plane and with heading and speed as degrees of freedom. A number of assumptions are made to simplify the analysis, both for illustration of the concepts and tractability of metrics estimation. Figure 5-1 depicts in two dimensions (x, y) the trajectory solution space of an aircraft A flying towards a destination fix at $(x_{dest}, y_{dest})$. Aircraft A may select a trajectory by selecting a heading profile h(x, y) (several example are displayed in the figure) while keeping its speed v(x, y) along the path constant at a value V. In this analysis, the aircraft trajectory is also constrained by maximum and minimum headings ($h_{max}$ and $h_{min}$ respectively) at every point along the trajectory. These limits represent operational rather than physical constraints. They aim at confining the path stretch solution space to a reasonable area. For example, the heading bounds may be determined by a cone starting at the current position and surrounding the destination fix.[4] These heading limits also limit converging at the destination fix within a cone.
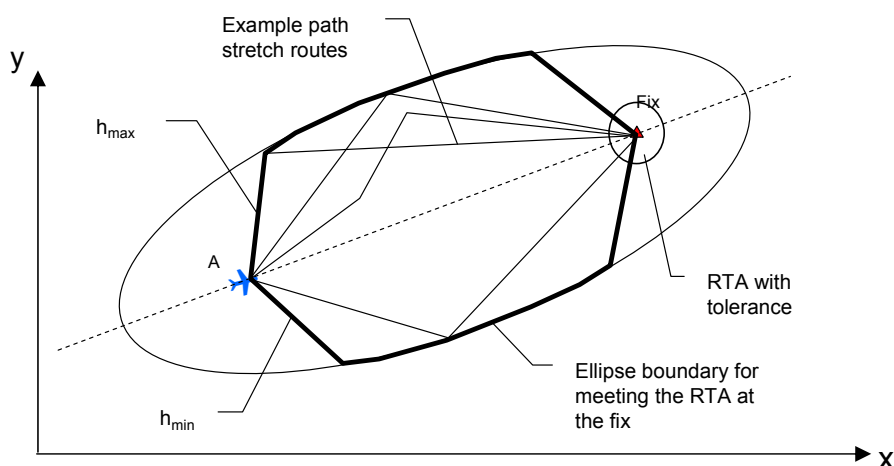


**Figure 5-1 Solution space with varying heading and constant speed**

Aircraft A faces a constraint to meet an RTA at the destination fix. The RTA constraint reduces the reachable set by eliminating non-feasible regions, which consist of the reachable states that, if reached, the allowable heading range is not effective in meeting

---

[4] In general these bounds are functions of the position along the trajectory and the previous heading used to get to that position (to avoid large heading changes). However, in this example, $h_{min}$ and $h_{max}$ are considered absolute and constant along the trajectory, for simplicity.

the RTA. To meet the RTA constraint at the destination fix, the path stretch solution space is limited to within an ellipse with focal points at the current and destination positions, as shown in Figure 5-1, for the fix point as the destination. The ellipse boundary results from the requirement that the trajectory length D is constant and equal to ((RTA – current time) times V). It corresponds to the trajectories that are anchored at the current and the destination positions and fully stretched outwards, resulting in a single heading change at the ellipse boundary. All other trajectories with length D and more than one heading change are stretched less and lie within the ellipse. If the destination allows a tolerance around it as shown in the figure, one such elliptical boundary corresponds to each allowable destination point within the tolerance. The path stretch solution space is then bound by the outmost one. Also, if the speed is allowed to vary between a minimum and a maximum value, the ellipse boundary corresponds to the longer distance required at the maximum speed as shown in Figure 5-2.
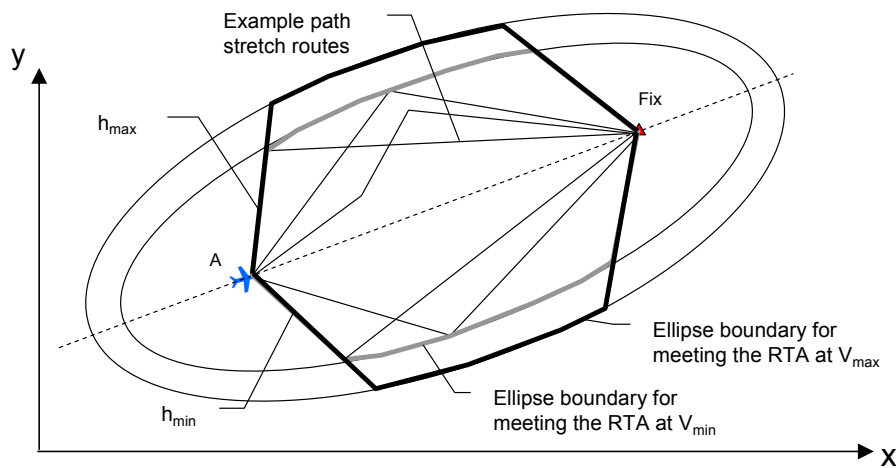


**Figure 5-2 Solution space with varying heading and speed**

While the elliptical boundary is an outer bound of the solution space, points within it may or may not be feasible depending on other constraints and operational assumptions. In this analysis the aircraft is assumed to follow segments of discrete time length, with constant heading and speed along each segment. The aircraft is assumed to make heading changes at specific instances in time separated by a time increment during which it maintains constant heading and speed. As discussed in the speed-only case (in Section 3.4.3), this assumption simplifies a method for estimating the metrics proposed. This discretization is demonstrated more explicitly by depicting the solution space in Figure 5-3 in three dimensions, x, y and time t with a constant speed assumption. Because the speed is constant in each segment, the solution space lies on a series of conical shells; each corresponds to the allowable heading range and makes a slope with the time axis equal to the constant speed V of the aircraft. As shown in the figure, the first conical shell starts at the current position. Then, the solution space remains on the conical shell as long as a selected heading is maintained constant, and a new cone originates from the point a new heading is selected. The new cone can be at the same or a new speed from the previous cone.
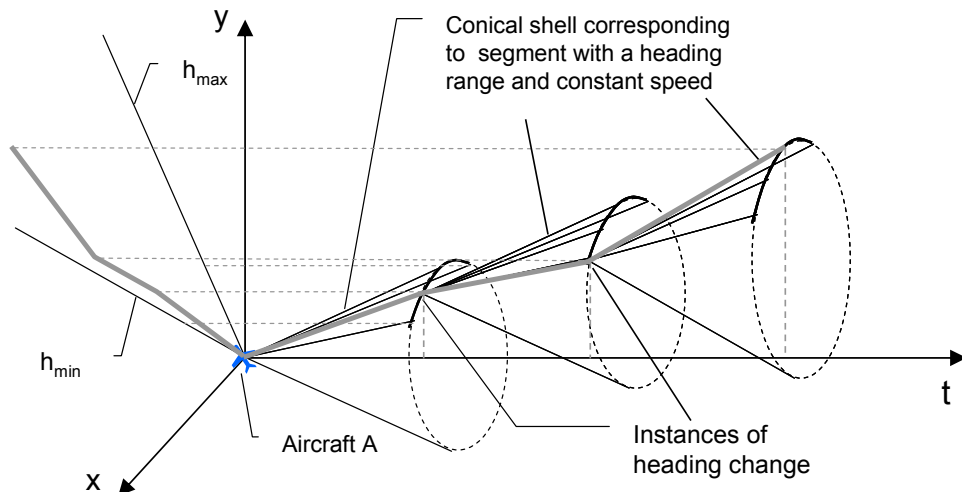
**Figure 5-3 Discretization of the solution space with varying heading and constant speed**

If the speed is allowed to vary between a maximum and a minimum speed, the solution space lies within a conical volume bounded by two conical shells, one corresponding to the minimum speed and one to the maximum speed. This is shown in Figure 5-4.
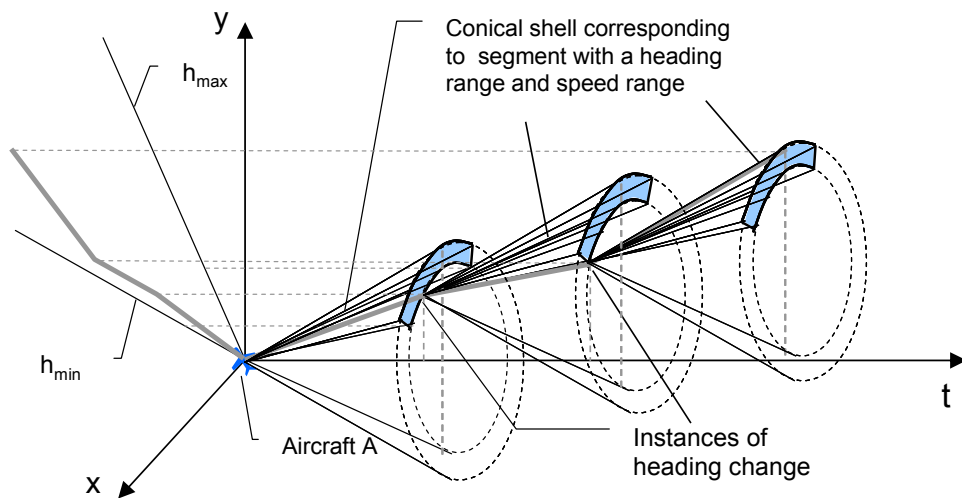


**Figure 5-4 Discretization of the solution space varying heading and speed**

In addition to the RTA constraint, aircraft A has to maintain separation from an intruder aircraft B (which may also represent in general a moving weather cell). This is depicted in Figure 5-5 by encircling the intruder aircraft with a circle of a radius equal to the minimum separation requirement (typically 5 nmi). The separation zone around the intruder aircraft becomes in the three dimensional space (t, x, y) a cylinder along its motion line, which is assumed to be along a constant speed and heading. For illustration, the impact of the separation zone on the solution space is depicted in Figure 5-5. Because of its maximum and minimum heading and speed constraints, aircraft A has to remain outside a hexagonal volume tangentially surrounding aircraft B's

50

cylindrical separation zone. This volume is bound by eight planes: each two opposing tangents resulting from a combination of heading and speed limits of the ownship aircraft relative to the intruder (There are four such combinations). Appendix A provides the equations for these planes. A point loses (or is imminent to lose) separation if it falls on the inside of all eight planes, within the time duration of the segment. The intersection of these planes with the solution space blocks areas in the x-y planes, as shown in the figure for one segment.[5] A trajectory that crosses this region loses separation with the intruder aircraft and is therefore infeasible. A trajectory (which corresponds to heading and speed profiles in this case) is feasible if it lies entirely in feasible regions. Therefore, for the aircraft to meet the RTA and be conflict free, its trajectory has to lie with the elliptical boundary of Figure 5-2 and remain outside the volume around aircraft B of Figure 5-5.
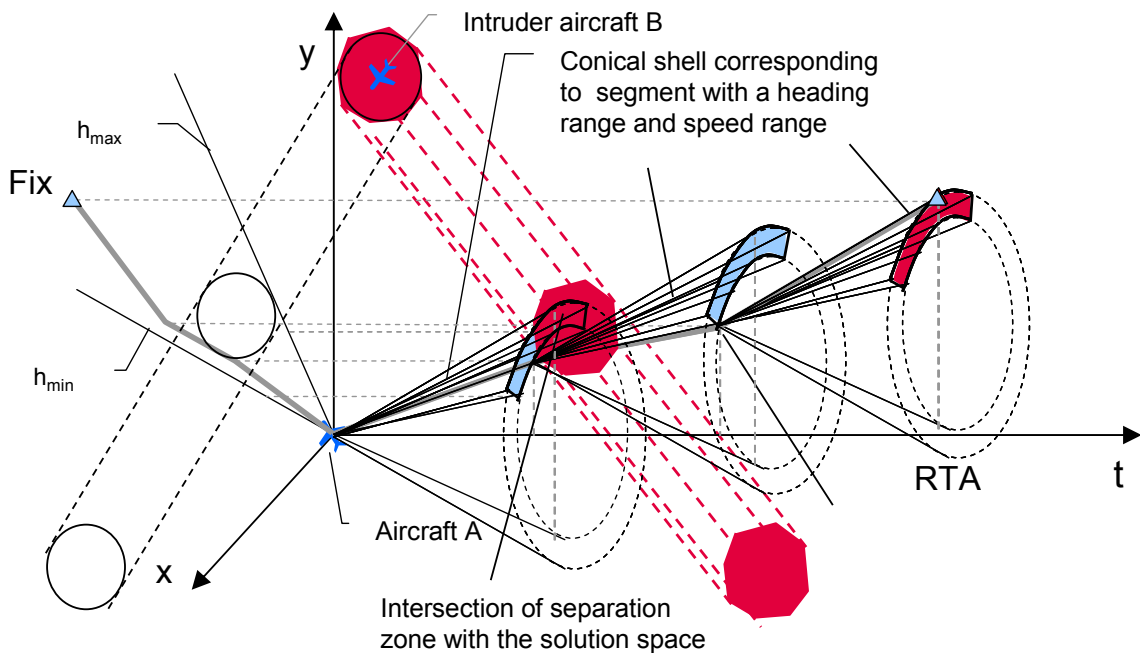


**Figure 5-5 Solution space with RTA and conflict constraints and heading and speed DOF**

Imposing more constraints further limits the trajectory solution space of the aircraft. The locations and tolerances of RTAs or the conflict regions may leave no feasible trajectory that is conflict free and meets all RTA constraints. In this case, the aircraft trajectory is said to be over-constrained and requires relaxation of some constraints. Figure 5-2 demonstrates how relaxing a constraint by increasing the RTA tolerance opens up solution space, by pushing outward the elliptical boundary allowing more feasible

---

[5] Hazards are similarly modeled as circles with zero speed. Therefore, the hazard circle is enclosed with four tangent planes rather than eight.

trajectories. A trajectory is said to be excessively constrained if the constraints allow some feasible trajectories without sufficient flexibility, which is defined below.

## 5.2  Definition of Trajectory Flexibility Metrics

The notion of "trajectory flexibility" was defined in Section 3 as the ability of the trajectory (and hence the aircraft following the trajectory) to abide by all constraints imposed on it while mitigating its exposure to risks that cause violation of these constraints. Examples of these constraints include the heading limits, RTAs, and loss of separation, described in the previous sections, but in general they include any constraints that intend to achieve ATM and aircraft objectives. They define the trajectory solution space, as was shown in Figure 3-3 for the speed degree of freedom case and here in Figure 5-2 in the case with both heading and speed as degrees of freedom.

Risk of constraint violation is represented by disturbances that alter the images depicted in these figures causing the aircraft trajectory to violate or potentially violate constraints. Disturbances were classified in Section 3 into state or constraint disturbances. These disturbances generalize to the speed and heading degrees of freedom with the extension of the possible state change to include heading as shown in Figure 5-6. As mentioned in Section 3, state disturbances result in aircraft state deviations along its trajectory. For example, the aircraft may pass through a turbulence region with uncertain wind speed, which results in the aircraft assuming one of many possible ground speeds in this region, some of which may lead to constraint violation. Constraint disturbances result in deviations in the constraints that define the aircraft trajectory solution space. They may be new constraints or modifications of currently imposed or known potential constraints. They include many types such as new TFM restrictions or new potential conflicts with traffic or weather cells, of which limited or no information may be available at the prediction time.
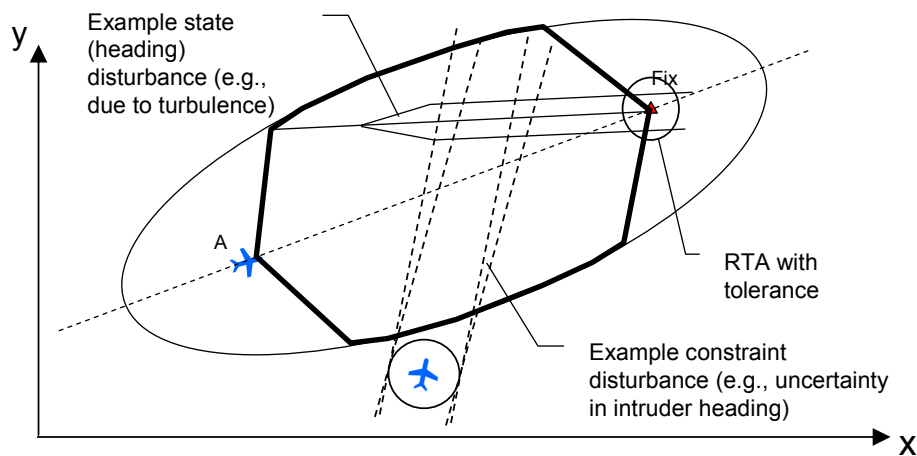


**Figure 5-6 State and constraint disturbances with heading and speed DOF**

Two trajectory characteristics relevant to measuring this notion of flexibility were identified in Section 3: robustness and adaptability. Metrics were also proposed for robustness and adaptability based on estimating the number of feasible trajectories

available to the aircraft to accommodate disturbances. In this section these definitions are generalized, essentially extending the notation to a plane rather than a line.

A robustness metric RBT(traj) is associated with a trajectory (traj) starting from a state (t, x, y) and ending at another state such as (RTA, $x_{dest}$, $y_{dest}$). RBT(traj) is measured with the probability of feasibility $P_f$(traj) of the trajectory, which can be estimated with partial information about state and constraint disturbances that represent the risk of constraint violation or infeasibility. Estimating $P_f$(traj) requires probabilistic models of the state and constraint disturbances. As an example, consider a state disturbance that makes every trajectory instance from a state (t, x, y) to the destination e.g., (RTA, $x_{dest}$, $y_{dest}$) possible with equal probability. In this case, the trajectory (traj) is modeled by N(t, x, y) instances ($traj_i$) each with equal probability

$$P_i(t, x, y) = \frac{1}{N(t, x, y)}, \text{ with } \sum_{i=1}^{i=N} P_i = 1.$$

Each constraint situation c divides the total set of trajectories N(t, x, y) into two mutually exclusive subsets: $f_c$(t, x, y) the set of feasible trajectories with respect to c and $i_c$(t, x, y) the set of infeasible trajectories with respect to c. Hence, N(t, x, y) = $f_c$(t, x, y) + $i_c$(t, x, y). Then, the following formula can be derived for robustness RBT(t, x, y) following the same method described in Section 3.3:

$$P_{f,c}(t,x,y) = \frac{f_c(t,x,y)}{N(t,x,y)} \qquad RBT(t,x,y) = P_f(t,x,y) = \sum_{c=1}^{c=C} P_c \times \frac{f_c(t,x,y)}{f_c(t,x,y) + i_c(t,x,y)} \qquad (6)$$

where $P_{f,c}$ is the probability of feasibility of the trajectory traj in a constraint situation c, and is equal to the ratio of the number of feasible trajectories $f_c$ to the total number of trajectories N. The constraints are modeled with C constraint situations c each with a probability $P_c$ with $\sum_{c=1}^{c=C} P_c = 1$.

**(2) Adaptability** is defined as the ability of the aircraft to change its planned trajectory in response to the occurrence of a disturbance that renders the current planned trajectory infeasible. An adaptability metric ADP(t, x, y) is associated with a state (t, x, y) along a trajectory and is measured by the number of feasible trajectories f(t, x, y) (with respect to all constraints) that are available for the aircraft to use at (t, x, y) to regain feasibility. Then, given the probability distribution ($P_c$) of each constraint situation c of C, ADP may be estimated by the average over C:

$$ADP(t,x,y) = f(t,x,y) = \sum_{c=1}^{c=C} P_c \times f_c(t,x,y). \qquad (7)$$

Adaptability decreases as the aircraft moves along a trajectory because the number of feasible trajectories decreases. The special case of robustness given by (6) (robustness to totally random state disturbances) increases over time because as the number of feasible trajectories (numerator) decreases the total number of trajectories (denominator) decreases more rapidly by both infeasible and feasible trajectories.

## 5.3  Estimation Method using Discrete Time, Speed and Heading

The calculation of the adaptability and robustness metrics requires estimation of the number of feasible trajectories from a state (t, x, y) to the destination (location, time, or both). A method was developed in Section 4.1 for varying speed along a fixed path. Here, this method is generalized to scenarios involving both speed and heading as degrees of freedom in situations involving RTA and separation constraints, under the two simplifying assumptions of discrete time, heading and speed, described above.

(1) The aircraft is assumed to follow segments of discrete time length, where instantaneous heading and speed changes can only occur at discrete instances in time that are ε apart.

(2) Heading h and speed V take discrete values between $h_{min}$ and $h_{max}$ and between $V_{min}$ and $V_{max}$ and are constant along each segment. (Altitude is not considered in this report.)

In addition to simplifying the estimation method, these assumptions are reasonable from an operational point of view considering the intended application of the trajectory flexibility metrics. Namely, the metrics are intended for relative comparison of trajectories over a long time horizon suitable for strategic planning (typical of traffic flow management planning horizon) as opposed to tactical maneuvering (where the dynamics of the speed and heading change are relevant).

Under these assumptions, the number of trajectories may be estimated using a convolution and filtering technique. Figure 5-7 demonstrates this method for calculating $f_c(t, x, y)$ from any point (t, x, y) to a destination specified by a point (RTA, $x_{dest}$, $y_{dest}$) and a tolerance circle around it in the x-y plane, in a constraint situation c that includes an instance of a potential conflict. The three-dimensional space is discretized into time steps ε-apart, where in each time step, the x-y plane is discretized into square cells. The function $f_c(t, x, y)$ is estimated for each cell. Assume the function $f_c(t_j, x, y)$ at time $t_j$ is known. The function $f_c(t_{j-1}, x, y)$ at the previous time step $t_{j-1}$ can be obtained by convoluting $f_c(t_j, x, y)$ and the function $g_k(x, y)$, which represents the number of trajectories that reach from a point k=($t_{j-1}$, x(k), y(k)) at time step $t_{j-1}$ to the next time step $t_j$. The function g is independent of time. There is one trajectory that reaches from point k at step $t_{j-1}$ to each of a set of discrete locations at step $t_j$ – each corresponds to one pair of discrete heading and speed values. Therefore, the reachability function $g_k(x, y)$ which is shown as a conical shell in Figure 5-7 is given by:

$$g_k(x, y) = 1 \; : (t_j, x, y) \in$$
$$\{(t_j, x(k) + V_{min} \cos(h_{min})\varepsilon, y(k) + V_{min} \sin(h_{min})\varepsilon), \cdots,$$
$$(t_j, x(k) + V_i \cos(h_i)\varepsilon, y(k) + V_i \sin(h_i)\varepsilon), \cdots,$$
$$(t_j, x(k) + V_{max} \cos(h_{max})\varepsilon, y(k) + V_{max} \sin(h_{max})\varepsilon)\}$$
$$g_k(x, y) = 0 \qquad \text{elsewhere}$$

(8)
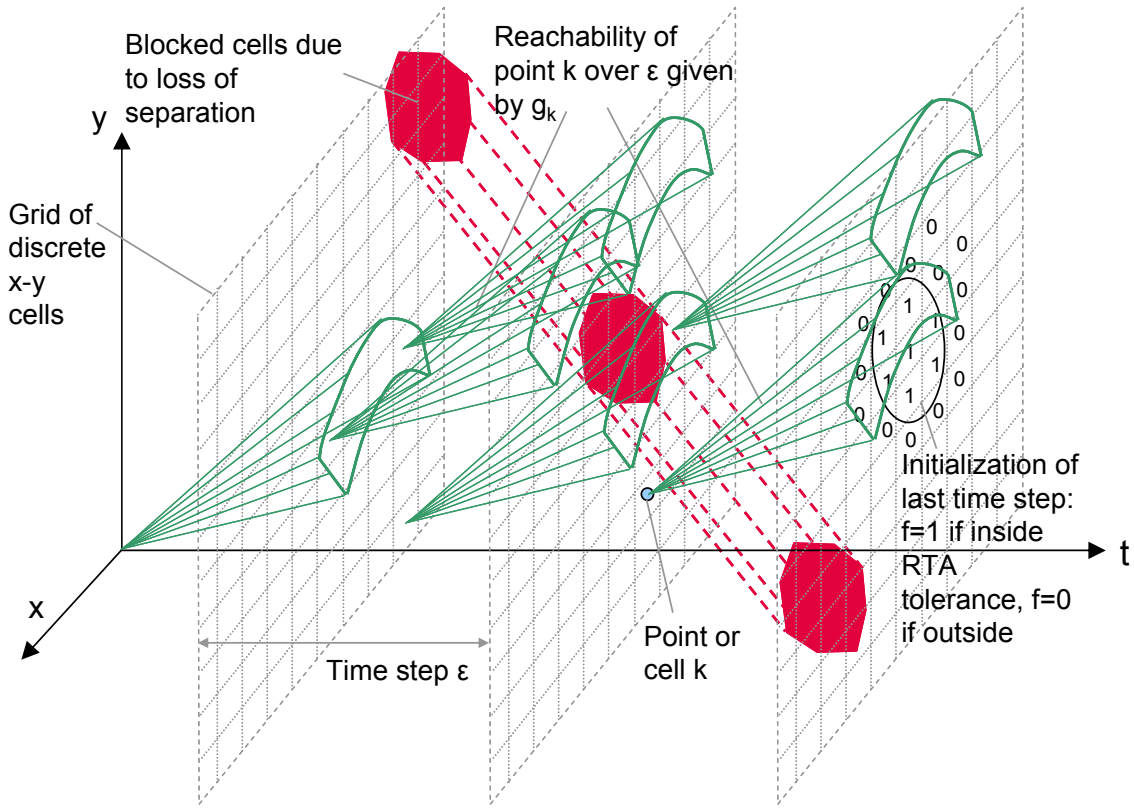
**Figure 5-7 Estimation of number of feasible trajectories with heading and speed DOF**

The convolution operation amounts to calculating $f_c(t_{j-1}, x(k), y(k))$ at point k, by multiplying the values of $f_c(t_j, x, y)$ by the number of trajectories that reach from point k to $(t_j, x, y)$ and adding them, and then repeating the operation for each point k in the x-y plane at time step $t_{j-1}$. However, if the point k is infeasible (for example due to loss of separation) then $f_c(t_{j-1}, x(k), y(k)) = 0$. This requires a filtering step before each convolution operation to zero out the values at infeasible states. Substituting a dummy variable τ to denote sliding the point k in the x-y plane, the function $f_c(t_{j-1}, x, y)$ is given by the following equation, representing convolution and filtering for infeasibility:

$$f_c(t_{j-1}, x, y) = \sum_{\lambda} \sum_{\tau} f_c(t_j, \tau, \lambda) g(x - \tau, y - \lambda) \text{ if feasible}$$

$$f_c(t_{j-1}, x, y) = 0 \qquad\qquad\qquad \text{if infeasible}$$

(9)

This operation is applied starting from the destination step t = RTA and proceeding backwards to the current state. The destination time step is initialized by setting $f_c(RTA, x, y) = 1$ at the feasible states and zero elsewhere as shown in Figure 5-7.

To compute the total number of trajectories, N(t, x, y) used in the denominator of the robustness metric RBT, certain constraints are excluded from the filtering process (namely the constraints with respect to which robustness is computed). In this report robustness only to loss of separation with traffic and hazards is considered. Therefore, the numerator filtering was applied to all cells that lead to separation loss as well as cells that lead to violating speed and heading limits or violating the RTA constraint. On

the other hand, filtering ignored loss of separation but was applied to the RTA and heading and speed limit constraints for calculating the denominator.

Separation zones are modeled as circles with given radii surrounding each intruder aircraft trajectory. Because a trajectory consists of discrete segments, each with constant speed and heading, the circle moves with constant speed and heading for the duration of each segment. In each segment, the circle is enclosed with eight tangent planes, each two opposing tangents resulting from a combination of heading and speed limits of the ownship aircraft relative to the intruder (There are four such combinations). A cell loses (or is imminent to lose) separation if it falls on the inside of all eight planes, within the time duration of the segment. The intersection of these planes with the solution space blocks polygon areas in the x-y grids, as shown in Figure 5-7 for one segment. Hazards are similarly modeled as circles with zero speed. Therefore, the hazard circle is enclosed with four tangent planes rather than eight.

Under probabilistic models of disturbances, the estimation process is repeated for each constraint situation c. Then, the estimates $f_c(t, x, y)$ are averaged over all situations C to obtain the adaptability or robustness metrics (6) and (7). The convolution operation produces an exponential growth of the number of feasible trajectories $f_c(t, x, y)$ backwards with time, depicting the decrease of adaptability with time. The infeasible regions eliminate trajectories as the function $f_c(t, x, y)$ is zeroed at these states. This produces troughs or valleys in the function $f_c(t, x, y)$ depicting the impact of constraints. This behavior is demonstrated in the example shown in Figure 5-8 which depicts an implementation of the estimation algorithm in MATLAB.
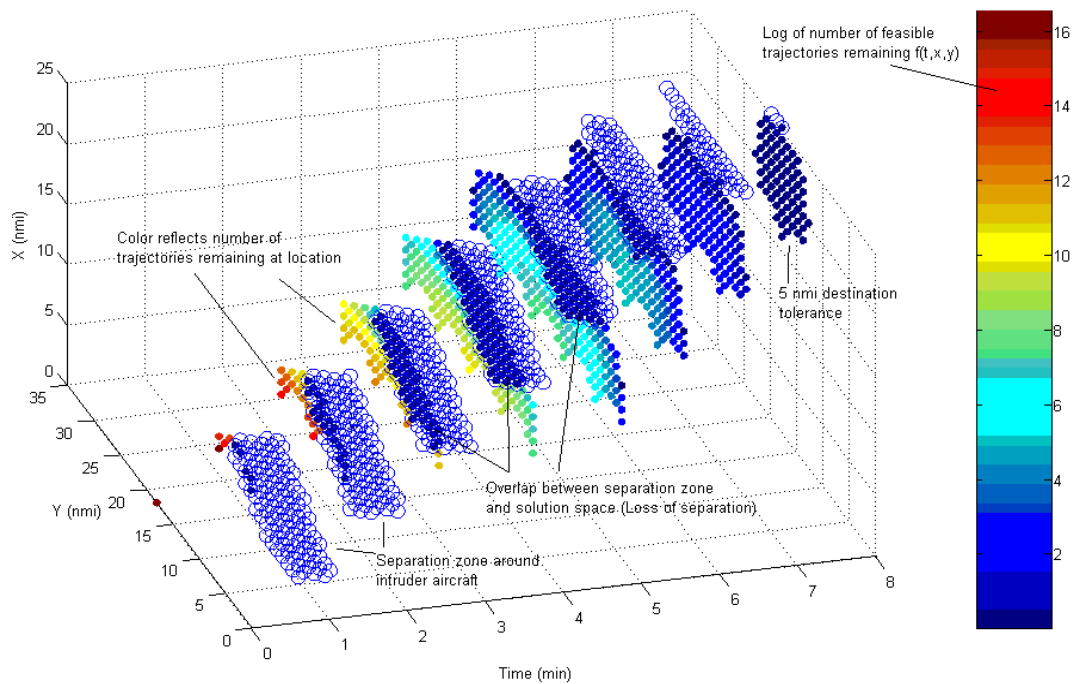


**Figure 5-8 Trajectory number estimation example with heading DOF**

This example consists of an aircraft with a current state of (0, 0, 18 nmi) and with an RTA constraint to be at (8 min, 20 nmi, 18 nmi) with a tolerance of 5 nmi around the destination location. In addition the aircraft path is impacted by a potential conflict with an intruder aircraft moving across at a heading of 20 degrees from the right hand side of the aircraft. Both aircraft have a speed of 240 kts. Figure 5-8 shows in a t-x-y space the trajectory solution space of the aircraft with $h_{min}$ and $h_{max}$ set at –60 and +60 degrees, respectively. The intruder aircraft separation zone is shown by non-filled circles at each time step. It also shows, as colored filled circles (the log value of) the number of feasible trajectories f(t, x, y), remaining at each point, estimated with time increments of 1 min and heading increments of 20 degrees. The color scale ranges from dark blue for the lowest number of trajectories to dark red for the largest number. Figure 5-8 shows the exponential decline of f(t, x, y) from the origin towards the destination and the filtering out of trajectories in the dark blue (zero value) circles that are intersected by the separation zone caused by the potential conflict  region.

An identical convolution/filtering process may be applied in the reverse direction starting from the current state towards the destination, yielding the number of trajectories (total or feasible) that lead to each point (t, x, y). Denoting this number by b(t, x, y), then for each point to be feasible there should be at least one trajectory to reach it from the current state and at least one trajectory to reach the destination from it. In other words the feasibility condition at a point (t, x, y) may be written as: $f(t, x, y) \times b(t, x, y) > 0$. These infeasible points are eliminated in Figure 5-8 showing the effect of discretization, where certain locations are unreachable from the current state due to the discrete heading and time assumptions.

## 5.4  Analysis Case and Preliminary Insights

A simple scenario was analyzed to demonstrate how the adaptability and robustness metrics described in the previous subsection can be used in trajectory flexibility planning with the heading degree of freedom. In this analysis, the discretized metrics estimation over the solution space is used as a map to assess the adaptability and robustness of specific trajectories. Each trajectory is laid over the map and the number of trajectories that remain to the destination at each point along it is identified, as absolute value for adaptability and in relative terms for robustness. These numbers are then compared among different trajectories to select the optimal one based on adaptability, robustness, or a tradeoff between them. In this analysis, the trajectories tested are generated independently of the map. Therefore, they do not have to abide by the discretization assumptions that were used to generate the map and may contain loss of separation. For example, a trajectory may have a heading that does not belong to the discrete set of headings used in the map and may change a heading at a time different than the discrete times used in the map for heading change. In these cases, the adaptability at a point along the trajectory is still measured by the number of trajectories remaining given the discretization assumptions from that point on, regardless of how the aircraft got to that point. This analysis is applied in the following scenario.

## 5.4.1  Analysis Scenario

The scenario analyzed, depicted in Figure 5-9, is a simplified representation of an aircraft (A) planning its trajectory between two streams of traffic, one along its direction and one in the opposite direction. The aircraft is constrained by a heading between –60 and +60 degrees relative to the line of sight between the current position (x= 0, y = 18 nmi) and the destination fix position at (x = 20, y = 18 nmi). It is also constrained to a constant speed of 240 kts. It has to meet an RTA at the destination fix at (8 min) with a tolerance of 5 nmi radius around the destination. Two intruder aircraft proceed on either side of the aircraft with a constant speed of 240 kts. Aircraft B starting at (x = 0, y = 6 nmi) and at a heading of 0 degrees, along the same direction of aircraft A, and aircraft C starting at (x = 20 nmi, y = 30 nmi) and with a heading of 180 degrees in the opposite direction to aircraft A.
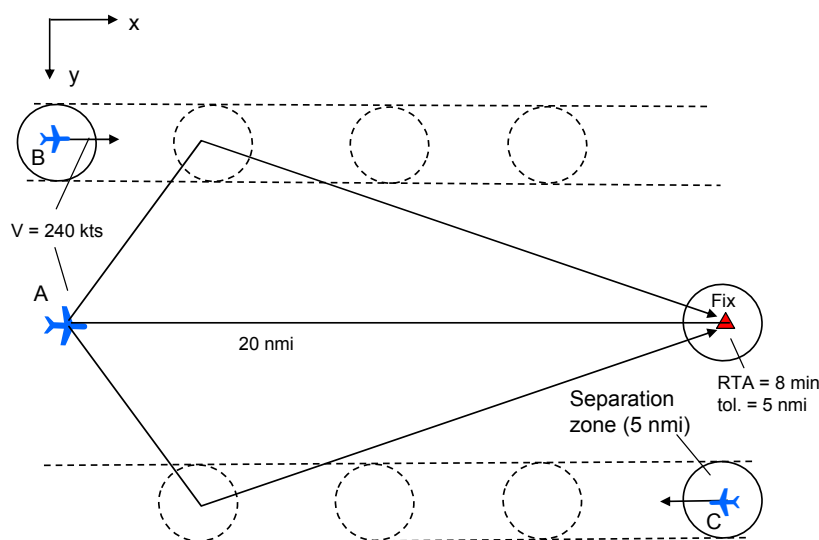


**Figure 5-9 Analysis scenario with heading DOF**

## 5.4.2  Adaptability-Based Trajectory Planning

The adaptability analysis of the scenario is shown in Figure 5-10, using the estimation method of the number of trajectories with 1-min time increments and 10-degree heading increments. Adaptability is shown as a color scale, showing the log value of the remaining number of feasible trajectories f(t, x, y) at each cell. Dark blue indicates lowest values (including the ones that overlap the separation zone) and dark red indicate highest values. A most adaptable heading profile would attempt to be as close as possible to the adaptability maxima at each time step, while ensuring reachability along the trajectory. Algorithms for finding such an optimum trajectory using the adaptability map are subject of the next section. Preliminary insights are made in this analysis by showing in Figure 5-10 the maximum values with X symbols connected with a line. Also, two single-turn trajectories are depicted, one starting at +60 degree heading and one starting with –60 degree heading and both ending at the destination fix. The following observations are made from Figure 5-10:

**Figure 5-10 Adaptability analysis with heading DOF**

(1) The opposing aircraft (C) impact is minimal in the time steps 8 to 5 where its separation zone does not overlap the solution space. Its impact is then concentrated at time steps 3 and 4 where its separation zone eliminates a large number of trajectories (see the large cluster of dark blue circles at step 4). On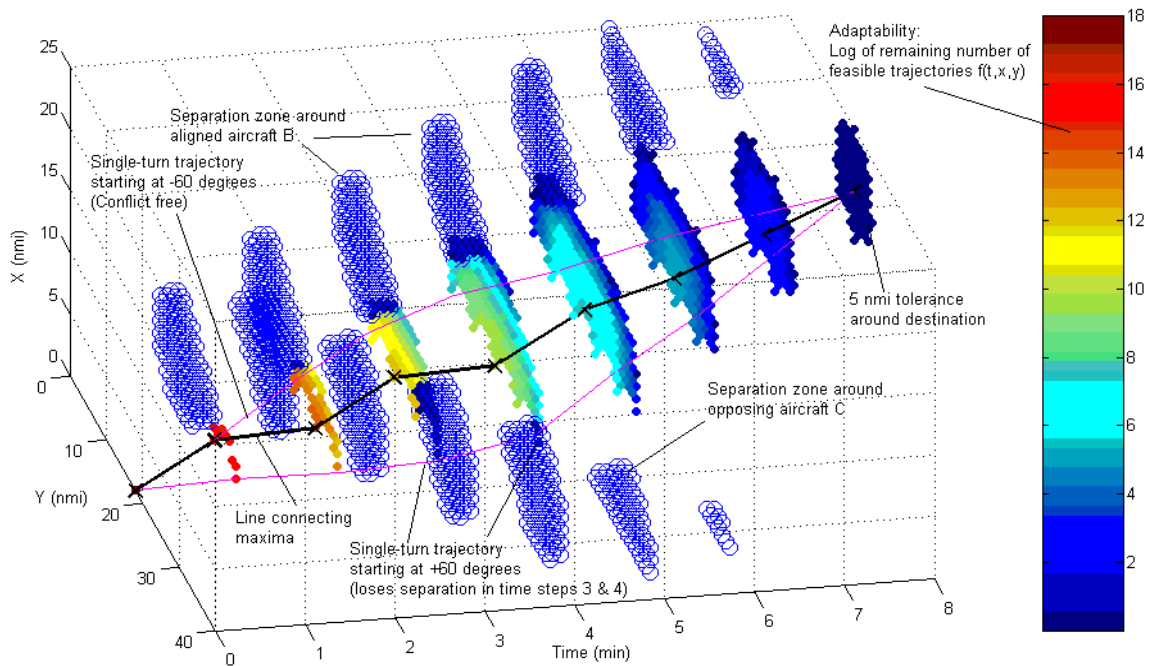 the other hand, the aligned aircraft (B) impact is higher at the later time steps and is maintained throughout the time horizon where its separation zone overlaps the solution space in almost every time step. However, the cumulative filtering by the aligned aircraft B, although spread over time, is less severe, resulting in higher number of trajectories remaining on the 'left' side of aircraft A than at the 'right' side.

(2) As a result of the previous observation (1), the adaptability maxima indicate that the aircraft would optimize adaptability by flying first away from the opposing aircraft (C) and towards the aligned aircraft (B). Then, after clearing the impact of aircraft C, it would opt to fly away from aircraft B increasing its separation from it. Finally, it proceeds towards the destination using a central line where neither aircraft has an impact on the solution space (the central line is selected to break ties between many equally adaptable locations).

(3) If the aircraft is to optimize adaptability it has to make more than one turn (heading change). If it is limited to a single turn, for example, it would choose the one that starts at –60 degrees, over the one that starts at +60 degrees. In fact, the figure shows that the one starting with +60 degrees loses separation with aircraft C at time steps 3 and 4.

## 5.4.3  Robustness-Based Trajectory Planning

Figure 5-11 repeats the analysis of Figure 5-10 based on maximizing robustness rather than adaptability, using the ratio of f(t, x, y) to N(t, x, y), thus assuming totally random state disturbance. For comparability with the adaptability analysis of Figure 5-10, in this example the total number of trajectories N(t, x, y) allowed by state (heading) variation is limited to the ones that meet the destination RTA constraint. This assumes that meeting the RTA constraint is totally robust to heading changes and robustness only with respect to meeting the conflict constraint is considered. Color is again used to depict robustness, with a color scale showing the lowest ratios as dark blue and the highest ratio (of 1) as dark red. In addition to the observations in the adaptability analysis, the following observations are made from Figure 5-11:
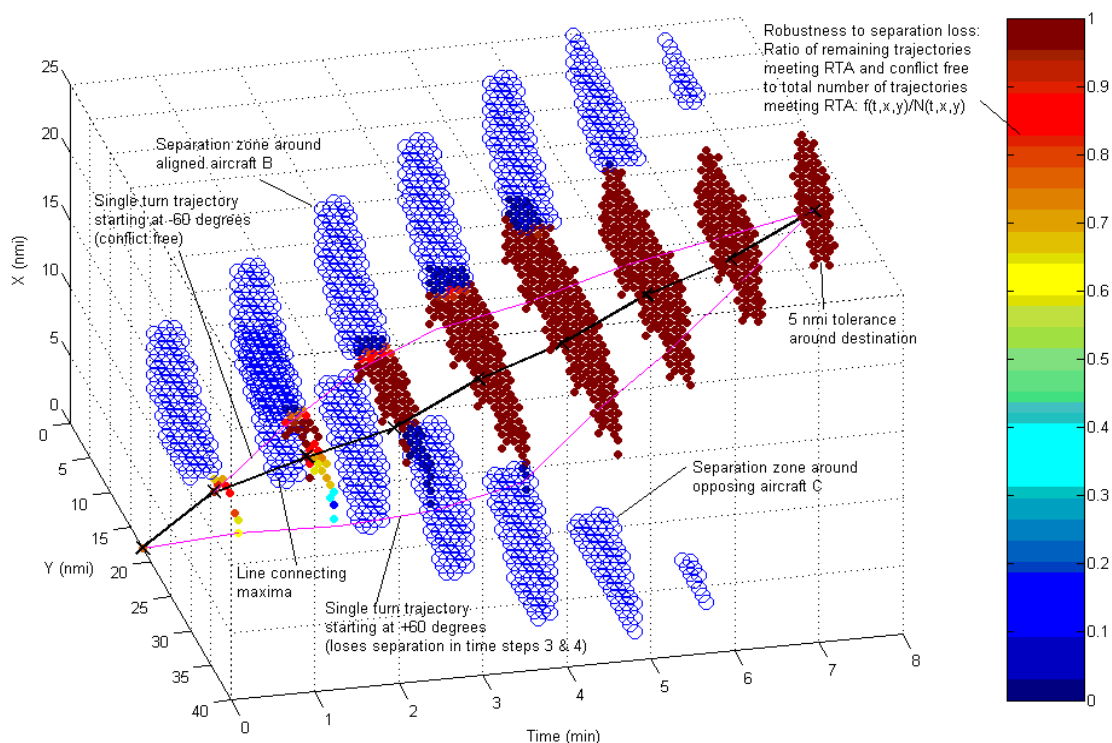


**Figure 5-11 Robustness analysis with heading DOF**

(1) Robustness (in this special case) increases over time, as opposed to adaptability which decreases over time, reaching a maximum value of one (100 percent robust) near the destination.

(2) The robustness maxima indicate that the aircraft would optimize robustness also by flying first away from the opposing aircraft (C) and towards the aligned aircraft (B). Then after clearing the impact of aircraft C, it would opt to fly away from aircraft B increasing its separation from it. Finally, it proceeds towards the destination using a central line where neither aircraft has an impact on it (the central line is again selected by breaking ties between many equal options). This robustness result in

60

this scenario is similar to the case of adaptability, which is not necessarily always the case.

### 5.4.4 Note on Traffic Complexity Impact

The metrics proposed in this section will be used for trajectory flexibility planning and constraint minimization and analyzing the impact on traffic complexity in Section 6. However, preliminary insights can be gained from this scenario. Traffic complexity involves a large number of factors. In this scenario, two factors may be identified as relevant, one related to the relative heading of the aircraft and one related to the proximity between them. The complexity of the traffic situation depends on how these factors trade, which is often subjective. However, the following observation may be made based on the most flexible trajectory (heading profile) selected by the aircraft. It is observed that the aircraft minimized the confrontation with the opposing traffic when its impact dominated (early), at the expense of closer proximity to the aligned traffic. Then when the opposing traffic was not a factor, it was advantageous to reduce its proximity to the aligned traffic in later time steps. Although anecdotal, these observations give preliminary insight on the possible positive impact that may be expected on traffic complexity in more elaborate scenarios.

# 6  Analysis of Impact on Traffic Complexity

Trajectory flexibility metrics have been defined to represent robustness and adaptability to the risk of violating separation, airspace hazards, and traffic flow management constraints. In this section, the impact of using these metrics on traffic complexity is analyzed. Two scenarios are analyzed in two-dimensional en route airspace, where each aircraft must meet a required time of arrival (RTA) in a one-hour time horizon using speed and heading degrees of freedom. Simultaneously, each aircraft preserves its trajectory flexibility, using the defined metrics, to mitigate the risk of loss of separation with the other aircraft and hazards. The effects were quantified using traffic complexity metrics based on Lyapunov exponents [40], flow pattern consistency, and proximity. The experiments showed promising results in terms of mitigating complexity as measured by these metrics.

## 6.1  Traffic Complexity Metrics

The impact of planning trajectories using the adaptability and robustness metrics on traffic complexity was assessed using three main indicators: an intrinsic trajectory-based complexity metric, consistency of a resulting flow pattern, and proximity between aircraft.

The intrinsic traffic complexity metric is based on the non-linear dynamic system modeling of the aircraft trajectories. This metric identifies any kind of trajectories organization in the airspace by the mean of Lyapunov exponents map computation. Based on the observations of the aircraft (positions, speed vectors and times), a non linear space-time dynamic system has to be adjusted with the minimum error.[6]

$$\dot{\vec{X}}(t) = f(\vec{X}, t)$$

$$\min \sum_{i=1}^{i=N} \sum_{k=1}^{k=K} \left\| V_i(t_k) - f(\vec{X}_i, t_k) \right\| \tag{10}$$

where N is the number of aircraft and K the number of samples per aircraft trajectory.

There are many classical ways of obtaining a class of parameterized vector fields that fulfill the fitting requirement. Among them, vector splines allow control of the smoothness of vector fields, which is important in this case because civil aircraft maneuvers are based on low acceleration guidance laws. The vector field is designed to minimize a function form

$$\min \int_{R^4} \int_R \alpha \left\| \nabla \mathrm{div} \vec{f}(\vec{X}, t) \right\|^2 + \beta \left\| \nabla \mathrm{curl} \vec{f}(\vec{X}, t) \right\| + \left\| \frac{\partial \vec{f}(\vec{X}, t)}{\partial t} \right\| d\vec{X} dt \tag{11}$$

---

[6] The symbol "f" is used here to represent the dynamic system evolution for consistency with the literature. It is not the number of trajectories used in the previous sections of this document.

with α, β ,γ positive real numbers controlling the smoothness of the approximation by focusing on constant divergence or constant curl.

Computing traffic complexity for a given traffic situation requires interpolating a vector field given only samples (positions and speeds of aircraft at given times). Vector spline interpolation seeks the minimum error between the observation and the model. This adjustment is done with a Least Square Minimization (LMS). The metric chosen for complexity computation relies on a measure of sensitivity to initial conditions of the underlying dynamic system called Lyapunov exponents. The Lyapunov exponents are closely related to the singular values of the gradient matrix on the vector field at a given point.

$$\kappa(\vec{f}) = \frac{1}{n} \sum_{i=1}^{i=n} \left\| D_{\vec{X}} \vec{f}(\phi(t,\vec{X})) \right\| 2 \tag{12}$$

where $D_{\vec{X}}$ is the gradient matrix of the field at point $\vec{X}$ and $\phi(t,\vec{X})$ the point trajectory of the dynamic system at point $\vec{X}$.

When Lyapunov exponents are high, the trajectory of a point under the action of the dynamic system is very sensitive to the initial conditions (or parameters on which the vector field may depend), therefore, the situation in the future is unpredictable. On the other hand, small values of the Lyapunov exponents mean that the future is highly predictable (very organized traffic). So, the Lyapunov exponent map determines the area where the underlying dynamic system is organized. It identifies the places where the relative distances between aircraft do not change with time (low real value) and the ones where such distance changes a lot (high real value). More information about this metric may be found in [40].

Flow pattern consistency was also measured by the percentage of aircraft that followed a consistent pattern. The pattern was readily apparent visually so no clustering technique was employed in the scenarios analyzed in this report. The pattern was scenario dependent.

Traffic proximity was measured by the number of aircraft-seconds that are less than a threshold distance apart.

## 6.2  Cost Function and Trajectory Building

Given the structure of the solution space, dynamic programming offers a straightforward method to build an optimal trajectory. Using recursive back-propagation and starting from the final time step, the minimum cost of proceeding from each cell to the destination is computed and stored. This minimum cost $Q(t, x(k), y(k))$ for each cell k is computed by minimizing, over its reachable cells given by $\{(t+1, x, y) : g_k(t+1, x, y) \geq 1\}$ [7] in the next time step $t+1$, the sum of the minimum cost $Q(t+1, x, y)$ already computed for

---

[7] Gk may be larger than one because a square cell of large dimensions may contain more than one reachable point, depending on the resolution of the discretization.

each of the reachable cells (t+1, x, y) plus the cost of proceeding from k to that cell, given for short by q(k → (t+1, x, y)). A generic formula is:

$$Q(t,x(k),y(k)) = \underset{x,y:g_k(t+1,x,y)=1}{\text{Min}} \{Q(t+1,x,y) + q(k \rightarrow (t+1,x,y))\} \tag{13}$$

Four functions for the local cost, q, were used in the experiments reported in this report. A function representing minimal path length was used as a baseline. Functions representing maximizing adaptability, maximizing robustness, and maximizing both combined with minimizing path length:

$$q(k \rightarrow (t+1,x,y)) = \text{distance}(k \rightarrow (t+1,x,y)) = \text{dist} \tag{14}$$

$$q(k \rightarrow (t+1,x,y)) = -\text{ADP}(k) \tag{15}$$

$$q(k \rightarrow (t+1,x,y)) = -\text{RBT}(k) \tag{16}$$

$$q(k \rightarrow (t+1,x,y)) = -\text{ADP}(k) - a^{T-t}\text{RBT}(k) + b^{T-t}\text{dist} \tag{17}$$

where a and b are weights that trade robustness and distance, respectively, with adaptability. They are raised to the power of time (T-t) (measured from the final time step) to account for the exponential growth of ADP. Note that while the accumulated distance over time is minimized, ADP and RBT are maximized at each time step (because their accumulation at any point is identical over all trajectories to the destination).

After storing the optimal costs for each cell, a forward loop builds a trajectory by tracing the optimal cells starting from the initial state. Any ties between cells were broken randomly.

The estimation technique and trajectory optimization algorithm were implemented in a MATLAB tool. The resulting trajectories were analyzed using the traffic complexity metrics described in Section 6.1. First, the two scenarios reported in this paper are described. Second, observations are made on the impact of trajectory planning, using the four cost functions (14) through (17), on traffic complexity.

## 6.3  Analysis Scenarios

The first of two scenarios consists of a line of weather cells leaving two holes for which two flows of traffic compete as shown in Figure 6-1. The two traffic flows travel in opposite directions: one starts at x = 0, y = −120 nautical miles and heads towards x = 0, y = 80 nautical miles. The other flow starts at x = 0, y = 120 and ends at x = 0, y = −80 nautical miles. Five weather hazard cells are modeled as circles with a radius of 20 nautical miles, and located at x = 0 and y = {0, ±70, ±120 nautical miles}. The geometry of the hazards and of the traffic start and end positions is selected to provide symmetry, such that the path length alone is not a differentiator for selecting among the two holes. This ensures highlighting the impact of the robustness and adaptability metrics compared to shortest path. Each traffic flow is generated with random entry times separated by intervals between five and seven minutes. All aircraft are limited to headings of ±60 degrees relative to the centerline connecting the start and end positions, with 10-degree increments. They are also limited to a speed between 240 and 360 knots with 10-knot increments. Each aircraft is assigned an RTA at the destination

that forces the aircraft to path stretch to meet the RTA. This was ensured by setting the RTA up to 10 minutes above the travel time at minimum speed along a straight path. The RTA is met exactly with no tolerance at the destination point allowed.
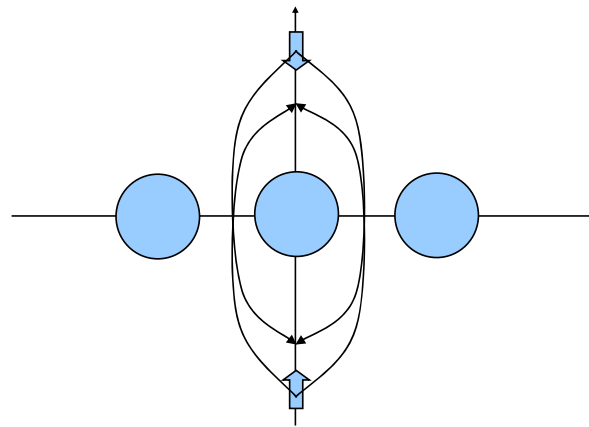


**Figure 6-1 Two holes in weather line scenario**

The second scenario consists of a weather cell that causes four traffic flows crossing at right angles to go around the weather cell, in a roundabout, as shown in Figure 6-2. The weather cell is modeled as a circle with radius of 30 nautical miles located at (x = 0, y = 0). The four traffic flows originate at (x = 0, y = −120), (x = 0, y = 120), (x = −120, y = 0) and (x = 120, y = 0). They end respectively at (x = 0, y = 80), (x = 0, y = −80), (x = 80, y = 0) and (x = −80, y = 0). All units are in nautical miles. Eight other hazard circles are added at the corners to increase the traffic interaction around the hazard located in the center. The speed and heading limits and increments are the same as in the first scenario. The entry times for each flow ranged between 6 and 8 minutes.
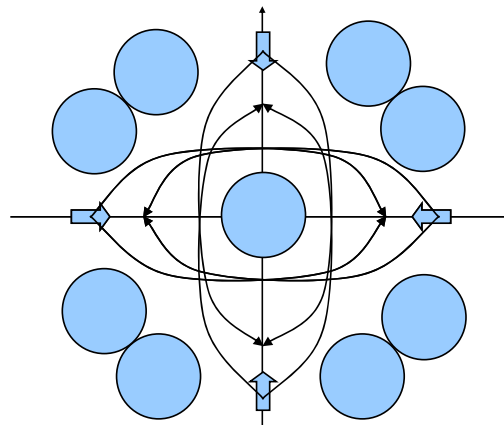


**Figure 6-2 Round about scenario**

In both scenarios, each aircraft plans a trajectory to meet the RTA (using speed reduction and path stretching), optimizing the four cost functions (14) through (17). Time increments of 2 minutes and square x-y cells of 2 nautical miles are used in the estimation of the number of trajectories. The first aircraft does not encounter any traffic as it plans its trajectory. Then, each following aircraft plans its trajectory assuming

knowledge of the trajectories of all preceding aircraft. These trajectories are surrounded by separation zones that, in addition to the weather hazards, are avoided by the aircraft. Hazards and separation zones reduce the number of feasible trajectories. Therefore, earlier aircraft are given priority while each later aircraft encounters exceedingly more traffic. No dynamic trajectory modification is considered in the experiments run for this analysis. Each aircraft generates one trajectory upon its entry and maintains this trajectory throughout. Also, the experiment runs considered only deterministic aircraft behavior. One trajectory is considered for each aircraft with probability of one. However, the separation requirement around each aircraft was set to 10 nautical miles (instead of the required 5 nautical miles) in order to capture the higher uncertainty in the rather long time horizon of these experiments.

Each scenario contained 80 aircraft distributed evenly among the flows. The resulting trajectories consist of heading and speed decisions at each two-minute increment. They are then interpolated with 30 second time steps assuming constant speed and heading in each two-minute time increment. Finally, they are analyzed for traffic complexity.

Figure 6-3 shows an example of the adaptability metric (ADP) at one time step of the solution space, for an aircraft that encounters the hazards of the first scenario. Color shades are used to depict the log of the number of feasible trajectories. Figure 6-4 shows an example of the robustness metric (RBT) at one time step of the solution space using color shades. Note that adaptability is highest near the center of the solution space around the central hazard, while robustness is highest near the extremities of the solution space away from the central hazard. Also, note that robustness here is with respect to the hazards and loss of separation only and not to the RTA constraint or the speed and heading limits. Finally, it should be noted that the solution space is smaller in Figure 6-4 because it is an earlier time step and that these figures are in a relative frame with respect to an aircraft (hence the hazard y-location is 120 nautical miles rather than zero).
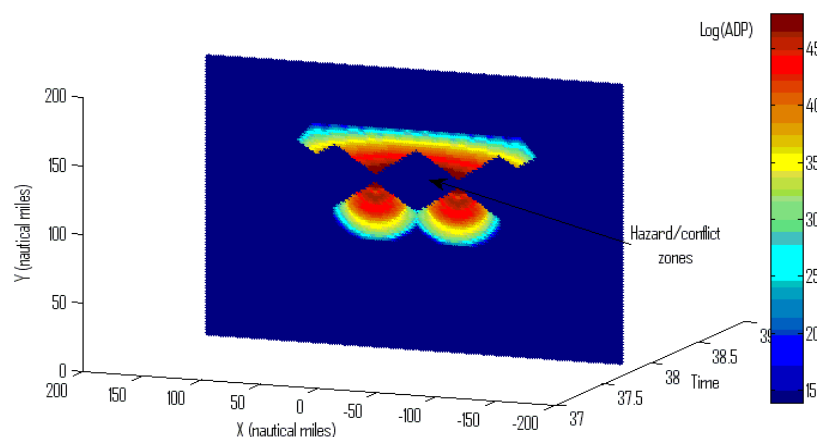


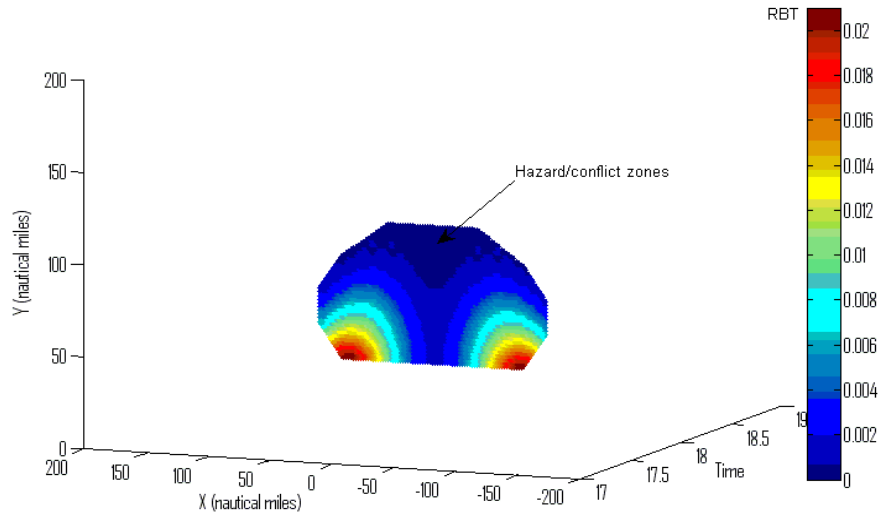**Figure 6-3 Example of adaptability metric map**

**Figure 6-4 Example of robustness metric map**

## *6.4  Results and Observations*

Figure 6-5 (a-e) demonstrates the resulting flow patterns in the first scenario and Figure 6-6 (a-e) those in the second scenario, using an eight-minute time history. As a baseline, the shortest path cost function (14) was run twice, once without avoiding the other traffic (case a) and once with avoiding it (case b). Traffic avoidance was turned off in case a to depict current practice where conflict avoidance is only applied in a short time horizon of 10 to 20 minutes. Shortest-path with traffic avoidance in case b sets another baseline for demonstrating the marginal effect of using the adaptability and robustness metrics in cases c-e. When using the adaptability and robustness metrics, (cases c-e), traffic is naturally avoided because the number of trajectories from cells that lose separation is zero. However, avoiding loss of separation is not guaranteed because of the coarse discretization of the solution space. The greater the time and space between increments, the greater the chance of losing separation.

Traffic complexity was measured using the metric given by Equations (10)-(12). The resulting complexity maps (Lyapunov exponents) are shown as background to the traffic scenarios in Figure 6-5 and Figure 6-6. The maps in Figure 6-5 were derived using a twelve-minute window and the ones in Figure 6-6 using a three-minute window (the twelve-minute average did not highlight enough details in this case). The Lyapunov exponent maps demonstrate the predictability of the flow in the snap shots used in these figures. Note that the color scale is unique for each of the cases, but the numbers on the scale can be compared between cases. The high numbers indicate less predictability and hence less organized traffic areas as discussed in Section 6.1.

67
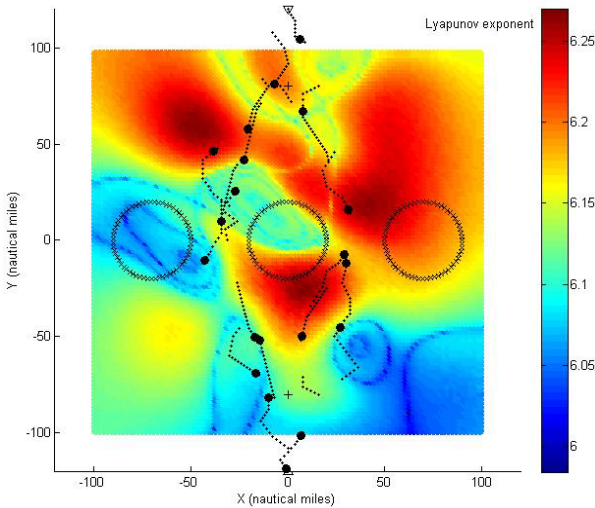
(a) Shortest path without traffic avoidance
Pattern: No specific pattern.
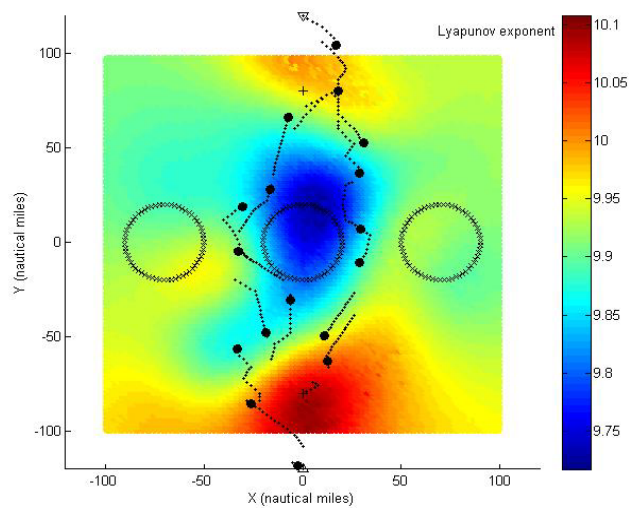
(b) Shortest path with traffic avoidance
Pattern: northbound mostly through left hole,
southbound mostly through right hole
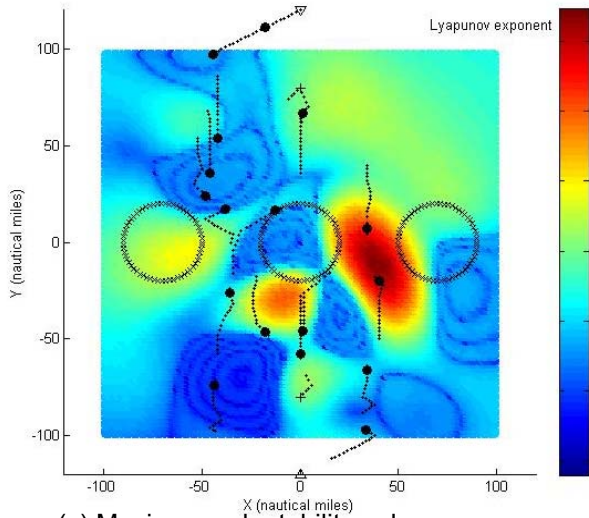
(c) Maximum adaptability only
Pattern: outer lanes before hole, along
centerline after the hole
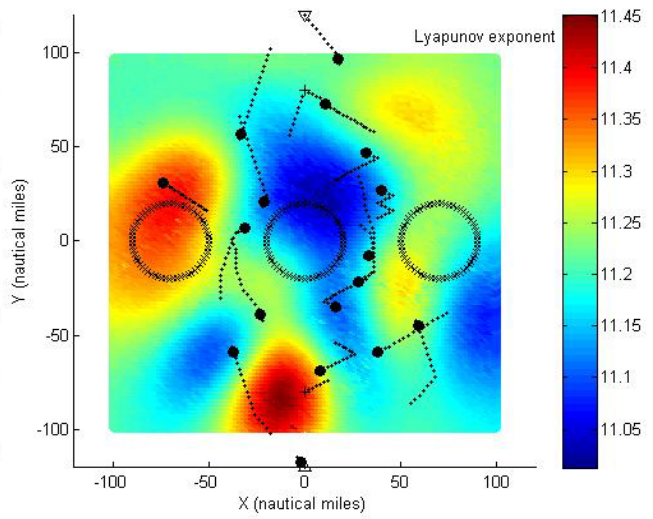
(d) Maximum robustness only
Pattern: spread out as possible

(e) Maximum adaptability and
robustness, and shortest path

Pattern: mostly northbound through
right hole, southbound through left
hole
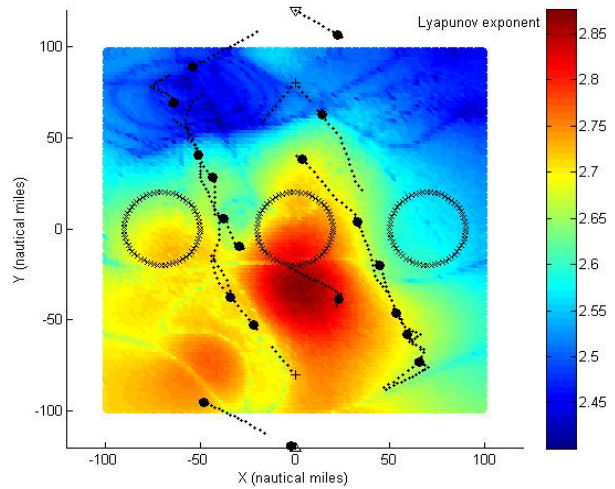
**Figure 6-5 Flow patterns in weather line scenario**

68
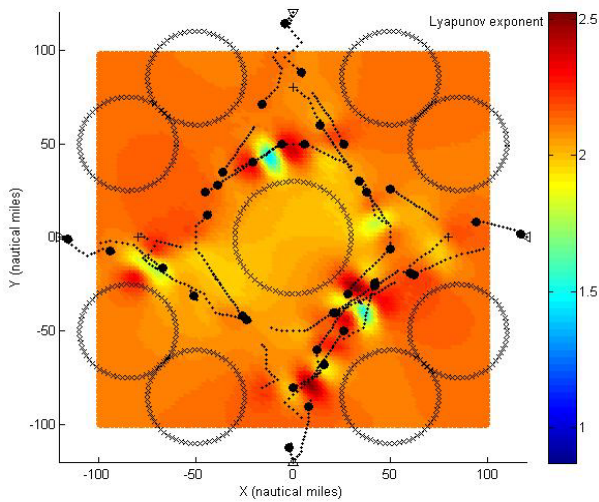
(a) Shortest path without traffic avoidance
Pattern: 60% of aircraft counterclockwise
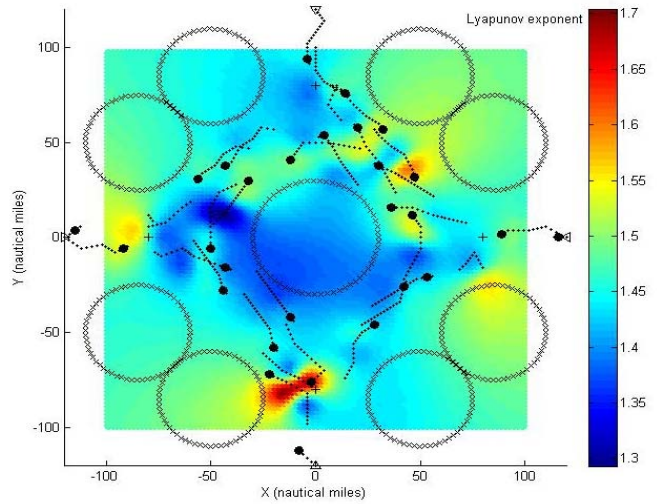
(b) Shortest path with traffic avoidance
Pattern: 68% of aircraft counterclockwise
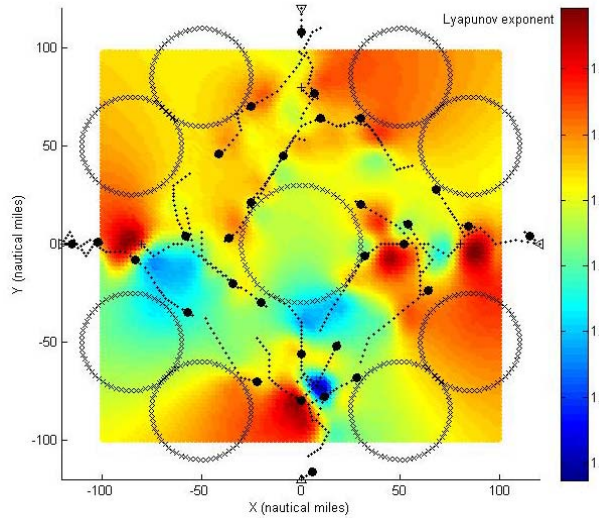
(c) Maximum adaptability only
Pattern: 97% of aircraft counterclockwise
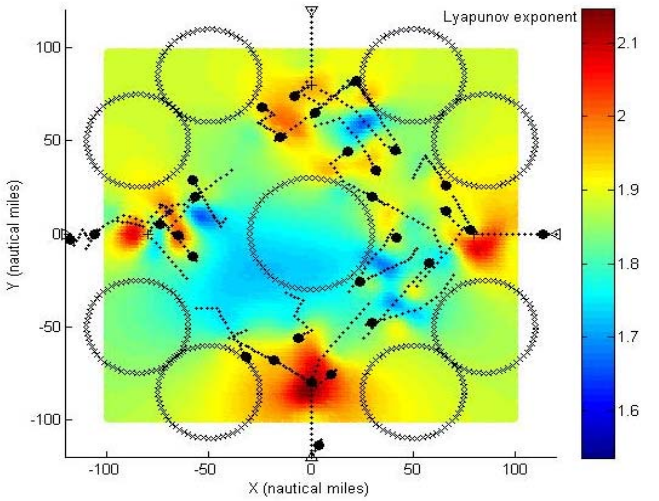
(d) Maximum robustness only
Pattern: 70% of aircraft counterclockwise

(e) Maximum adaptability and robustness, and shortest path

Pattern: 84% of aircraft counterclockwise
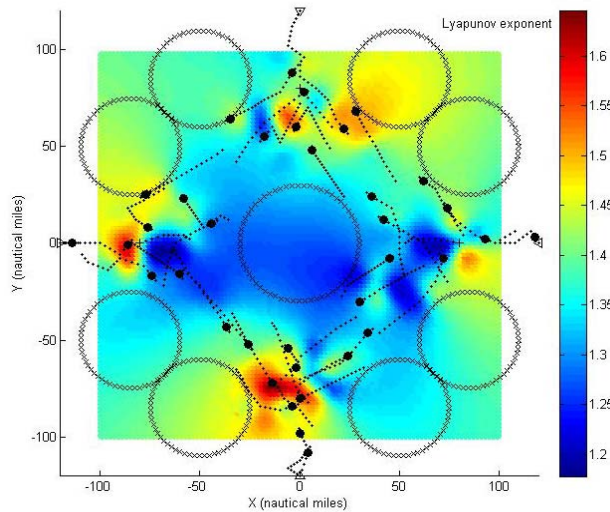
**Figure 6-6 Flow patterns in round about scenario**

Figure 6-5 and Figure 6-6 demonstrate that, in both scenarios, using robustness and adaptability as objectives for individual trajectory planning resulted in more structured aggregate traffic flow. Looking at the headings of the aircraft, shown by a black circle at the end of the eight minute history trail, and at the complexity maps, one can see the following: In case a, which used shortest path without traffic avoidance, aircraft varied in selecting their path relative to the hazard in both scenarios resulting in closer proximity and more random flow patterns. This is captured by a wide and unorganized spread of high-Lyapunov-exponent areas in case a of both figures.

All the other cases resulted in a more structured traffic pattern but in a different manner: In case b of Figure 6-5, which used shortest path but avoided traffic, most aircraft traveled through the holes in a uniform direction, with occasional misalignment. In case c of Figure 6-5, which used adaptability, aircraft formed outer lanes before the hazard and traveled along the centerline afterwards. This pattern resulted because adaptability tended to concentrate the aircraft trajectory close to the centerline connecting the initial and final locations. This is because the number of feasible trajectories is highest near the centerline (as shown in Figure 6-3) which caused the aircraft to hug to central hazard. The holes in this scenario were large enough to allow the aircraft to travel through them in both directions. This caused locally high Lyuaponov exponents as shown in the right hole of Figure 6-5 c. On the other hand, robustness, which was used in case d, tended to send the aircraft away from each other and from the hazards increasing the spacing between them. This caused aircraft in case d to spread out more than in cases b and c, and to exhibit a less structured manner. This was also captured by areas of low predictability around strayed aircraft in Figure 6-5 d. Aircraft in both cases c and d separated from each other more than in cases a and b. In case e, the aircraft formed a unidirectional flow through each of the holes. One can see in Figure 6-5 e the valleys (low exponent values) along this unidirectional flow through the holes. Aircraft that did not follow this pattern are surrounded with high exponent areas.

In the round about scenario of Figure 6-6, most aircraft turned around the central hazard in a uniform direction relative to the shortest path case a. This is indicated in the figure by the percentage of aircraft that selected the counterclockwise direction. This percentage is higher in cases c-e (70-97 percent) than cases a and b (60-68 percent). The Lyapunov exponent again captures this effect. Case a in Figure 6-6 has high exponent areas concentrated around the central hazard where aircraft paths cross each other randomly without avoidance. In cases b through e, the high exponent values are concentrated near the sources and destinations while the movement areas around the central hazard are relatively more organized and predictable.

In Figure 6-5 and Figure 6-6, cases c and d exhibited the lowest Lyapunov exponent values compared to the other cases, reflecting more organized and predictable patterns for one time step. Figure 6-7 shows the average Lyapunov exponents for a series of maps over time for the scenario of Figure 6-6. This average value represents the minimum information (in the Shannon sense) that has to be brought to the system to fully organize the traffic (with the same speed in the same direction). Figure 6-7 shows that case a, has the highest average value most of the time. This is consistent with the lack of organization relative to the other cases. On the other hand, case c has the lowest average most of the time also consistent with the most structured flow pattern

indicated in Figure 6-6. The corresponding plot for the scenario in Figure 6-5 did not show such a consistent difference in the average Lyapunov exponent between the cases. This may be attributed to the fact that the patterns in this scenario were less structured over the full map area and dominated by local misalignments.
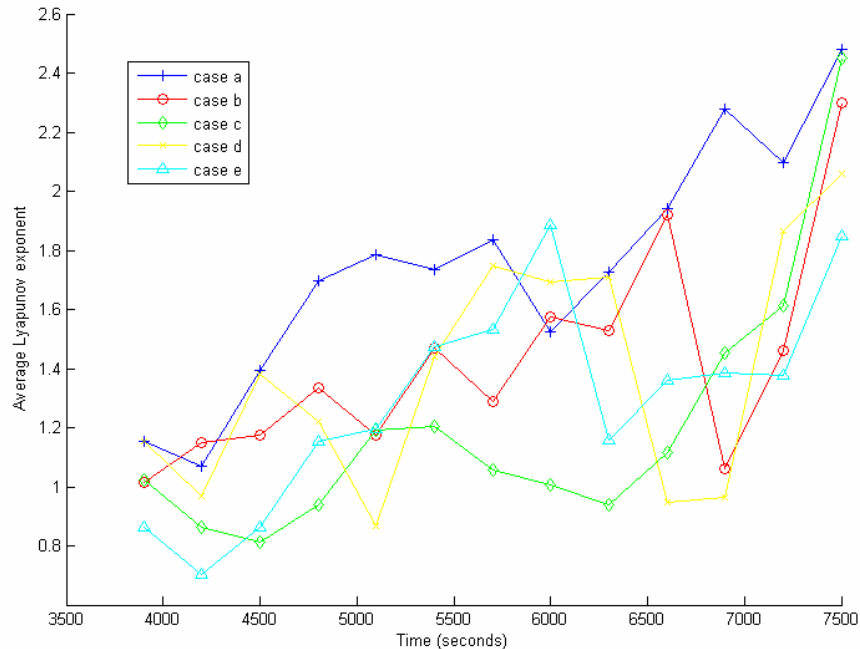


**Figure 6-7 Average Lyapunov exponent for round-about scenario**

The manner and degree to which the traffic self organizes depends on a number of factors. For example, the following additional observations are made:

(1) cases e of Figure 6-5 and Figure 6-6 combine shortest path, adaptability and robustness in the cost function (17), with a = 40 and b = 5000. These cases exhibited aspects from each of the b, c, and d cases: Because of robustness, aircraft spread out more. Because of adaptability, they formed a lane closer to the centerline especially after the hazard. Because of minimizing distance, trajectories are smoother. The weights used in this example were not optimized and the tradeoff between these factors is a subject of further research.

(2) The density of the traffic, a function of both the arrival rate and the size of the hazards, affects the pattern. For example, the aircraft managed to go through the holes in Figure 6-5 in both directions, which caused high complexity areas captured well by the Lyapunov exponents in Figure 6-5 case c.

(3) The first aircraft in the scenario does not encounter any traffic and hence makes random decisions if there are ties between trajectories. The emerging pattern of the traffic depends on these early decisions. For the same reason, when the traffic density declines the pattern may switch to a new one.

(4) All aircraft in these scenarios used the same objective function. This induces implicit coordination and rules and influences the emerging pattern.

(5) The shortest path case, with traffic avoidance (b) is closer to the adaptability case (c) than the robustness case (d). This is because the shortest path is close to the centerline where adaptability is high. The shortest path trajectory, however, differs from the most adaptable trajectory because it uses the minimum speed (to minimize path stretching). Therefore, these trajectories were smother and exhibited less turns. Adaptable trajectories, on the other hand, tended to zigzag around the centerline.

The resulting aircraft trajectories were also analyzed for proximity.

Figure 6-8 (a and b) display, respectively for the two scenarios of Figure 6-5 and Figure 6-6, the number of aircraft-seconds when aircraft were less than 20 nautical miles apart, over the duration of each scenario.
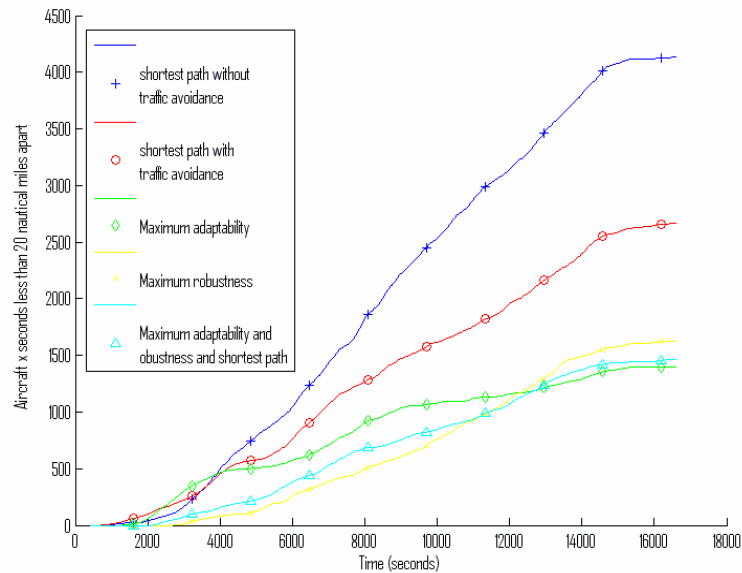


(a) Traffic complexity for the first scenario (two
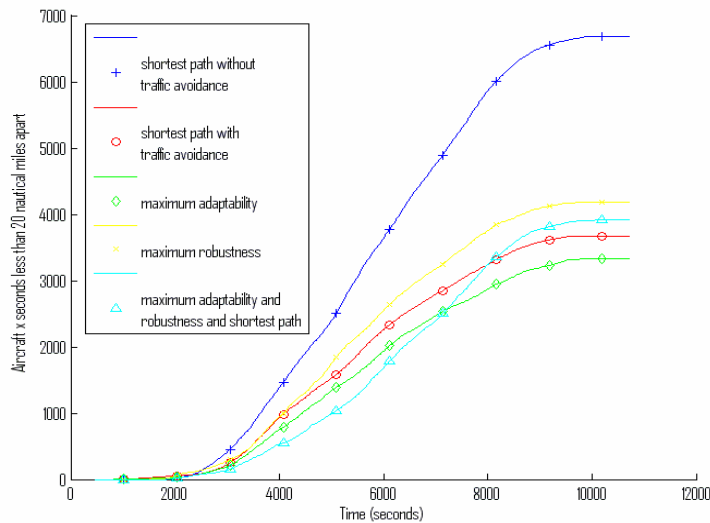


(b) Traffic complexity for the second scenario (round about)

**Figure 6-8 Traffic proximity for the two scenarios**

72

These figures show that, as expected, for both scenarios the case (a) where aircraft used shortest path without traffic avoidance exhibited the highest rate of close proximity. In the first scenario (the two-hole scenario of Figure 6-5) the shortest path with traffic avoidance (case b) exhibited significantly higher proximity than the other cases (c-e) that used adaptability and/or robustness. This suggests that, at least in this scenario, the use of adaptability and/or robustness metrics increases the separation between aircraft over simple traffic avoidance. However, this was not apparent in the second scenario (the roundabout scenario of Figure 6-6) where all cases that avoided traffic (b-e) exhibited similar proximity.

# 7 Preliminary Notes on Constraint Minimization

The research described in the previous sections focused on the trajectory flexibility preservation function which was described in Section 2.2. This was appropriate because flexibility preservation was more central to testing the hypothesis of the impact of preserving flexibility on traffic complexity. As a result, the constraint minimization function, which was described in Section 2.3, was de-emphasized because its role is secondary in terms of further increasing trajectory flexibility. This section describes initial thoughts on the constraint minimization function, which will be investigated more thoroughly in future research.

To limit the scope, the constraints discussed in this section are limited to those that are intended to achieve the objectives of the ATM system, such as safety and efficiency. Constraints that stem from users attempting to maximize their business objectives are ignored. Hence, the constraints addressed are mainly generated by the air traffic service provider (ATSP). As described in Section 2.3, constraint minimization is a shared responsibility between the ground-based ATSP and the flight crews of autonomously operating aircraft. ATSPs are responsible for generating constraints and transferring these constraints to the flight crews. Flight crews are responsible for adhering to these constraints unless negotiating a change to one or more constraints.

In addition, no attempt is made here to comprehensively identify the different types of constraints that may be imposed, which will be addressed in future research, Rather, this section describes initial thoughts on the responsibilities of the ATSP and flight crew in generating and negotiating constraints (respectively), with some constraint examples.

## 7.1 ATSP Constraint Generation

The ATSP is responsible for maintaining safe operations within the controlled airspace. With respect to autonomously flying aircraft, where the ATSP does not directly control the aircraft's trajectory to provide separation assurance, the ATSP maintains safe operations by applying constraints on the autonomous aircraft. To enable an adequate amount of aircraft autonomy, ATSP-generated constraints should only be applied when necessary and should be designed to apply the minimum level of constraint on the aircraft's trajectory that maintains safe operations.

Controllers apply a wide range of constraints to managed aircraft, e.g., from tactical heading clearances to flight plan route changes. While no attempt is made here to comprehensively identify all types of constraints that may be imposed by the ATSP, two categories are distinguished, strategic and tactical constraints. In this context, strategic constraints are defined as those that can be applied directly to the routes within the autonomous aircraft's flight management system (FMS). To ensure increased autonomy and flexibility for autonomous aircraft, it is proposed that only strategic constraints should be applied to autonomous aircraft. More tactical constraints, such as giving the aircraft a heading to maintain, would compromise the aircraft's ability to fulfill its requirements for autonomous flight (e.g., maintain self-separation). If these types of ATSP-generated tactical constraints were deemed necessary, and it was determined to not be possible to specify strategic constraints to achieve the same ATM objectives with

sufficient flexibility to achieve them (e.g., busy terminal area), it may be that the environment was incompatible with autonomous flight. Examples of strategic constraints are position constraints (e.g., an arrival fix), crossing restrictions (time, altitude, speed), path specifications (e.g., cruise altitude), airspace restrictions, and traffic separation [54]. Some of these constraints may be applied with tolerance limits.

The strategic constraints vary in the amount of flexibility they leave for the autonomous aircraft. For example, the most effective type of ATSP-generated constraint for an autonomous aircraft is a required-time-of-arrival (RTA) constraint at a waypoint or boundary. This constrains the aircraft to pass through a given waypoint (or cross a defined boundary[8]) at a specified time, but does not constrain the aircraft's trajectory in any other way. When the RTA is applied to a specific waypoint, the autonomous aircraft is constrained to pass through that waypoint, so there is a constraint on possible lateral paths available to the aircraft. From an ATSP perspective, RTA constraints are excellent for controlling the demand on a given airspace resource (e.g., a region of airspace), but could theoretically also be used to maintain separation between a specific ATSP managed aircraft and an autonomous aircraft. From a flight crew perspective, RTA constraints enable strategic maneuvering to maintain the RTA constraint while also self-separating the aircraft from other traffic and airspace hazards.[9] The generation of more than one RTA constraint for the same aircraft is also acceptable. The tolerance of meeting the RTA, both in time and space, is another aspect that may control the amount of flexibility afforded to the aircraft.

Other types of constraints typically add more limitations on the autonomous aircraft's trajectory than RTA constraints. For example, a cruise altitude constraint could be used to temporarily keep an autonomous aircraft out of a region of airspace (e.g., if the aircraft desired to climb or descend through the airspace), especially if the constraint were an "at or above" or "at or below" constraint. Using a cruise altitude constraint, especially an "at" constraint, could be severely limiting, reducing the degrees of freedom available for self-separation as well as potentially impacting the aircraft's ability to properly manage its trajectory (e.g., not enabling the aircraft to initiate the descent phase of flight). The more restrictive the constraint, the more likely the autonomous aircraft will need to negotiate a relaxation for one or more constraints.

## 7.2  Flight Crew Negotiated Constraint Relaxation

Negotiation to relax (i.e., eliminate or modify to make less restrictive) an ATSP-generated constraint can be desired/required by the flight crew under a variety of

---

[8] It is assumed that the autonomous aircraft would be able to convert a boundary restriction into an equivalent waypoint restriction for application to an FMS route.

[9] This assumes that the RTA does not force a conflict with a traffic or area hazard. The requirement that an ATSP-generated RTA constraint does not create a conflict between the constrained aircraft and another hazard (e.g., with a managed aircraft crossing the same fix at the same time) at the constrained point is assumed a responsibility of the ATSP when generating the constraint. Otherwise, the situation is considered to be over-constrained, that is, no trajectory solution exists that satisfies all of the constraints.

situations. First, the flight crew may not be able to accommodate all of the constraints issued to the aircraft. In this situation, the aircraft is said to be overly constrained. This may be due to performance limitations of the aircraft or may be due to an inability to maintain self-separation while achieving the constraints. Similarly, the aircraft may be forced to perform an unexpected tactical maneuver that causes the flight crew to be unable to maintain a constraint (tactical conflict resolution algorithms are often not required to maintain strategic constraints, since this could limit their ability to maintain self-separation). Finally, the flight crew may determine that the constraints issued can be met, but that the solutions available are not sufficiently flexible (i.e., do not maintain an acceptable level of robustness and/or adaptability) and that a future disturbance is likely to make the constraints unachievable. In this situation, the aircraft is said to be excessively constrained.

If negotiation is desired/required, the flight crew should provide enough information to the ATSP such that the ATSP can generate a new set of constraints that achieve the original ATSP objectives while meeting the requirements of the aircraft. It is unlikely that the flight crew will be able to propose a complete set of new requirements for the ATSP to consider, since the flight crew is unaware of the objectives that the ATSP is required to achieve. It is more likely that the flight crew will return a range of acceptable/desired values for a given constraint or a request to eliminate a specific constraint. The ATSP will have to take this information into account when attempting to generate a new set of constraints. The definition of what data should be sent by the flight crew to enable quick and effective negotiation still needs to be developed.

# 8 Demonstration of Initial Trajectory Flexibility Preservation Functionality in AOP

A limited version of the trajectory flexibility preservation function was implemented in the NASA ATOL AOP platform for demonstration purposes. The objective was to show that the AOP platform is capable of performing route optimization using the approach to trajectory flexibility preservation described in this report. This section describes the current capabilities of AOP to demonstrate use of the flexibility preservation algorithm.

This kind of enhancement had not been previously performed in the AOP environment, which contained only conflict detection and resolution functionality exercised within a 20 minute time horizon. Trajectory flexibility planning applies both within and outside the conflict resolution horizon. However, as described in the previous sections of this report, the focus of the analysis and experiments has been on the longer time horizon beyond conflict resolution. The longer-term focus was selected for two reasons: to test the hypothesized impact of flexibility preservation on traffic complexity, which is more relevant in the longer horizon, and to defer dealing with the interaction with the conflict resolution function until the flexibility metrics have matured. For the same reasons, the AOP platform demonstration included only trajectory flexibility planning in the longer horizon. This selection allowed the new capability to be separated architecturally from the conflict detection and resolution functions. However, it also required some modifications to enable inputs to the trajectory flexibility function that are typically not available in the shorter conflict detection and resolution horizon. As a result, the trajectory that is computed by the trajectory flexibility function is not currently reconciled with the trajectory that the conflict resolution function builds (in case there is a conflict detected). In a fully integrated implementation, the conflict resolution trajectory would typically override the initial part of the trajectory built by the longer-horizon trajectory flexibility preservation function. This integration is a subject of future research and development.

The trajectory computed by the trajectory flexibility preservation function is intended as a long-horizon, rough guidance to the aircraft in terms of waypoints and times and speeds at these waypoints. This flexible trajectory guidance is then inputted to the FMS. However, integration with the requirements of current FMS technologies has not been addressed in this research. As evident from the analyses and experiments described in the previous sections, the trajectory flexibility metrics and methods were developed in an abstract context without consideration of a specific platform. This was justified because the main purpose of the research was testing the hypothesized impact of trajectory flexibility preservation on traffic complexity, and it was intended to apply to both distributed and centralized environments. In this project, the methodology was exercised in a distributed environment.

In the development of the AOP demonstration capability, it was assumed that the FMS may be able to adhere to some of the flexible trajectory guidance but may override other aspects of it as needed to meet objectives that have higher priority than flexibility, particularly in the short-horizon. The implementation of a demonstration capability in AOP highlighted certain aspects of the methods and algorithms developed in the MATLAB environment that require adjustment to reconcile the FMS requirements. One

example that stood out was the use of the speed degree of freedom which was assumed to be available for trajectory flexibility planning (along with path stretching) in the MATLAB algorithm. The FMS on the other hand does not assume a speed input and may override such a speed when, for example, it attempts to meet an RTA. Nevertheless, these restrictions were ignored in the demonstration capability, and the speed profile was computed along with the path stretching by the trajectory flexibility function.

The AOP demonstration conducted in NASA's ATOL successfully showed that high-fidelity flight-deck automation supporting autonomous flight can be adapted to incorporate real-time execution of the trajectory flexibility preservation methodology described in this report. The trajectory flexibility algorithm demonstration was only run on one aircraft in the ATOL environment. It is planned to extend this feature to compute the flexibility optimization for more than one AOP-equipped aircraft during the same simulation. There are many details to be decided regarding this distributed implementation of flexibility planning for complexity management, such as whether the data broadcast from each aircraft would need to be modified to enable the extended look-ahead times required by the trajectory flexibility algorithm.

In the AOP demonstration capability, only deterministic conflicts were implemented in the trajectory flexibility algorithm. As in the MATLAB experiments, it was decided that deterministic conflicts will suffice (with increased separation zone size to represent uncertainty) in providing data about the traffic aircraft. Therefore, there is currently no capability to assign probabilities to different paths of the traffic aircraft. If this decision is revisited in the future, it would still be possible to modify the AOP flexibility capability to take into account a stochastic nature of the traffic data. Also, it was decided that only the traffic hazards would be considered in the initial AOP demonstration. The MATLAB trajectory flexibility algorithm is capable of taking into account both area hazards and traffic hazards. It is planned to include the area hazards in the computations of the AOP flexibility algorithm as well.

The AOP demonstration capability included the three main objective functions used in finding the optimum route that were used in the MATLAB experiments: finding the shortest path to destination, finding the most adaptable path to destination, and finding the most robust path to destination. It would also be possible to have a weighted combination as an objective function or several objective functions with a ranked priority, and it was demonstrated that any of those methodologies can be computed by the AOP software. The current version of the software defaults to the robustness methodology as the highest priority when computing the flexibility algorithm. One of the future extensions will be to provide an easy interface to select which methodology should take priority.

It should be emphasized that more research is required to reach the full potential of AOP for computing and using the flexibility algorithm. For example, it is not certain how the FMS would react to an uploaded optimum route computed by the flexibility algorithm, how the algorithm should be integrated with the conflict resolution function, and what display and interface capabilities are appropriate to allow the flight crew to interact with the flexibility planning function. Future research will address these issues.

# 9 Summary and Conclusions

The work presented in this document constitutes preliminary and investigatory research efforts towards testing the two hypotheses stated in Section 1.1. The first hypothesis speculates that by each individual aircraft autonomously preserving adequate flexibility in accommodating disturbances, a traffic situation that is less complex will naturally result. The second hypothesis speculates that by minimizing the constraints imposed on the aircraft trajectory, without jeopardizing the intended ATM objectives, aircraft flexibility is increased and hence complexity mitigation is further enabled.

Testing these hypotheses fundamentally supports improving ATM operations, both centralized and distributed. However, a concept of distributed operations was formulated to provide a specific operational context for the research.

In this concept the flexibility preservation function is conceived as an airborne function that supports the pilot in autonomously selecting a trajectory which minimizes the aircraft risk exposure to disturbances. Two situations were distinguished: exposure to conflicts with other traffic within a separation assurance horizon, and exposure to disturbances outside the separation assurance horizon stemming for example from traffic congestion and weather systems. In both situations the flexibility preservation function is hypothesized to result in trajectories that lead to lower conflict rates and less complex traffic situations. The research presented focused on the longer horizon while the shorter horizon will be addressed in future research.

In the described concept, the constraint minimization function is conceived as primarily a centralized function that supports ground-based traffic managers in imposing just enough constraints on aircraft trajectories to achieve ATM objectives such as separation assurance and flow management. However, pilots may negotiate constraint minimization with the traffic managers when required from the airborne perspective. Limited research has been conducted on the constraint minimization function. Particularly, cost minimization was considered in the context of trajectory flexibility planning since the planning was done in the presence of constraints and the risk was defined in terms of constraint violation. In addition initial thoughts on the responsibilities of the pilot and traffic manager were provided, preparing for future investigation. Further analysis and development of the constraint minimization function was deemphasized because it is a ground based function, and currently the NASA ATOL capabilities do not support ground agents.

After defining the concept of operations, the focus of the remainder of the document concentrated on mathematically defining trajectory flexibility metrics, developing estimation methods for these metrics, and using these metrics in experiments that involve planning flexible trajectories and testing the impact on traffic complexity. The analysis resulted in defining flexibility in terms of two key characteristics, robustness and adaptability to the disturbance. Then, metrics were developed to measure robustness and adaptability. Robustness is measured by the probability of feasibility, and in a special case, using the ratio of the number of feasible trajectories, given the disturbance with respect to which robustness is measured, to the number of feasible trajectories without the disturbance. Adaptability is measured using the absolute number of trajectories that are feasible given the disturbances. A method to estimate the

number of trajectories under different constraint/disturbance impacts was suggested. The estimation method discretizes time into time steps during each speed and heading are assumed constant. It also discretizes space into cells. It uses a convolution process to estimate the number of trajectories between time steps while filtering for infeasibility due to violating RTA, traffic and hazard constraints. The approach was gradual, starting with one degree of freedom, namely speed, and then generalizing to speed and heading as degrees of freedom.

Using these metrics and their estimation method, experiments were conducted in MATLAB to test the impact of trajectory flexibility preservation on traffic complexity. The analysis demonstrated that using adaptability and robustness metrics in planning flexible aircraft trajectories results in traffic complexity mitigation. The impact was quantified using a Lyapunov-exponent-based traffic complexity metric, flow pattern consistency and a proximity rate measurement. Two scenarios showed signs of self separation and self organization when using these metrics.

The flexibility metrics can be combined with other metrics in the trajectory planning of pilots, airlines, and traffic managers. By incorporating these metrics, the contribution of each aircraft to traffic complexity would be reduced, even without explicit coordination among aircraft or for the aircraft by a ground system. The results reported are promising, and open the door for a wide range of future research. Future research is proposed in the next section.

# 10 Future Work

The following list includes areas of future research extension.

1. Further analysis of impact on traffic complexity. The research conducted to date included analyzing the impact of trajectory flexibility preservation on a limited number of traffic complexity metrics. These metrics included the Lyapunov-based metric and simple measurements of proximity between aircraft and the structure of a traffic pattern. While the early signs are promising in terms of mitigating complexity as measured by these metrics, the research requires further and more thorough analysis. This includes: Continuing the investigation of the impact in the Lyapunov exponent metric to fully understand the observed behavior; analyzing the impact on other metric such as those listed under the notion of dynamic density; investigating other metric possibilities, such as identifying patterns using clustering techniques; and investigating various other scenarios.

2. Extension of the metrics and analysis to altitude. The current metrics and analysis scenarios have been limited to speed and heading degrees of freedom, in two-dimensional airspace. Research is needed to extend to the altitude degree of freedom. This will enable using altitude in the en route environment as well as applying the flexibility preservation function to an environment that included climb and descent.

3. Extension of the current trajectory flexibility metrics and their estimation method. The robustness and adaptability metrics are currently considered under special cases of state and constraint disturbances. While their definitions are generic, the limitation to special cases was motivated by enabling tractable estimation techniques. Further research is needed to generalize these metrics to other state and constraint disturbances and combination of them.

4. Extension of flexibility preservation to within the conflict resolution horizon. The experiments have been focused to date on a long time horizon (about one hour) relevant for traffic flow management applications. The flexibility preservation function and algorithms were designed to apply both within the conflict resolution horizon (10-20 minutes) and beyond. Further experiments are needed to investigate the effectiveness of the metrics and algorithms within the conflict resolution horizon. In this horizon the function assists in selecting conflict free trajectories that are also flexible, in the sense of robustness and adaptability to risk.

5. Validation of the trajectory flexibility metrics. The robustness and adaptability metrics were selected as representation of trajectory flexibility, because the notion of flexibility was defined as the ability of the aircraft to mitigate its exposure to risk. These metrics succeeded in producing the hypothesized impact on traffic complexity, at least according to the preliminary indications. However, the metrics have not been analyzed in terms of their ability to mitigate risk. In other words a validation analysis is needed to demonstrate that these metrics indeed represent the ability of the aircraft to mitigate its risk exposure. Experiments need to be designed and conducted to perform this

validation with different risk exposure scenarios. This may also lead to insights on the relation between these metrics and other ATM aggregate concerns such as safety and user objectives. It may also lead to other metrics or variations on these metrics to represent trajectory flexibility.

6. Investigation of real-time applicability of the methods and algorithms. The current estimation methods and trajectory selection algorithms were based on simplicity. Computational load was not a concern since the intended use was a test of a hypothesis rather that a real-time application (even in experimental setting such as human in the loop simulations). To support future human-in-the-loop experiments and to investigate possible future employment in airborne or ground systems, the computational load needs to be investigated. This research includes testing the tradeoff between accuracy and computation load. It includes investigating the impact of a number of factors on this tradeoff, such as the discretization resolution and the algorithms used. This research is critical in the conflict resolution horizon where both accuracy and computation speed are more critical due to safety concerns and the shorter time horizon. Real time implications also include interfacing with the airborne or ground systems. For example the methods and algorithms need to account for the requirements of the FMS in airborne applications.

7. Extension to dynamic and stochastic trajectory planning. The current experiments were conducted under static and deterministic scenarios. In other words, each aircraft generates a trajectory once upon entry into the system and maintains it throughout without dynamic re-planning over time. Also each hazard or intruder was considered known with a single predicted trajectory. Research is needed to extend the planning to be dynamic to accommodate uncertainty. Extension is also needed to model uncertainties in constraints and aircraft state and to plan in the presence of such uncertainty. The research has considered uncertainty; however, the experiments were conducted in a deterministic environment mainly for computational concerns. Therefore, this research includes identifying uncertainty modeling approaches that mitigate the combinatorial explosion issues. It also includes investigating algorithmic approaches that include uncertainty, such as extending the current dynamic programming algorithm.

8. Investigation of other algorithmic approaches. The current algorithm selected was dynamic programming. Other algorithmic approaches may be more efficient for real-time application. Other concerns include synergy with algorithmic approaches used for conflict resolution (such the genetic algorithm used for AOP's conflict resolution).

9. Investigation and extension of the cost functions. Limited research has gone into designing the cost function of the trajectory flexibility planning. The experiments were conducted with limited selections of the cost function that are not optimized, but were sufficient to demonstrate a number of alternative behaviors combining adaptability and robustness. Further research is needed to investigate variations of the cost function and their impact on traffic complexity and risk mitigation. This research includes investigating different weight parameters to combine adaptability and robustness and

combining adaptability and robustness with other metrics that are of concern to the user and service providers. This research also includes investigating different cost functions for different aircraft in the scenario. Current experiment used a single identical cost function for all aircraft, which induces implicit coordination. Varying aircraft cost functions to represent individual and possibly competing behavior and attitude may increase complexity and reduce predictability. Therefore, experiments are needed to assess the impact of such variations on the underlying hypothesis.

10. Extension of the constraint minimization function. Limited research has been conducted on the constraint minimization function. Particularly, constraint minimization was considered in the context of trajectory flexibility planning since the planning was done in the presence of constraints and the risk was defined in terms of constraint violation. Further analysis and development of the cost minimization function was deemphasized because it is a ground based function, and currently the NASA ATOL capabilities do not support ground agents and interaction between the air and the ground. While, this function may continue to be deemphasized for the same reasons, research need to be extended to at least the airborne side of the constraint minimization and negotiation function.

11. Conducting an AOP experiment. The current experiments have been conducted in using a MATLAB suite that was developed for this purpose. Most of the research extensions described above can be conducted in the MATLAB environment. However, real-time issues will need to be investigated by conducting human-in-the-loop type experiments in ATOL. As functionalities are being developed in MATLAB, the mature ones will be transferred to AOP for demonstration purposes and to support future experiments in ATOL.

# 11 References

[1]. Joint Planning and Development Office, "Next Generation Air Transportation System Integrated Plan," URL: http://www.jpdo.gov/library/NGATS_v1_1204r.pdf

[2]. Wing, D., 2005, "A Potentially Useful Role for Airborne Separation in 4D-Trajectory ATM Operations," AIAA-2005-7336.

[3]. NASA, 2004, "DAG-TM Concept Element 5 En Route Free Maneuvering for User-Preferred Separation Assurance and Local TFM Conformance Operational Concept Description," AATT Project Milestone 8.503.10, NASA Airspace Systems Program Office, Washington D.C.

[4]. NASA, 2004, "DAG-TM Concept Element 11 Terminal Arrival Self-Spacing for Merging and In-Trail Separation Operational Concept Description," AATT Project Milestone 8.652.7, NASA Airspace Systems Program Office, Washington D.C.

[5]. Erzberger, H., T.J. Davis, and S.M. Green 1993, "Design of Center-TRACON Automation System," *Proceedings of AGARD Meeting on Machine Intelligence in ATM*, Berlin, Germany.

[6]. Coppenbarger, R., Lanier, R., Sweet, D., and Dorsky, S., "Design and Development of the En Route Descent Advisor (EDA) for Conflict-Free Arrival Metering," AIAA-2004-4875, 2004.

[7]. Ballen, M., V. Sharma, R. Vivona., E. Johnson, and E. Ramiscal, 2002, "A Flight Deck Decision Support Tool for Autonomous Airborne Operations," AIAA-2002-4554.

[8]. Consiglio, M.C., S.T. Hoadley, D.J. Wing, and B.T. Baxley, 2007, "Safety performance of Airborne Separation: Preliminary Baseline Testing," AIAA-2007-7739.

[9]. Vivona, R., D. Karr, and D. Roscoe, 2006, "Pattern-Based Genetic Algorithm for Airborne Conflict Resolution," AIAA-2006-6060.

[10]. Mondoloni, S., and S. Conway, 2001, "An Airborne Conflict Resolution Approach Using A Genetic Algorithm," AIAA-2001-4054.

[11]. Mondoloni, S., Ballin, M., and Palmer, M., 2004, "Airborne conflict resolution for flow-restricted transition airspace" AIAA-2004-4991.

[12]. Barhydt, R., and P. Kopardekar, 2005, "Joint NASA Ames/Langley Experimental Evaluation of Integrated Air/Ground Operations for En Route Free maneuvering," 6th USA/Europe ATM R&D Seminar, Baltimore, MD.

[13]. Mediterranean Free Flight Programme Final Report, 2005, D821, http://www.medff.it/public/index.asp.

[14]. Blom H.A.P., B. Klein Obbink, and G.I. Bakker 2007, "Safety Risk Simulation of an Airborne Self Separation Concept of Operation," Proceedings of the AIAA Aviation Technology Integration and Operations (ATIO) Conference, Belfast, Northern Ireland, AIAA 2007-7729.

[15]. Hill, J.C., J.K. Archibald, W.C. Stirling, and R.L. Frost, 2005, "A Multi-Agent System Architecture for Distributed Air Traffic Control," AIAA-2005-6049.

[16]. Wollkind, S., J. Valasek, and T. Ioeger, 2004, "Automated Conflict Resolution for Air Traffic management Using Cooperative Multiagent Negotiation," AIAA-2004-4992.

[17]. Versteegt, H.H., and H.G. Visser, 2002, "Traffic Complexity Based Conflict Resolution," AIAA-2002-4443.

[18]. Tomlin, C, G. Pappas, and S. Sastry, 1998 "Conflict Resolution for Air Traffic Management: A Study in Multiagent Hybrid Systems" IEEE transactions on Automatic Control, Vol. 43, No. 4, April, 1998.

[19]. Tomlin, C., I. Mitchell, and R. Ghosh, 2001, "Safety Verification of Conflict Resolution Maneuvers," IEEE Transactions on Intelligent Transportation Systems, Vol. 2, No. 2, June 2001.

[20]. Iyengar, S., C. Jorgensen, V. Rao, and C. Weisbin, 1986, "Robot Navigation Algorithm using Learned Spatial Graphs," Robotica, Vol. 4, No. 2, pp. 93–100.

[21]. Khatib, O., 1986, "Real-Time Obstacle Avoidance for Manipulators and Mobile Robots," International Journal of Robotics Research, Vol. 5, No. 1, pp. 90–98.

[22]. Koren, Y.and J. Borenstein, 1991, "Potential Field Methods and Their Inherent Limitations for Mobile Robot Navigation," In IEEE Conference on Robotics and Automation, pp. 1398-1404, Sacramento, CA, April 1991.

[23]. Sigurd, K and J. How, 2003, "UAV Trajectory Design Using Total Field Collision Avoidance," AIAA-2003-5728.

[24]. Eun, Y., and H. Bang, 2006, "Cooperative Control of Multiple Unmanned Aerial vehicles using the Potential Field Theory," AIAA-20345-674, Journal of Aircraft, Vol 43, No. 6, pp. 1805-1814.

[25]. Shimoda, S., Y. Kuroda, and K. Iagnemma, 2005, "Potential Field Navigation of High Speed Unmanned Ground Vehicles on Uneven Terrain," in *Proceedings of the IEEE International Conference on Robotics and Automation*, Barcelona, Spain, April 2005.

[26]. Clark, C. and S. Rock, 2001, "Randomized Motion Planning for Groups of Nonholonomic Robots," International Symposium of Artificial Intelligence, Robotics and Automation in Space.

[27]. Hsu, D., J.C. Latombe, and R. Motwani, 1997, "Path Planning in Expansive Configuration Spaces," in Proceedings of the IEEE International Conference on Robotics and Automation, pp 2719-2726.

[28]. Hsu, D., R. Kindel, J.C. Latombe, and S. Rock, 2000, "Randomized Kinodynamic Motion Planning with Moving Obstacles," in Workshop on the Algorithmic Foundations of Robotics.

[29]. Kindel, R, D. Hsu, J.C. Latombe, and S. Rock, 2000 "Kinodynamic Motion Planning Amidst Moving Obstacles," in Proceedings of the IEEE Conference on Robotics and Automation, pp. 537-544.

[30]. Lamiraux, F., E. Ferre, and E. Valle, 2004, "Kinodynamic Motion Planning: Connecting Exploration Trees Using Trajectory Optimization Methods," Proceedings of International Conference on Robotics and Automation, 2004

[31]. Barraquand, J.and J.C. Latombe, 1993, "Nonholonomic Multibody Mobile Robots: Controllability and Motion Planning in the Presence of Obstacles," Algorithmica, 10:121-155.

[32]. LaValle, S. M. and J. J. Kuffner, 2001, "Randomized Kinodynamic Planning," International Journal of Robotics Research, 20(5):378-400, May 2001.

[33]. Lamiraux, F.and D. Bonnafous, 2002, "Reactive Trajectory Deformation for Nonholonomic Systems: Application to Mobile Robots." In Proceeding of the IEEE International Conference on Robotics and Automation, pp. 3099-3104, Washington D.C., May 2002.

[34]. Clark, C., Rock, S., and Latombe, J-L., 2003, "Motion Planning for Multiple Mobile Robot Systems using Dynamic Networks", Proceedings of IEEE Conference on Robot and Automation.

[35]. Kopardekar, P. and Magyarits, S., 2002. "Dynamic density: Measuring and predicting sector complexity" Proceedings of the 21st Digital Avionics Systems Conference.

[36]. Histon, J. M., Aigoin, G., Delahaye, D., Hansman, R. J., and Puechmorel, S. 2001, "Introducing structural considerations into complexity metrics." Proceedings of the 4th USA/Europe Air Traffic Management R&D Seminar, Sante Fe, NM.

[37]. Davison, J., Histon, J., Ragnarsdottir, M., Major, L., Hansman, R.J. "Impact of Operating Context on the Use of Structure in Air Traffic Controller Cognitive Processes". Proceedings of the 5th USA/Europe Air Traffic Management R&D Seminar Budapest, Hungary.

[38]. Athenes, S., Averty, P., Puechmorel, S., Delahaye, D., and Collet, C., 2002, "ATC Complexity and Controller Workload: Trying to Bridge the Gap. HCI-Aero 2002 International Conference on Human-Computer Interaction in Aeronautics.

[39]. Delahaye, D. and Puechmorel, S., 2000, "Air Traffic Complexity: towards intrinsic metrics. Proceedings of 3rd USA/Europe Air Traffic Management R&D Seminar, Napoli, Italy.

[40]. Delahaye, D., Puechmorel, S., Hansman, J., and Histon, J., 2003, "Air traffic complexity based on non linear dynamical systems" Proceedings of the 5th USA/Europe Air Traffic Management R&D Seminar, Budapest, Hungary.

[41]. M. Ishutkina, E. Feron, K. Billimoria, 2005, "Describing Air Traffic Complexity Using Mathematical Programming" AIAA-2005-7453.

[42]. Aigoin, G. ,2001, "Air Traffic Complexity. Modeling", Master Thesis. ENAC: France.

[43]. Granger, G., and Durand, N., XXXX" A traffic complexity approach through cluster analysis," Proceedings of the 5th USA/Europe Air Traffic Management R&D Seminar, Budapest, Hungary.

[44]. Billimoria, K., and Lee, H., 2005, "Analysis of aircraft cluster to measure sector-independent airspace congestion", AIAA 2005-7455.

[45]. Riley, V., G. Chatterji, W. Johnson, R. Mogford, P. Kopardekar, E. Sierra, and G. Lawton, 2004, "Pilot perceptions of airspace complexity, part 2," DASC.

[46]. Sridhar, S., Seth, K., and Grabbe, S., 1998, Airspace Complexity and its Application in Air Traffic Management", Proceedings of the 2nd USA/Europe Air Traffic Management R&D Seminar, Orlando, FL.

[47]. Masalonis, A., Callaham, M. Wanke, C., 2003, "Dynamic density and complexity metrics for realtime traffic flow management", Proceedings of the 5th USA/Europe Air Traffic Management R&D Seminar, Budapest, Hungary.

[48]. Idris, H., D. Wing, R. Vivona, and J.L. Garcia-Chico, 2007, "A Distributed Trajectory-Oriented Approach to Managing Traffic Complexity," AIAA-2007-7731.

[49]. Idris, H., R. Vivona, J.L. Garcia-Chico, and D. Wing, 2007, "Distributed Traffic Complexity Management By Preserving Trajectory Flexibility," Proceeding of the 26th Digital Avionics Systems Conference.

[50]. Idris, H., R. Vivona, and D. Wing, "Metrics for traffic complexity management in self-separation operations," Air Traffic Control Quarterly, Volume 17, Number 1, 2009.

[51]. Idris, H., T. El-Wakil, and D. Wing, 2008, "Trajectory planning by preserving flexibility: metrics and analysis," Proceedings of the AIAA Guidance Navigation and Control (GNC) Conference, AIAA-2008-7406, 2008.

[52]. Idris, H., D. Delahaye, and D. Wing., "Distributed Trajectory Flexibility Preservation for Traffic Complexity Mitigation," Proceedings of the 8th USA/Europe Air Traffic Management R&D Seminar, Napa valley, California, 2009.

[53]. Idris, H., T. Hsu, R. Vivona, and S. Green, 2003, "Time Based Conflict Resolution Algorithm and Application to Descent Conflicts," AIAA-2003-5517.

[54]. Wing, D., "Performance Basis for Airborne Separation," Proceedings of the 26th International Congress of the Aeronautical Sciences, 2008-8.7.1, Anchorage, AK, 2008.

# Appendix A. Conflict Zone Geometry

In this appendix, the equations for defining the conflict zone in the t-s domain and in the t-x-y domains are given based on the derivation in [53]. In addition, the equations for determining if a point is inside or outside the zone are given.

Figure A-1 shows the geometry of an intruder aircraft traveling at a constant ground speed across a straight line segment. It also shows the resulting conflict zone in the t-s domain.
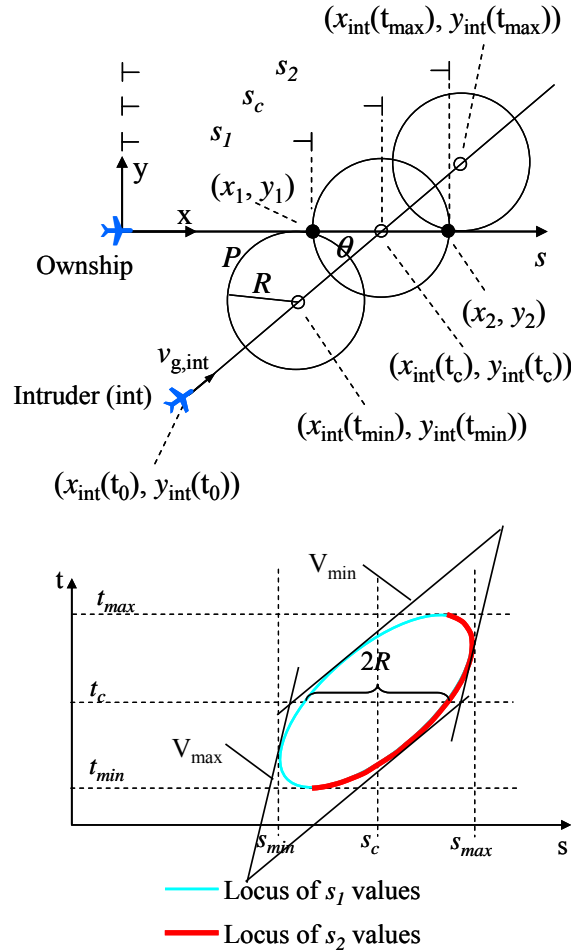


**Figure A-1 Conflict zone geometry**

The following equations are for the boundaries of the elliptical conflict zone in the t-s domain. The derivation can be read in [53].

$$s_1(t) = x_{\text{int}}(t_0) + v_{\text{g,int}} t \cos\theta - \sqrt{R^2 - (v_{\text{g,int}} t \sin\theta + y_{\text{int}}(t_0))^2}$$

$$s_2(t) = x_{\text{int}}(t_0) + v_{\text{g,int}} t \cos\theta + \sqrt{R^2 - (v_{\text{g,int}} t \sin\theta + y_{\text{int}}(t_0))^2}$$

The four tangency lines are found by a constraint optimization problem. The problem maximizes and minimizes the t-intercept of the lines with slopes $v_g = V_{min}$ and $v_g = V_{max}$, (i.e., shifting the lines up/down) subject to constraints of remaining on the loci given by $s_1$ and $s_2$ above. Details can be found in [53].

In the (t,x,y) domain, the conflict volume is found similarly by constructing tangent planes to the intruder aircraft surrounding cylinder. These can be found using the following equations and steps:

Given intruder speed $V_{int}$ and heading $h_{int}$ and ownship speed limits $V_{min}$, $V_{max}$ and heading limits $h_{min}$ and $h_{max}$ and minimum separation R:

(1) Find four relative angles where i and j are min or max

$$h_{rel,i,j} = \arctan(\frac{V_i \sin(h_j) - V_{int}\sin(h_{int})}{V_i\cos(h_j) - V_{int}(h_{int})})$$

(2) Find eight tangency points

$$x_{tan,k} = \pm\frac{R\times\tan(h_{rel,i,j})}{\sqrt{\tan^2(h_{rel,i,j})+1}} + x_{int} \quad , \quad y_{tan,k} = \mp\frac{R}{\sqrt{\tan^2(h_{rel,i,j})+1}} + y_{int}$$

(3) Find 8 planes with norms $n_k$ and distances $d_k$:

$$n_k = \pm(\cos(h_{rel,i,j}), \sin(h_{rel,i,j}),0)\times\text{Unit}(V_i\cos(h_{int}), V_i\sin(h_{int}),1)$$

$$d_k = n_k\cdot(x_{tan,k}, y_{tan,k},0)$$

(4) Point (t,x,y) is in conflict if and only if

$$(x,y,t)\cdot n_k < d_k, \forall k$$

# REPORT DOCUMENTATION PAGE

| 1. REPORT DATE *(DD-MM-YYYY)* | 2. REPORT TYPE | 3. DATES COVERED *(From - To)* |
|---|---|---|
| 01-09-2009 | Contractor Report | |

| 4. TITLE AND SUBTITLE | 5a. CONTRACT NUMBER |
|---|---|
| Trajectory-Oriented Approach to Managing Traffic Complexity: Trajectory Flexibility Metrics and Algorithms and Preliminary Complexity Impact Assessment | NNA07BB26C |
| | **5b. GRANT NUMBER** |
| | |
| | **5c. PROGRAM ELEMENT NUMBER** |
| | |

| 6. AUTHOR(S) | 5d. PROJECT NUMBER |
|---|---|
| Idris, Husni; Vivona, Robert; Al-Wakil, Tarek | |
| | **5e. TASK NUMBER** |
| | |
| | **5f. WORK UNIT NUMBER** |
| | 411931.02.51.07.01 |

| 7. PERFORMING ORGANIZATION NAME(S) AND ADDRESS(ES) | 8. PERFORMING ORGANIZATION REPORT NUMBER |
|---|---|
| NASA Ames Research Center        NASA Langley Research Center <br> Moffett Field, CA 94035        Hampton, VA 23681-2199 | |

| 9. SPONSORING/MONITORING AGENCY NAME(S) AND ADDRESS(ES) | 10. SPONSOR/MONITOR'S ACRONYM(S) |
|---|---|
| National Aeronautics and Space Administration <br> Washington, DC 20546-0001 | NASA |
| | **11. SPONSOR/MONITOR'S REPORT NUMBER(S)** |
| | NASA/CR-2009-215933 |

**12. DISTRIBUTION/AVAILABILITY STATEMENT**
Unclassified - Unlimited
Subject Category 03
Availability: NASA CASI (443) 757-5802

**13. SUPPLEMENTARY NOTES**
Technical Monitor: David J. Wing, Langley Research Center. This work was performed and funded under Ames contract NNA07BB26C, but monitored and published by Langley Research Center.
Idris, Vivona, and Al-Wakil: L3 Communications, 300 Concord Road, Suite 400, Billerica, MA 01821

**14. ABSTRACT**

This document describes exploratory research on a distributed, trajectory oriented approach for traffic complexity management. The approach is to manage traffic complexity based on preserving trajectory flexibility and minimizing constraints. In particular, the document presents metrics for trajectory flexibility; a method for estimating these metrics based on discrete time and degree of freedom assumptions; a planning algorithm using these metrics to preserve flexibility; and preliminary experiments testing the impact of preserving trajectory flexibility on traffic complexity. The document also describes an early demonstration capability of the trajectory flexibility preservation function in the NASA Autonomous Operations Planner (AOP) platform.

**15. SUBJECT TERMS**

Air traffic management; Constraint minimization; Distributed control; Self-separation; Traffic complexity; Trajectory flexibility

| 16. SECURITY CLASSIFICATION OF: | | | 17. LIMITATION OF ABSTRACT | 18. NUMBER OF PAGES | 19a. NAME OF RESPONSIBLE PERSON |
|---|---|---|---|---|---|
| a. REPORT | b. ABSTRACT | c. THIS PAGE | | | STI Help Desk (email: help@sti.nasa.gov) |
| | | | | | **19b. TELEPHONE NUMBER** *(Include area code)* |
| U | U | U | UU | 92 | (443) 757-5802 |